RESEARCH ON THE TRANSMISSION OF ELECTROMAGNETIC SIGNALS BETWEEN MINE WORKINGS AND THE SURFACE

Richard G. Geyer
George V. Keller
Takashi Ohya

Prepared for:
DEPARTMENT OF THE INTERIOR
BUREAU OF MINES
WASHINGTON, D.C.

Colorado School of Mines
Golden, Colorado 80401

USBM Contract No. H0101691

"Research on the Transmission of Electromagnetic Signals Between Mine Workings and the Surface"

Richard G. Geyer
George V. Keller
Takashi Ohya

Colorado School of Mines

USBM CONTRACT REPORT H0101691

Date: January 10, 1974

DEPARTMENT OF THE INTERIOR
BUREAU OF MINES
WASHINGTON, D.C.

FOREWORD

This report was prepared by Richard G. Geyer under USBM Contract No. H0101691. The contract was initiated under the Coal Mine Health and Safety Research Program. It was administered under the technical direction of the Pittsburgh Mining and Safety Research Center with Mr. Howard E. Parkinson acting as the technical project officer. Mr. Alan Granruth was the contract administrator for the Bureau of Mines.

This report is a summary of the work recently completed as part of this contract during the period June 15, 1970 to October 1, 1973.

This technical report has been reviewed and approved.

ACKNOWLEDGMENTS

We wish to acknowledge the advice, comments, and encouragement given over the past three years by Mr. Howard E. Parkinson, Dr. James Powell, and Mr. John Murphy of the Pittsburgh Mining Research Center relating to the work reported here. We especially wish to acknowledge the helpful advice and assistance given by Dr. James R. Wait of CIRES.

ABSTRACT

One aspect of a program to improve the chances of survival following coal mine disasters is the development of a communications system which will allow surviving miners to make their circumstances known to rescue teams. At present, it appears that an electromagnetic system may be most practical.

The development and design of an effective electromagnetic communications link for signalling between mine workings and the surface requires knowledge of pertinent physical properties of the rocks overlying the mine workings and the characteristics of the ambient noise against which a communications signal must be recognized. Knowledge of the overburden electrical transmission properties is useful not only for determining a practical operating transmitter frequency at a given mine, but also for ensuring the best possible electromagnetic coupling for routine or emergency communication purposes.

Field studies of the electrical transmission properties of the overburden of coal mines in Colorado, Illinois, and Pennsylvania generally show that a relatively uniform and unimodal electrical conductivity distribution exists provided that the region has not been subject to considerable structural or metamorphic deformation such as that observed in the Gary District of West Virginia. Measurements of ambient surface electromagnetic noise levels at several mines in Colorado, Illinois, and West Virginia were taken and analyzed and are presented in the form of amplitude histogram plots both as a function of frequency and time of day. These amplitude histograms may be used in conjunction with overburden resistivity data in implementing an uplink communications beacon system which will yield a specified signal-to-noise ratio at the surface.

Numerous C.W. field transmission tests were made in various coal mining environments with use made of either a buried vertical-axis transmitting loop or a short insulated grounded current line. These transmission tests were made from 20 Hz to 20,000 Hz in frequency and at several geographic surface receiving sites. The results of these field measurements show, in general, good agreement with theoretically calculated results. Since the produced surface magnetic field from a buried vertical-axis loop source or the produced surface horizontal electric field from a buried horizontal current line show better agreement with theoretical results, they could be used for beacon location system.

One criterion would be in detecting the equatorial and polar null lines of the horizontal electric field component which is normal to the direction of emplacement of a buried transmitting line current source. A second criterion would be in the surface mapping of the maximum in the vertical magnetic field directly over a vertical-axis loop transmitter and the associated null in the vertical magnetic field at a horizontal offset distance which is about 1.4 times the depth of burial of the transmitter. Finally, a third criterion would lie in the surface mapping of the null in the horizontal magnetic field directly over the vertical-axis beacon and the associated maximum in the horizontal magnetic field at an offset distance from the transmitter axis of half the depth of burial of the loop transmitter.

In mapping the vertical magnetic field over a buried vertical-axis loop transmitter, the size effect of the transmitter loop must be taken into account

when the separation distances between the transmitter and receiving sensor are less than ten times the effective radius of the source loop; increasing the size of the transmitting source relative to the source-receiver separation distance shifts the null in the vertical magnetic field to greater offsets. In mapping either the vertical or horizontal magnetic field over a buried vertical-axis loop transmitter, care should be exercised in ascertaining that measured nulls and maxima are along radials through the axis of the buried source loop.

For the main part, coupling experiments show that ambient electromagnetic noise in coal mining districts is less of a problem above 1000 Hertz. But secondary and perhaps undesirable maxima and null phenomena (as well as penetration problems) would occur in many coal mine provinces in the behavior of the surface horizontal magnetic field (over a buried vertical-axis loop transmitter) if transmission frequencies as high as 10 kHertz were used.

CONTENTS

	Page
FOREWORD	i
ACKNOWLEDGMENTS	i
ABSTRACT	ii
INTRODUCTION	1
ELECTRICAL PROPERTIES STUDIES	3
Resistivity of Coal	3
Resistivity of Overburden	4
Galvanic Method	9
Overburden Electrical Conductivity Distribution at Imperial and Eagle Coal Mines, Colorado	9
Overburden Electrical Conductivity Distribution at Montour No. 4 Coal Mine, Pennsylvania	13
Inductive Method	20
NOISE ENVIRONMENT STUDIES	24
Gary No. 14 Coal Mine, West Virginia	26
Peabody No. 10 Coal Mine, Illinois	26
Imperial and Eagle Coal Mines, Colorado	26
APPLICATION OF FIELD STUDIES	29
Vertical-Axis Loop Transmitter	29
Grounded Horizontal Electric Line Transmitter	30
THROUGH-THE-EARTH TRANSMISSION TESTS	37
Inferences to Location	37
Passive Detection of a Buried Loop from the Surface	42
Downlink Pulse Signalling to Underground Mine Working	54
Theoretical Considerations	54
Experimental Downlink Pulse Signalling	60
Continuous Wave Field Transmission Tests	62
Horizontal Electric Field Measurements - Buried Line Source Transmitter - U.S. Bureau of Mines Experimental Coal Research Mine, Bruceton, Pennsylvania	64

Page

Vertical Magnetic Field Measurements - Buried Vertical-Axis Loop Transmitter - U.S. Bureau of Mines Experimental Coal Research Mine, Bruceton, Pennsylvania 69

Vertical Magnetic Field Measurements - Surface Vertical-Axis Loop Transmitter - U.S. Steel Robena No. 4 Coal Mine, Uniontown, Pennsylvania. 79

Horizontal Magnetic Field Measurements - Buried Vertical-Axis Loop Transmitter - U.S. Bureau of Mines Experimental Coal Research Mine, Bruceton, Pennsylvania 81

SUMMARY. 89

APPENDICES

A. Histograms/Gary No. 14 Coal Mine, Gary, West Virginia. 95

B. Histograms/Peabody No. 10 Coal Mine, Pawnee, Illinois. 104

C. Histograms/Eagle Coal Mine, Erie, Colorado 113

REFERENCES 122

Research on the Transmission of Electromagnetic Signals Between Mine Workings and the Surface

INTRODUCTION

Underground mining of coal remains one of the most hazardous of occupations, despite intensive efforts by government, industry, and labor to reduce the hazards. One of the most frustrating aspects of attempts to reduce the number of fatalities in coal mine operations is that of not being able to communicate with miners trapped underground immediately after some type of catastrophic accident. When a gas explosion takes place, it is difficult to pinpoint the areas of a mine affected from the surface. Tens or even hundreds of miners may survive the initial effects of such a catastrophe, and their longer-term survival will depend on their taking the proper action, such as barricading themselves in a remote part of the mine, or seeking out an unobstructed exit from the mine. Normal communications are usually completely disrupted at the moment of the catastrophe, at a time when effective communication is essential. Therefore, there is a need for an emergency communications system for use under such circumstances, a system which would be sufficiently portable that a transceiver could be carried readily by groups of miners, or even individual miners at all times while they are underground.

The problems related to the development of an emergency communications system are only partly technical in nature, but to a large extent, the design of a workable system will depend on human engineering factors which are sometimes difficult to formalize. The problem is that of providing a miner underground with a communications system which will fulfill one or both of two requirements; that of indicating the location of the trapped miners, and that of providing some transfer of information between the miner and other people at the surface of the earth. If a communications system with a high capacity for transmitting information could be provided to the miner, these problems might be solved at the same time. Therefore, an important aspect of a communications system is the amount of information that can be transmitted over it per unit time. For voice transmission, data rates of about 3000 bits per second are necessary; while data rates as low as one bit per second or even one bit per minute might be used for the transmission of a simple code. Voice transmission would be more desirable than the use of a slow code, but as one might expect, the higher the data rate for the system, the greater will be the complexity, weight, and power requirements. Thus, in designing a workable system, we may expect there to be a tradeoff between data rate on the one hand, and portability on the other.

A second important property of a communications system is whether it is one-way or two-way. A simple communications system would allow the trapped miner to make his presence known to people on the surface, but would not allow communication from the surface to underground (e.g., hammer tapping). In an emergency it is of prime importance that up-link communications, from the miner to the surface, be established first so that rescue teams may know if there is anyone alive underground and where they may be. However, it is also important to have a down-link so that information can be passed to the buried miner. Such information might advise him as to the wisest course of action to ensure survival, or

would assure him that rescue attempts were proceeding, and so, prevent him from taking unwise actions on his own. Of particular interest is the possibility that the up-link and the down-link would not need to be symmetrical with respect to data rate. It would be quite reasonable to use a low-data-rate up-link system if a high-data-rate down-link system were available. In this way, specific questions along with instructions for a simply coded reply could be transmitted downward.

In order to design a workable electromagnetic communications system coordinating both technical requirements and human engineering, it becomes necessary to know a variety of design parameters which may be grouped into three classes as follows:

(1) the electrical properties of the rock overlying mine workings, which determine the relationship between the amount of energy or power applied to the transmitter and the strength of the signal as it propagates through the ground

(2) the ambient background electromagnetic noise levels at receiver locations, which determine the minimum level of signal strength that can be recognized

(3) the effect of mine workings and structures on the behavior of the communications signal.

Some of the above design parameters may differ for every mine so that for ultimate optimization of emergency communications systems, it would be necessary to have such information for every drift of every mine working.

Such an optimized system probably does not represent the desirable first step in developing an emergency communications system, but rather a longer range goal. At present, it would be preferable to specify a system which would not be sensitive to any but the most extreme differences in the character of a mine working, so that the same elements could be used by most mines. Thus, we may settle for near optimization based on the idea that similar mines in similar geological settings will be characterized by relatively narrow ranges for design parameters, and that these ranges may be determined with reasonable statistical reliability by making studies only over selected mines.

ELECTRICAL PROPERTIES STUDIES

The mathematical theory for the behavior of electromagnetic fields from an underground antenna, though tedious, has in recent years become somewhat well established (Wait and Campbell, 1953; Wait, 1962; Bannister, 1966; Sinha and Bhattacharya, 1966; Banõs, 1966; Wait, 1969; Wait, 1970; Wait, 1971c, 1971d; Wait and Hill, 1972a; Hill, 1973a; Hill and Wait, 1973c). In all such theoretical studies the electrical properties of the earth affect signal strength in a way which is determined by the wavenumber of the medium or media through which propagation takes place. The wavenumber is given by the expression:

$$\gamma^2 = 2\pi i f \mu\sigma - 4\pi^2 f^2 \mu\varepsilon \qquad (1)$$

where f is the frequency used in cycles per second, μ is the magnetic permeability of the medium in henries/meter, and ε is the dielectric constant in farads/meter (all quantities are expressed in MKS units in this report). Only one of these quantities, the frequency, is a design parameter. In order to specify values for the wavenumber in theoretical studies, it is reasonable to expect that statistical compilations of the other three factors might be needed, particularly as a function of frequency if any of the factors should be frequency-dependent.

Extensive tables of physical properties data are available in the literature which may be used to reduce the magnitude of the problems in compilation of pertinent data (Clark, 1966; Parkhomenko, 1967). Based on such tabulations, the generalization may be made that for the rocks normally occurring in the vicinity of coal mines, the magnetic permeability is not variable, but assumes a value quite close to that of free space, or $4\pi \times 10^{-7}$ henries/meter. As a consequence, it is not necessary to carry out any statistical analysis of magnetic permeability data for the purpose of this research.

However, the use of tabulated data on electrical conductivity and dielectric constant may not be entirely satisfactory. Coal mines are found rather near the surface in sedimentary sequences of rocks. Usually, the sedimentary rocks are those which were originally deposited in fresh or brackish water and, moreover, insofar as most coal mines are relatively near the surface, a significant fraction of the rock overlying a coal mine may have its properties modified by weathering. In a review of tabulated data on electrical properties, it becomes apparent that relatively few measurements have been made on such rock sequences. In considering the electrical properties of the rocks along a communications path between a mine working and the surface, it is convenient to consider coal and the overburden separately.

Resistivity of Coal

Studies of the electrical resistivity of coals have been carried out by many people (Parkhomenko, 1967; Krasnovskii, 1969; Baker et al, 1966; Tonkonogov and Veksler, 1971). Data on the resistivity of coals which may be found in literature do not always indicate the conditions under which measurements were made, such as the moisture content, temperature, measuring method, and so on. Baker and his coworkers reported that resistivity of anthracite depends on its moisture content, its temperature, the number of electrodes used to measure

resistivity, and whether the sample is cut parallel to or perpendicular to the bedding plane (Baker and others, 1966). Data reported by various authors are listed in Table 1 for six types of coal.

Of the values reported in Table 1, the highest resistivities were obtained for measurements made on samples obtained from a coal pile in a completely dry state. Lower values of resistivity are reported for naturally wet coal, while the resistivity of air-dried coal is about the same order of magnitude according to three references. However, A. F. Baker and others (1966) reported the resistivity of anthracite to be lower when it is dry than when it is wet.

The range of resistivities reported for coals is extremely wide, extending from the semiconducting to the insulating regions. Resistivity is a function of the physical and petrographic character of the coal, the mineral composition and the degree of metamorphism. Generally, the resistivity of coal can be correlated with texture and composition, but is a function of a greater number of variables than the properties of other rocks.

The basic petrographic constituents of coals are fusain, vitrain, durain, and clarain. The resistivity of dry samples of clarain and vitrain is more than 3×10^6 ohm-meter, while fusain has somewhat lower resistivity, 10 to 10^3 ohm-meter. As a result, the resistivity of a coal will depend on the relative proportions of these constituents.

The relation between resistivity of coals and their ash content is shown in Figure 1.

Dakhnov (see Parkhomenko, 1967) has analyzed data statistically, finding that the highest resistivities are found in gassing coal and greasy steam coal. According to Toporets (see Parkhomenko, 1967) long burning coals have the highest resistivities. Moreover, the amount of decrease in resistivity with increasing metamorphism depends on the type of metamorphism. A pronounced decrease in resistivity is found in coal fields subject to thermal metamorphism, particularly contact metamorphism.

The role played by the carbon ratio in determining the resistivity of coal with various degrees of carbonization is not uniform. For long-burning coal, gassing coal and greasy steam coal, the character of the relationship is one of decreasing resistivity with increasing carbon ratio, while in the case of anthracite, on the other hand, increasing the carbon ratio increases the resistivity. It must be noted that not only is the carbon ratio important, but also the ash content, which is related to the carbon ratio.

Resistivity of Overburden

Conduction in near-surface rocks is almost entirely through the water filling the pore spaces of the rocks, and so, prediction of electrical properties for the overburden is somewhat simpler than for coal seams. In water-bearing rocks, there tends to be a correlation between resistivity and geologic age, inasmuch as the amount of water decreases with age, and salinity tends to increase with age. Most studies of the electrical properties of sedimentary rocks have dealt with deep-seated formations that serve as oil and gas reservoirs, but a large amount of data on the resistivities of near-surface rocks is available in National

Coal quality	Source of data						
	1	2	3	4	5	6	7
Brown coal	-9×10^{10}	$10 - 2 \times 10^{2}$	$10^{7} - 10^{8}$	$10^{6} - 10^{8}$	$8 \times 10 - 1.8 \times 10^{2}$		
Gassing coal	1.7×10^{11}		2×10^{8}				
Greasy steam coal (bitumenous)	4.9×10^{10}	$10^{2} - 10^{4}$	10^{8}	$10^{6} - 10^{8}$		8 - 11	
Coaking coal	0.8×10^{10}					8 - 11	
Lumpy steam coal (super-bitumenous)	2.6×10^{9}	$10 - 10^{2}$				8 - 11	
Anthracite	3.0×10^{-1}	$10^{-3} - 10$	1				.6 - 1.5

TABLE I. Resistivity of Coal in ohm-meter

Source of data: 1. A. P. Kovalev, 2. V. M. Daknov, 3. A. A. Agroskin and I. G. Petrenko, 4. N. N. Shumilovskii, 5. F. Z. Kransnovskii, 6. M. P. Tonkonogov and V. A. Veksler, 7. A. F. Baker et al.

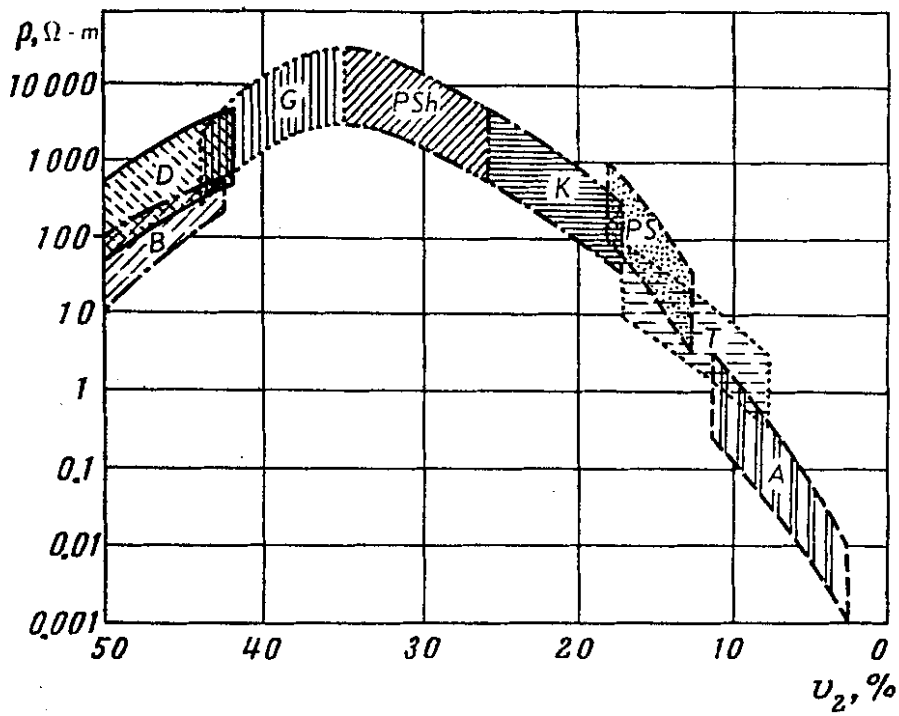

Fig. 1. Graph of the most probable values for the resistivity of coals of various grades as a function of quality. The ash content is plotted along the abscissa.

Bureau of Standards Circular 546 (Kirby and others, 1954). These earth resistivity values were estimated from the rate of decay in field strength about radio stations. Such surveys are required of all broadcast stations by the Federal Communications Commission. Resistivities determined from these field-strength surveys represent average values for rocks over an area of a few square miles about the broadcasting station to a depth of a few tens to a few hundreds of feet. The median value for slightly over 7000 measurements reported in Circular 546 is 143 ohm-meters.

Selecting from the 7000-odd measurements only those made over sedimentary rocks, the correlation between resistivity and geologic age shown in Figure 2 was obtained. Inasmuch as the age of the overburden over coal measures ranges from Carboniferous to Miocene, in most cases it is to be expected that the overburden will have resistivities lower than the median value of 143 ohm-meters mentioned above, probably near 60 to 70 ohm-meters.

In developing a workable emergency communications system, it is probably necessary to obtain statistical summaries of resistivity values for specific mines, rather than rely on the data presently in the literature.

Laboratory measurements on recovered samples may be subject to uncertain experimental errors, particularly since it is difficult to maintain or restore samples to their natural state with respect to water content - a factor which is quite important in making meaningful electrical properties measurements. Therefore it was decided that in this case in situ measurements of electrical properties would be preferable to laboratory studies.

Two approaches to the determination of electrical properties with surface-based equipment were used in our compilations. In one approach, current is introduced into the ground with electrode contacts and the potential established in the earth by this current is measured with a second pair of electrode contacts. In the other approach current is induced in the ground by a time-varying magnetic field with alternating current driven through a loop of wire or a grounded length of wire. The effect of the earth on this magnetic field is detected using a second loop of wire to measure the field at some moderate distance.

If the earth over a coal mine were completely uniform in electrical properties, the values for electrical conductivity determined from these two techniques would be the same. However, if the earth is stratified with layers having different electrical properties, as is most probably the case, the two techniques will provide somewhat different values for the average conductivity of the ground. This difference is a consequence of the electrical anisotropy which is observed in layered materials (Van'ian, 1965). When the earth is made up of a sequence of layers with differing conductivity, the average conductivity detected with current flowing perpendicular to the bedding will be less than the average conductivity detected with current flowing parallel to the bedding. The differences will be greater when the individual conductivities in the beds cover a wider range. The difference may be only a few percent in rocks which are uniform, or it may amount to a factor of 2 to 3 in rocks made up of layers with widely different individual conductivities. If the difference is significant for the typical rocks over coal mines, it may be of importance in comparing the merits of electromagnetic fields generated with grounded wire antennas and those

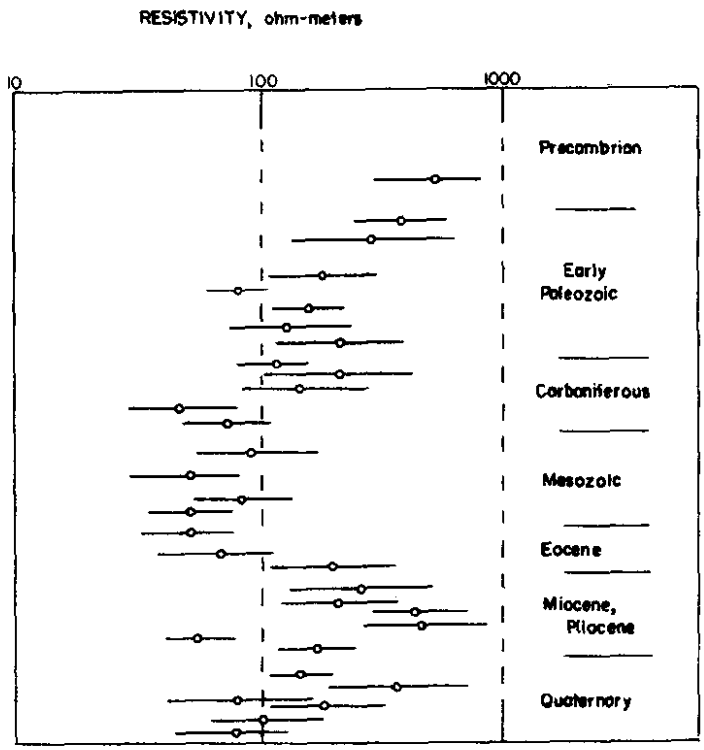

Fig. 2. Average resistivity for groups of sedimentary rocks with similar characteristics. Each circle indicates an average resistivity determined from 35 to 250 measurements about radio stations. The bar through each circle indicates the range within which 95 per cent of the values for that group of data fall.

generated with induction loops. Usually, the current field from a grounded wire will depend on the geometric average of the maximum and minimum conductivity measured along and across the bedding in a laminated sequence of rocks, while the field from a loop source lying in a plane parallel to the bedding of the rocks will depend on the maximum conductivity.

Galvanic Method

The system selected for the determination of electrical conductivity using electrode contacts is shown diagramatically in Figure 3. This particular arrangement of electrodes is one which exhibits a relatively low inductive coupling between the cables used to introduce current into the ground and the cables used to connect the measuring electrodes to the receiving equipment. With such an array, it is possible to determine the dielectric constant at low frequencies, if it is large enough, as well as the conductivity. The use of this electrode array in geophysical exploration has been described by Madden and Cantwell (1967).

In field experiments carried out over the Imperial and Eagle coal mines at Erie, Colorado, the Gary No. 14 coal mine at Gary, West Virginia, the Peabody No. 10 coal mine in Illinois, and the Montour No. 4 coal mine in Pennsylvania, typical currents of 1 to 5 amperes were used with an "a-spacing" of 30.5 meters. The maximum separation between electrodes A and M in Figure 1 was 243.8 meters. Measurements were made along short traverses, so that computed values of apparent resistivity might be presented in the form of pseudo-section.

With the dc measurement system described here, the current driven into the ground is in the form of square wave pulses; that is, the current is turned on to its dc level for a period of 10 seconds and then abruptly terminated. At the same time, the voltage between the measuring electrodes is recorded on a graphic recorder. A typical sample of acquired field data is shown in Figure 4.

If the dielectric constant in the earth is large at low frequencies, the voltage will not disappear abruptly as the current flow is terminated, but rather, there will be a transient decay from the static level observed during current flow. The characteristics of this transient decay may then be used to estimate the tangent of the loss angle, from which the low-frequency dielectric constant can be determined. However, in the measurements made at the above coal mines, the transient decay was so quick so as to be not detectable within the accuracy of the recording equipment. This observation means, as was expected, that the dielectric constant is not large enough to be significant in affecting electromagnetic propagation at low frequencies.

Overburden Electrical Conductivity Distribution at Imperial and Eagle Coal Mines, Colorado

Surface-based resistivity measurements using the axial dipole-dipole electrode configuration were made at the Imperial and Eagle Coal mines, Colorado, with a view toward the characterization of the geoelectric sections overlying the mine workings. Typical apparent resistivity sections along survey lines are given in Figures 5, 6, and 7. In plotting the sections, lines are drawn downward at angles of 45 degrees from the center of each dipole location, and measured apparent resistivity values are plotted at the appropriate intersections. It is apparent that the geoelectric section overlying the mine

DIPOLE - DIPOLE ARRAY

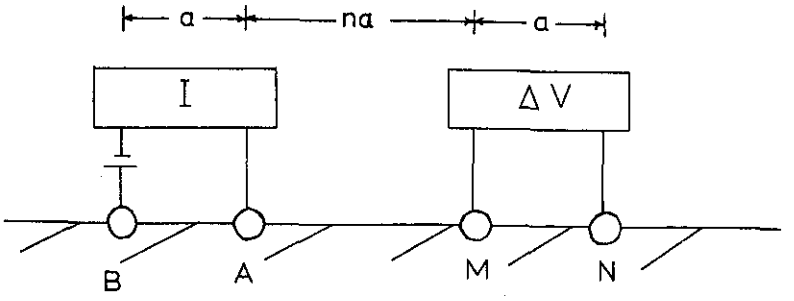

Fig. 3 Dipole-dipole array used in field determinations of electrical conductivity and dielectric constant. The spacing between electrodes A and M is increased stepwise to make a series of measurements with different effective penetrations into the earth.

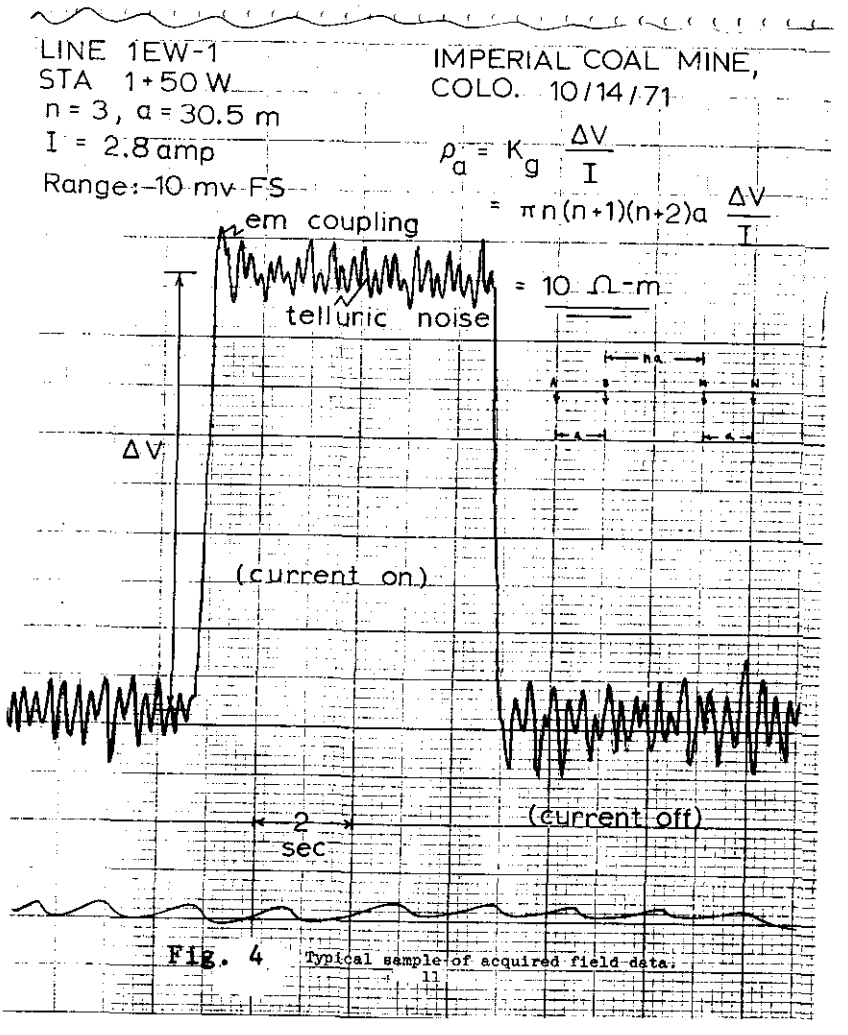

Fig. 4 Typical sample of acquired field data.

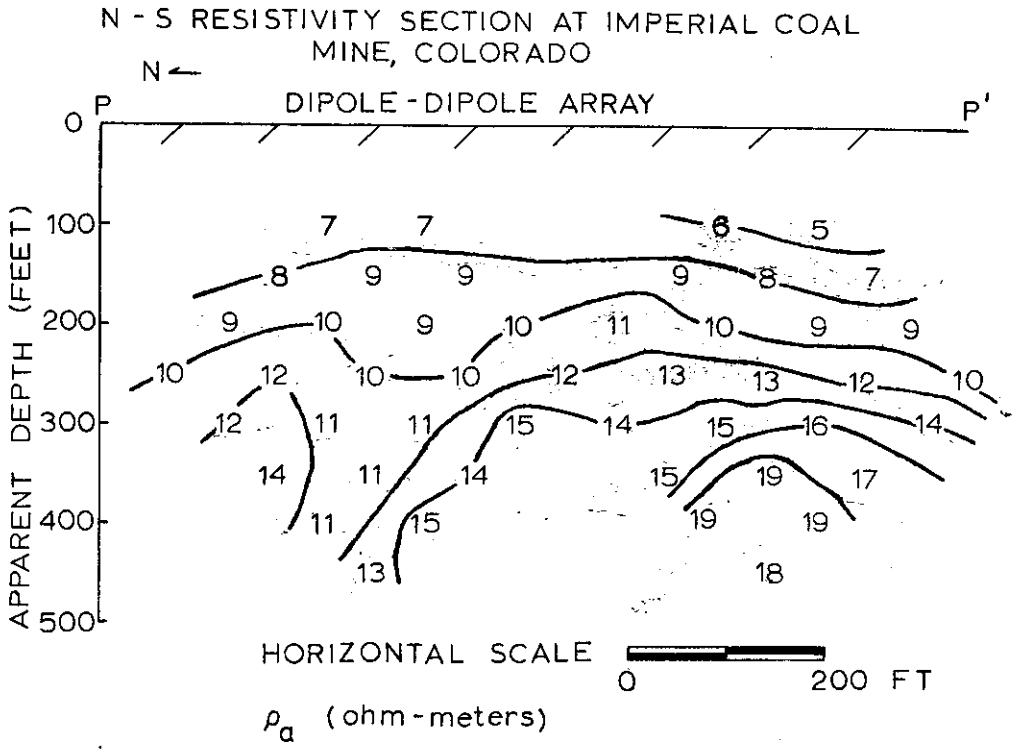
N - S RESISTIVITY SECTION AT IMPERIAL COAL MINE, COLORADO
N
P
DIPOLE - DIPOLE ARRAY
P'
APPARENT DEPTH (FEET)
0
100
200
300
400
500
HORIZONTAL SCALE
0
200 FT
ρ_a (ohm-meters)

Fig. 5

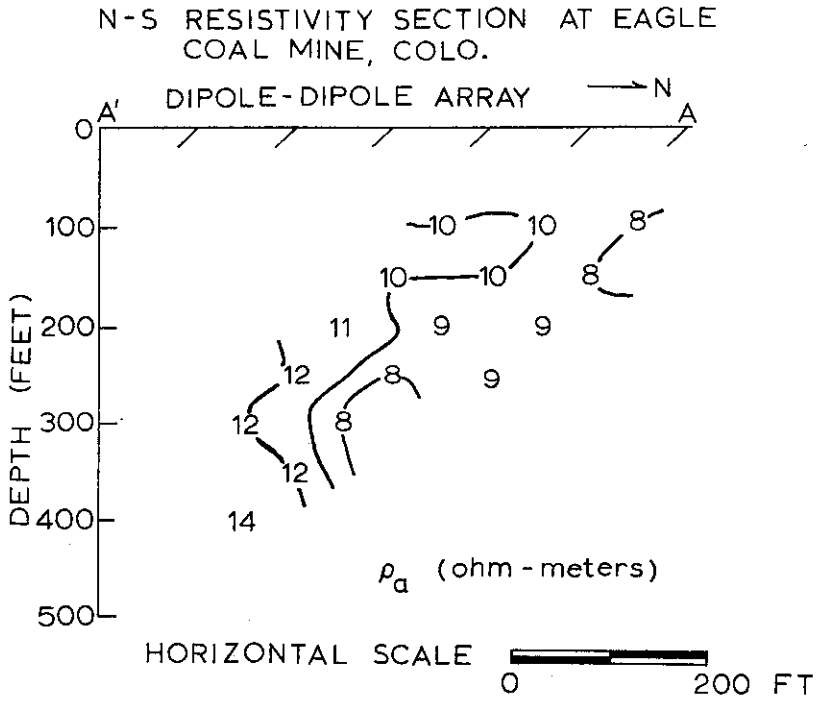
N-S RESISTIVITY SECTION AT EAGLE COAL MINE, COLO.
A'
DIPOLE-DIPOLE ARRAY
N
A
0
100
200
300
400
500
DEPTH (FEET)
ρ_a (ohm-meters)
HORIZONTAL SCALE
0
200 FT

Fig. 6

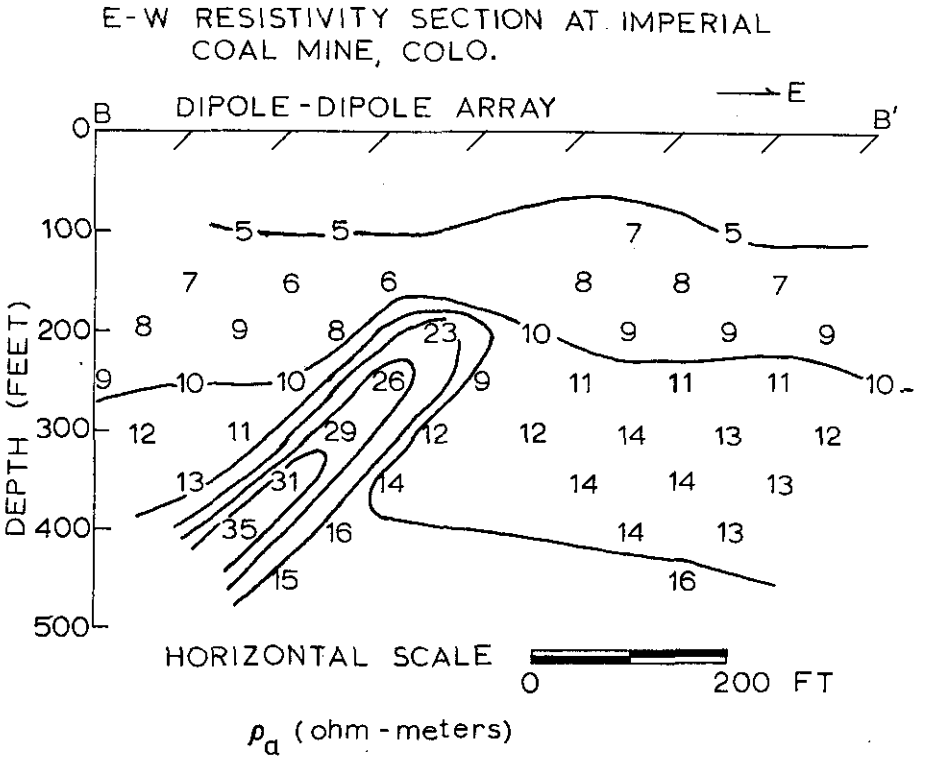
E-W RESISTIVITY SECTION AT IMPERIAL COAL MINE, COLO.
DIPOLE-DIPOLE ARRAY
E
B
B'
0
100
200
300
400
500
DEPTH (FEET)
HORIZONTAL SCALE
0
200 FT
ρ_a (ohm-meters)

Fig. 7

workings at the Imperial and Eagle mines is quite homogeneous, with an average resistivity of 12 ohm-meters.

A probability density plot of resistivity values of the overburden at Imperial and Eagle coal mines is inferred from Figures 5, 6, and 7 and is given in Figure 8. A unimodal distribution of apparent resistivity is evident. Plotting of the probability density functions in the manner portrayed by Figure 8 is useful for the optimal design of a mine beacon electromagnetic communications system, because the electromagnetic wave decays as a function of the wave number of the medium (Equation 1). If differing mining districts can be characterized by such probabilistic distributions (with regard to resistivity and electromagnetic noise), inasmuch as what may be optimal for communications in one mining district may not be optimal in another district.

For comparison, probability density plots of measured resistivity values of the overburden at Montour No. 4 mine, Peabody No. 10 mine, and Gary No. 14 mine are given in Figures 9, 10, and 11. All resistivity distributions appear unimodal in character; however, the spread in resistivity values measured at the Montour No. 4 mine is larger than that at the Imperial and Eagle mines and becomes even larger at the Gary No. 14 mine. On the other hand, the resistivity probability density plot for the Peabody No. 10 mine appears quite similar to that for the Imperial and Eagle mines. This comparison implies that electromagnetic transmissions through the earth, ambient noise and logistic factors being equal, would be less distorted by the resistivity distribution apparent at the Imperial and Eagle mines or at the Peabody No. 10 mine than by the resistivity distribution apparent at either the Montour No. 4 mine or the Gary No. 14 mine. Consequently, a theoretical model of a beacon source antenna immersed in an electrically and magnetically homogeneous halfspace (Wait, 1971d) would be applicable in mining provinces which have geoelectric sections similar to those measured at the Imperial and Eagle mines or the Peabody No. 10 mine and would yield insight into the behavior of electromagnetic transmissions. However, an analytic model applicable to a geoelectric section such as that encountered at the Gary No. 14 mine (Geyer and Keller, 1971a) would have to account not only for topography (Wait, 1971b), but also for the effect of electrical anisotropy and lateral inhomogeneities.

Overburden Electrical Conductivity Distribution at Montour No. 4 Coal Mine, Pennsylvania

Galvanic resistivity measurements of the geologic section collected over various profiles at the Montour No. 4 mine, Pennsylvania, are shown in section in Figures 12, 13, 14, 15, 16, 17, and 18. From the latter figures it is observed that a relatively homogeneous geoelectric section exists over the Montour No. 4 mine workings. Only along profiles P-P', P'-P'', A-A', A''-A''' are there suggestions of lateral inhomogeneities at depths beneath the surface ranging from 200 to 350 feet. It is noteworthy that all of these anomalous resistivities are high; at present no correlation has been made associating the resistivity highs with either the mine workings or perhaps resistive veins of subsurface coal. Since the average overburden conductivity at the Montour No. 4 mine is an order of magnitude lower than that measured at the Imperial and Eagle mines, an upper limit on the maximum operating frequency of a practical beacon electromagnetic system at the Montour No. 4 mine would be an order of magnitude higher than an upper limit for the same system in a mining province such as that

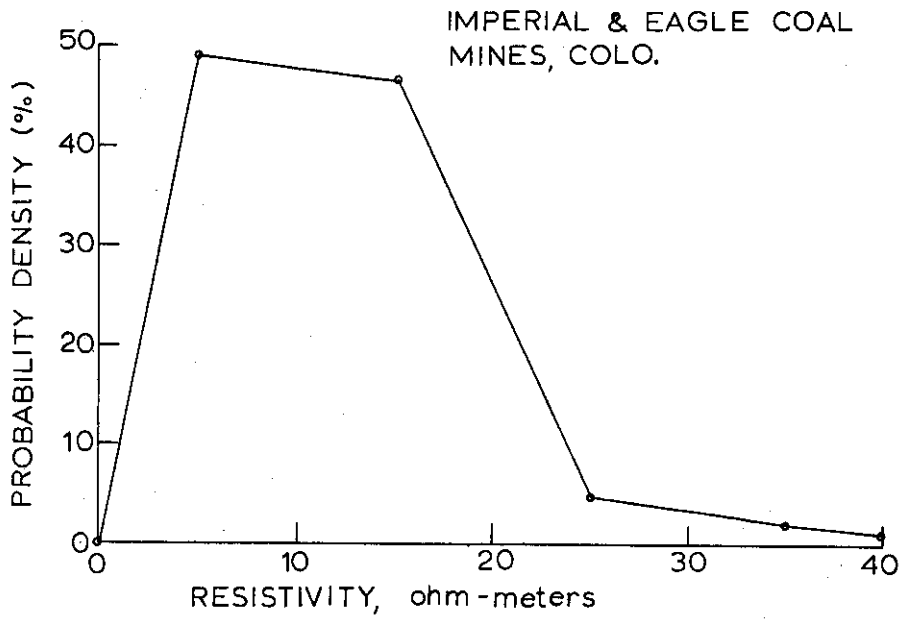
IMPERIAL & EAGLE COAL
MINES, COLO.
PROBABILITY DENSITY (%)
50
40
30
20
10
0
0
10
20
30
40
RESISTIVITY, ohm-meters

Fig. 8

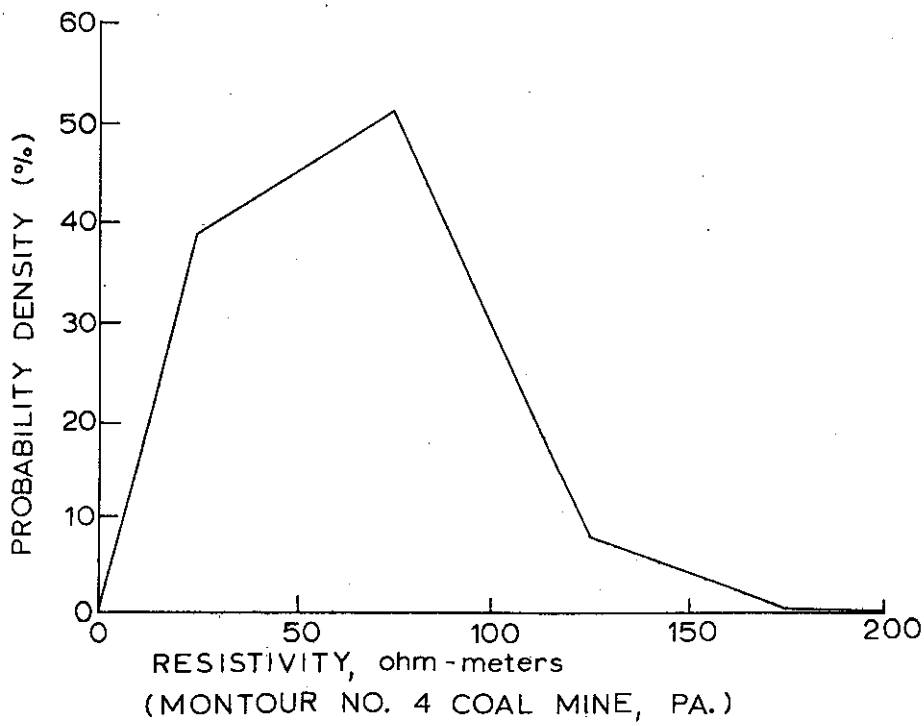
PROBABILITY DENSITY (%)
60
50
40
30
20
10
0
0
50
100
150
200
RESISTIVITY, ohm-meters
(MONTOUR NO. 4 COAL MINE, PA.)

Fig. 9

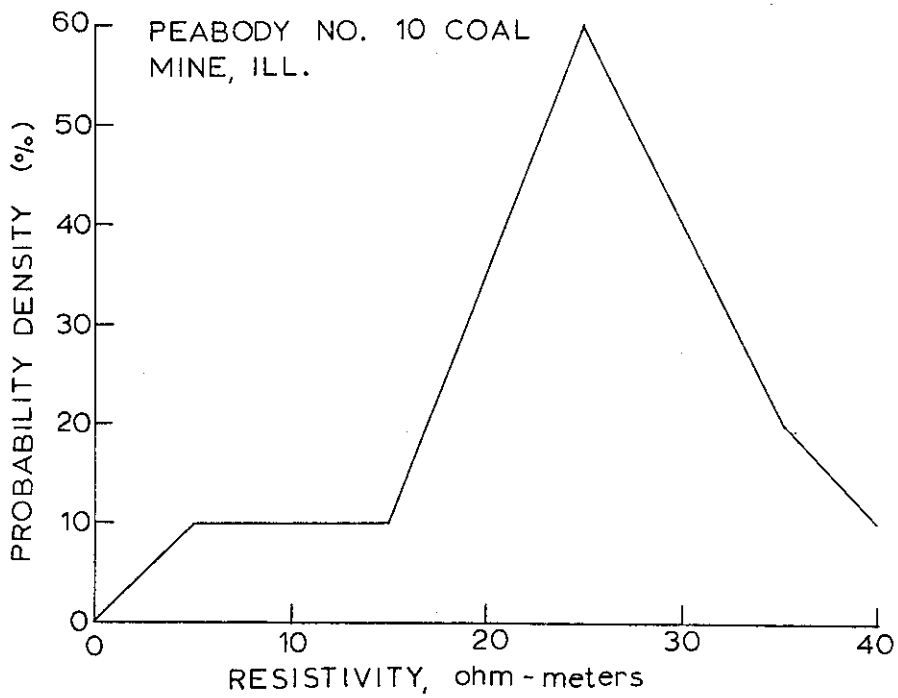
PEABODY NO. 10 COAL MINE, ILL.
PROBABILITY DENSITY (%)
60
50
40
30
20
10
0
0
10
20
30
40
RESISTIVITY, ohm - meters

Fig. 10

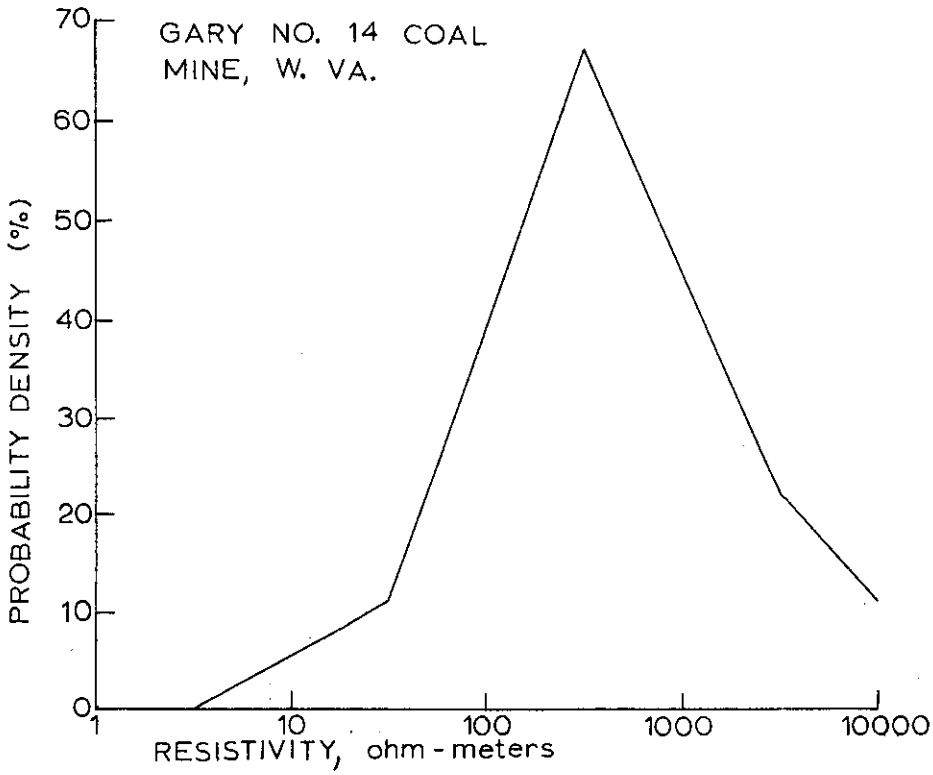
GARY NO. 14 COAL MINE, W. VA.
PROBABILITY DENSITY (%)
70
60
50
40
30
20
10
0
1
10
100
1000
10000
RESISTIVITY, ohm - meters

Fig. 11

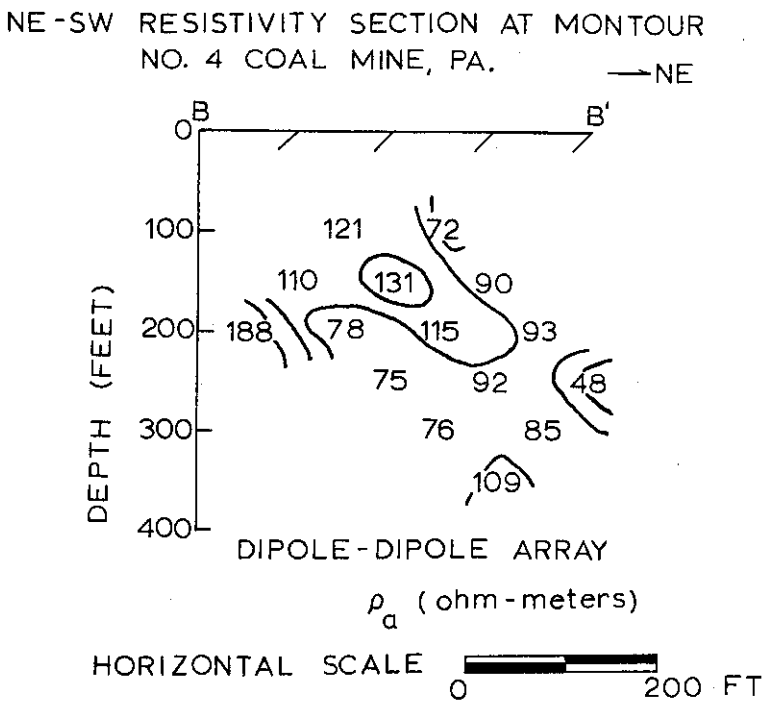
NE-SW RESISTIVITY SECTION AT MONTOUR
NO. 4 COAL MINE, PA.
NE
B
B'
0
100
200
300
400
DEPTH (FEET)
121
72
110
131
90
188
78
115
93
75
92
48
76
85
109
DIPOLE-DIPOLE ARRAY
ρ_a (ohm-meters)
HORIZONTAL SCALE
0
200 FT

Fig. 12

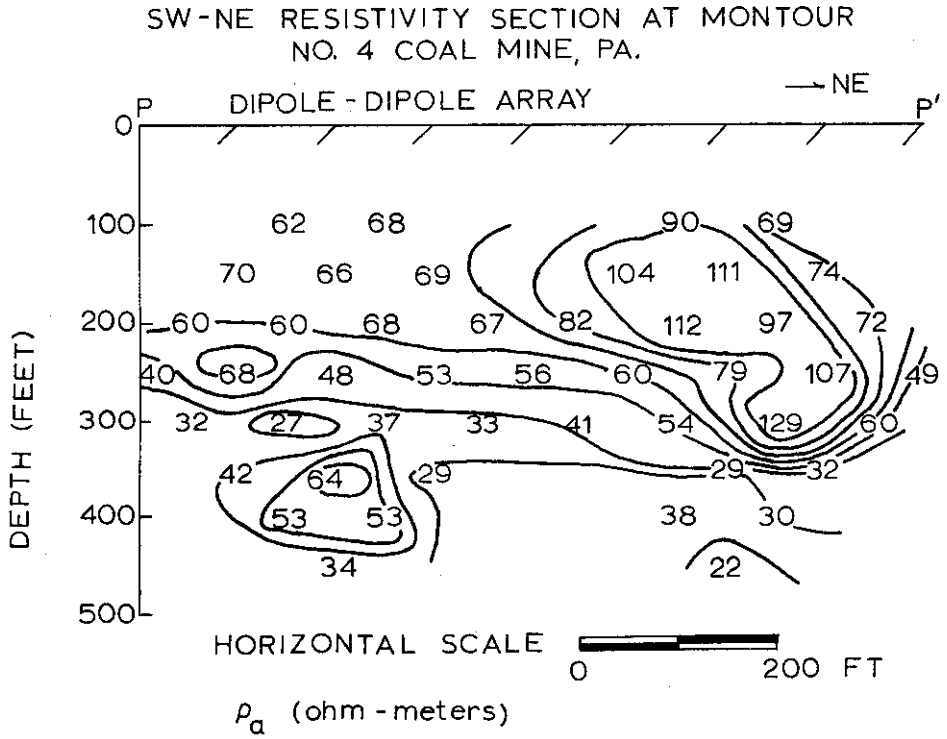
SW-NE RESISTIVITY SECTION AT MONTOUR
NO. 4 COAL MINE, PA.
NE
P
DIPOLE-DIPOLE ARRAY
P'
0
100
200
300
400
500
DEPTH (FEET)
62
68
90
69
70
66
69
104
111
74
60
60
68
67
82
112
97
72
40
68
48
53
56
60
79
107
49
32
27
37
33
41
54
129
60
42
64
29
29
32
53
53
38
30
34
22
HORIZONTAL SCALE
0
200 FT
ρ_a (ohm-meters)

Fig. 13

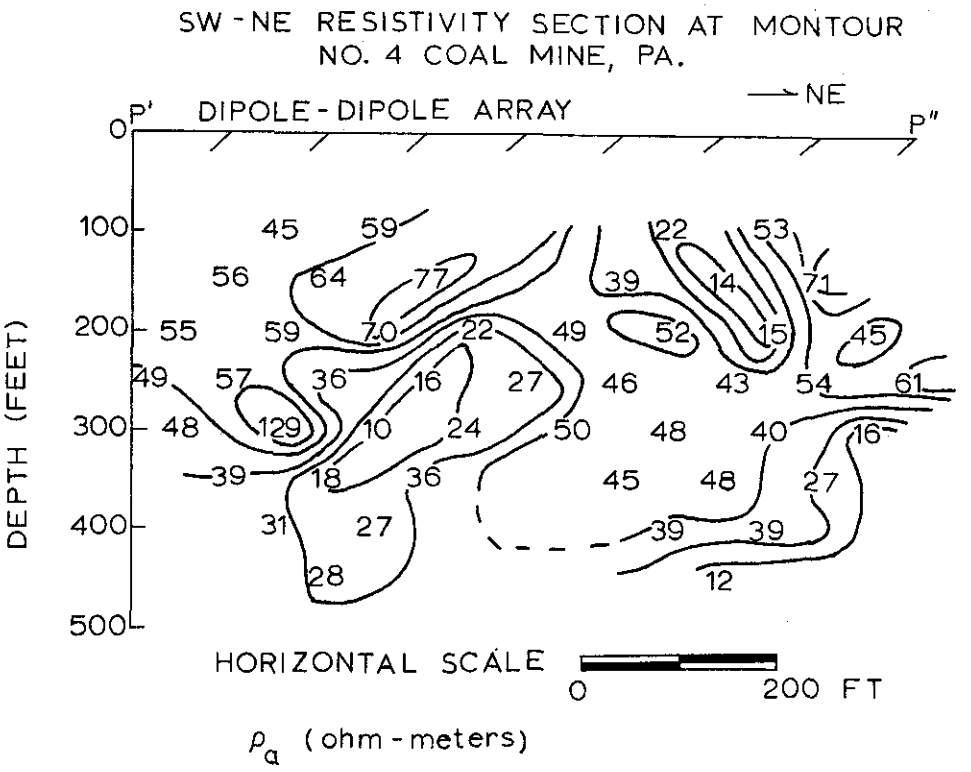
SW - NE RESISTIVITY SECTION AT MONTOUR
NO. 4 COAL MINE, PA.
NE
P' DIPOLE - DIPOLE ARRAY P"
DEPTH (FEET)
0
100
200
300
400
500
45 59 22 53
56 64 77 39 14 71
55 59 70 22 49 52 15 45
49 57 36 16 27 46 43 54 61
48 129 10 24 50 48 40 16
39 18 36 45 48 27
31 27 39 39
28 12
HORIZONTAL SCALE
0 200 FT
ρ_a (ohm - meters)

Fig. 14

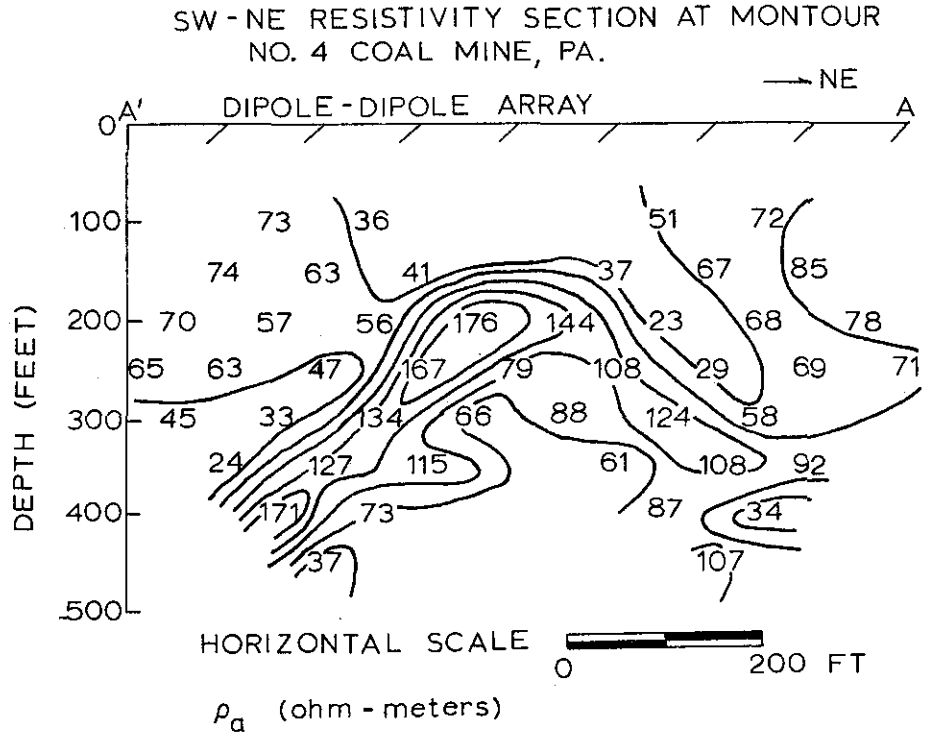
SW - NE RESISTIVITY SECTION AT MONTOUR
NO. 4 COAL MINE, PA.
NE
A' DIPOLE - DIPOLE ARRAY A
DEPTH (FEET)
0
100
200
300
400
500
73 36 51 72
74 63 41 37 67 85
70 57 56 176 144 23 68 78
65 63 47 167 79 108 29 69 71
45 33 134 66 88 124 58
24 127 115 61 108 92
171 73 87 34
37 107
HORIZONTAL SCALE
0 200 FT
ρ_a (ohm - meters)

Fig. 15

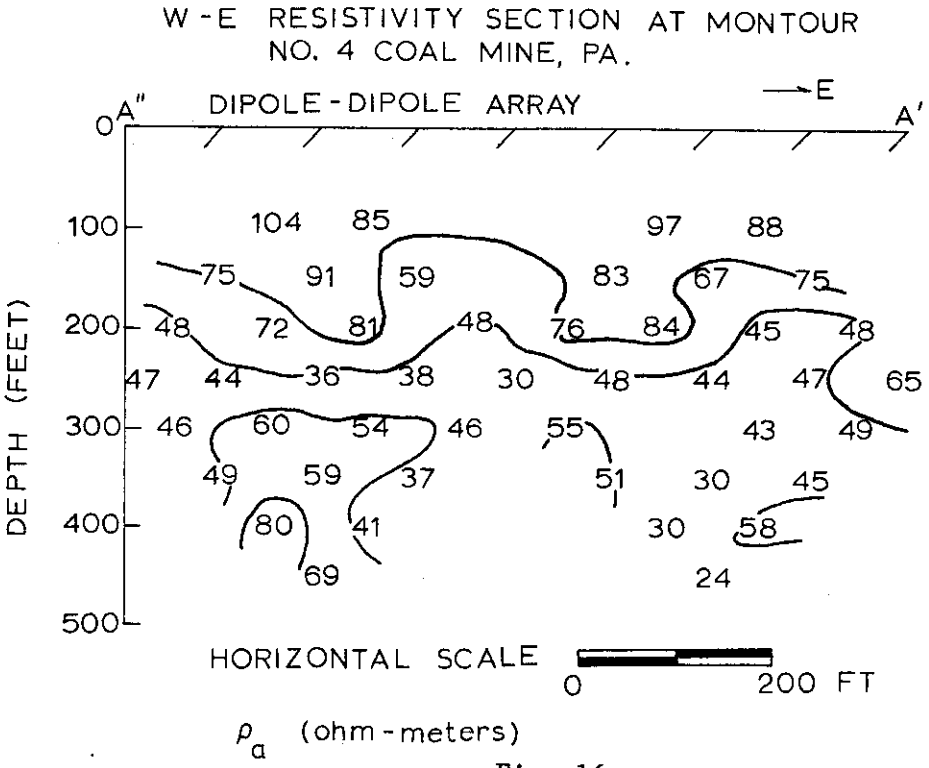
W - E RESISTIVITY SECTION AT MONTOUR
NO. 4 COAL MINE, PA.
DIPOLE - DIPOLE ARRAY
E
A"
A'
0
100
200
300
400
500
DEPTH (FEET)
104 85 97 88
75 91 59 83 67 75
48 72 81 48 76 84 45 48
47 44 36 38 30 48 44 47 65
46 60 54 46 55 43 49
49 59 37 51 30 45
80 41 30 58
69 24
HORIZONTAL SCALE
0
200 FT
ρ_a (ohm - meters)

Fig. 16

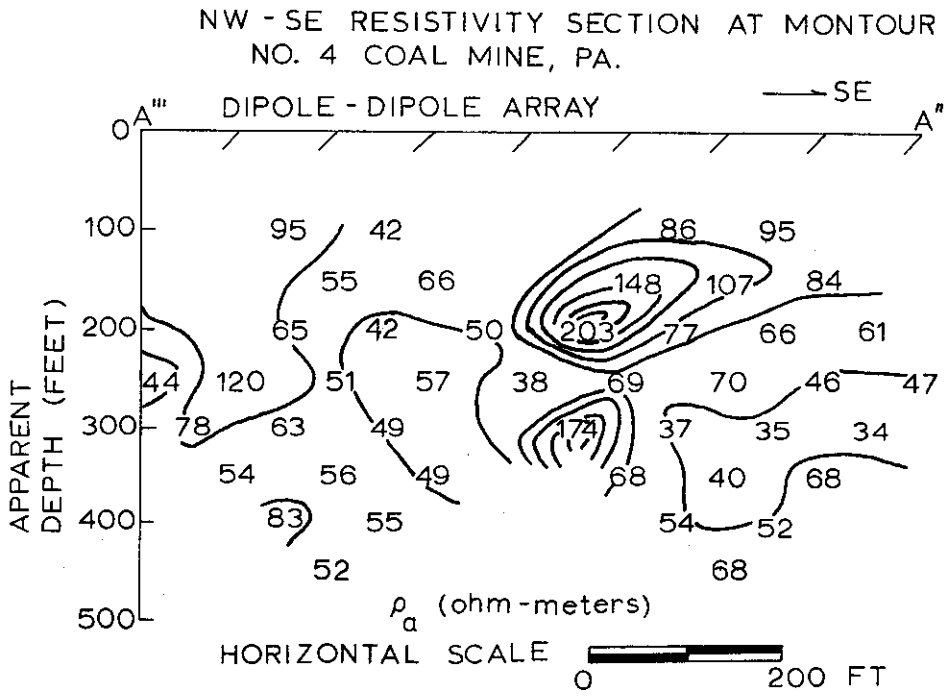
NW - SE RESISTIVITY SECTION AT MONTOUR
NO. 4 COAL MINE, PA.
DIPOLE - DIPOLE ARRAY
SE
A'''
A''
0
100
200
300
400
500
APPARENT DEPTH (FEET)
95 42 86 95
55 66 148 107 84
65 42 50 203 77 66 61
44 120 51 57 38 69 70 46 47
78 63 49 174 37 35 34
54 56 49 68 40 68
83 55 54 52
52 68
ρ_a (ohm - meters)
HORIZONTAL SCALE
0
200 FT

Fig. 17

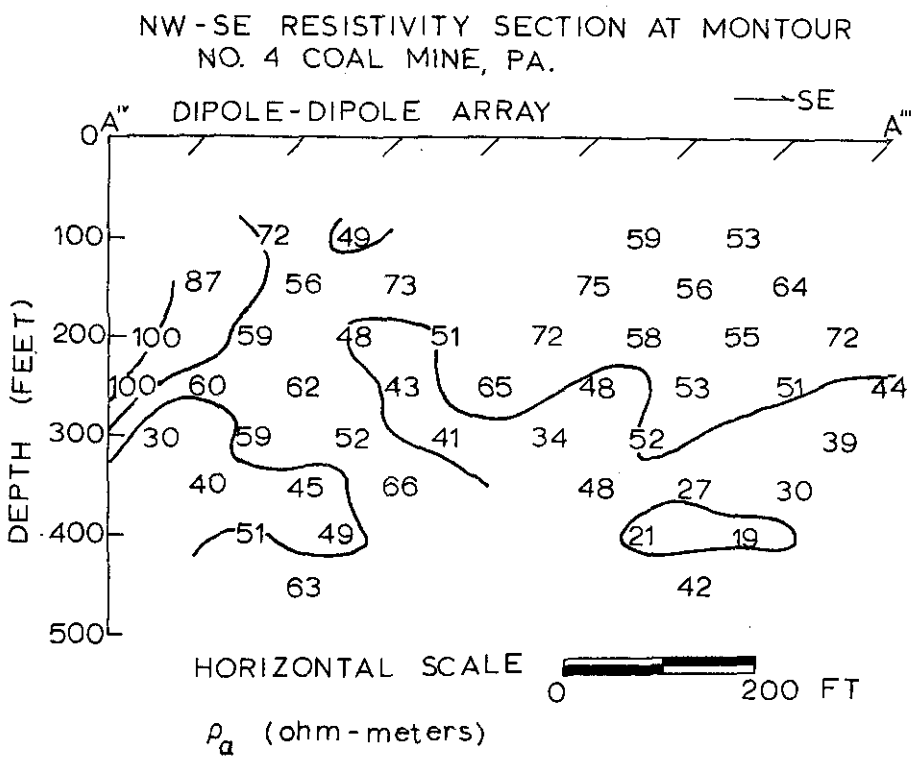
NW-SE RESISTIVITY SECTION AT MONTOUR
NO. 4 COAL MINE, PA.
DIPOLE-DIPOLE ARRAY
SE
A'' A'''
0
100
200
300
400
500
DEPTH (FEET)
72 49 59 53
87 56 73 75 56 64
100 59 48 51 72 58 55 72
100 60 62 43 65 48 53 51 44
30 59 52 41 34 52 39
40 45 66 48 27 30
51 49 21 19
63 42
HORIZONTAL SCALE
0 200 FT
ρ_a (ohm-meters)

Fig. 18

of the Imperial and Eagle mines, ambient noise, logistics, and through-the-earth communication distances being equal. In general, it is expected that the geologic regimen about other coal mines will be similar to that found in the experimental areas in which the geological character of the beds overlying a mine is simple. In other cases, where the character is more complex, it will probably be necessary to recognize the existence of several layers with different resistivities over a mine, and through which signals must propagate in an emergency communications system.

Inductive Method

Another surface-based approach for measuring the conductivity distribution of the overburden is that in which current is induced in the earth by a time-varying magnetic field with alternating current driven through a loop. The magnetic field of this induced current, which is affected by the resistivity distribution of the earth, is then measured with a second loop at some moderate distance away from the first. By varying the frequency at the source loop, variations of conductivity with depth may be ascertained, the lower frequencies sampling greater depths. One advantage to an inductive as opposed to a galvanic method is that the source and receiver positions may be kept fixed while the frequency is varied.

In dealing with such two-loop electromagnetic measurements it is convenient to use the concept of mutual impedances and ratios of mutual impedances. The mutual impedance Z between a source and a receiver is the ratio of the voltage induced in the receiver to the current I in the source. For two loops,

$$Z = V/I = -i\omega\mu NAH/I \tag{2}$$

where N is the number of turns of the receiving loop, A is the area of the receiving loop, and H is the magnetic field at the receiving loop. For two coplanar loops in free space separated by a distance R, the mutual coupling Z_o is, neglecting displacement currents,

$$Z_o = \frac{i\omega\mu_o N_1 N_2 A_1 A_2}{4\pi R^3} \tag{3}$$

where N_1 and N_2 are the number of turns on the loops, and A_1 and A_2 are the areas of the loops; Frischknecht (1967) gives the theoretical coupling ratio Z/Z_o for two horizontal coplanar loops at the surface of a two-layer earth (see Figure 19),

$$(Z/Z_o) = (Z/Z_o)' + B^3 T_o' \tag{4}$$

where $(Z/Z_o)'$ is the mutual coupling ratio for horizontal coplanar loops over a homogeneous earth given by (Wait, 1955),

$$(Z/Z_o)' = \frac{2}{\gamma^2 R^2}\{9-(9+9\gamma R + 4\gamma^2 R^2 + \gamma^3 R^3 e^{-\gamma R}\} \tag{5}$$

$\gamma^2 = i\omega\mu_o\sigma$, σ being the electrical conductivity in mhos per meter, μ_o the magnetic permeability of free space ($4\pi \times 10^{-7}$ henries/meter), and ω being the transmitter radian frequency. In the second term of (4),

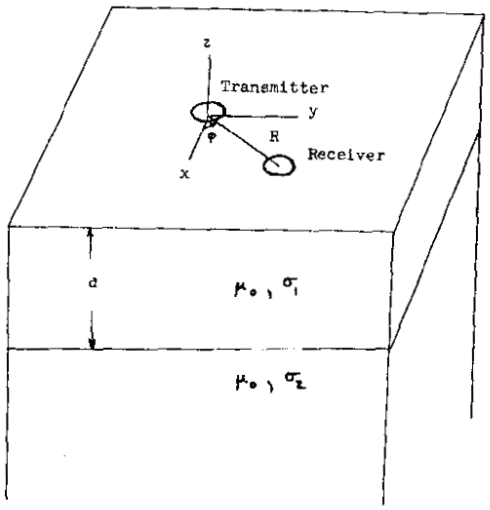

Fig. 19 Two horizontal coplanar loops at the surface of a two-layer earth.

$$T_o' = \int_o^\infty \tilde{R}(D_1 g) g^2 J_o(gB)\,dg - \int_o^\infty \tilde{R}(\infty_1 g) g^2 J_o(gB)\,dg \qquad (6)$$

where

$$\tilde{R}(D_1 g) = 1 - 2g \frac{(U+V) + (U-V)e^{-UD}}{(U+g)(U+V) - (U-g)(U-V)e^{-UD}}$$

$$U = (g^2 + 2i)^{\frac{1}{2}}$$

$$V = (g^2 + 2ik)^{\frac{1}{2}}$$

$$k = \sigma_2/\sigma_1$$

$$B = R/\delta$$

$$D = 2d/\delta$$

$$\delta = (2/\sigma_1 \mu_o \omega)^{\frac{1}{2}}$$

and J_o is the Bessel function of the first kind and of order zero. Frischknecht (1967) then evaluates both the amplitude and phase of the mutual coupling ratio Z/Z_o as a function of B for a number of k and D/B values.

Simple curve-matching techniques utilizing Frischknecht's reference curves may be used to interpret Z/Z_o sounding curves made over a two-layer earth. The procedure is to plot the field data (after correction for the calibration response of the receiver-amplifier system) on transparent bilogarithmic paper with $f^{\frac{1}{2}}$ along the abscissa. The field data are then superimposed on the appropriate set of reference curves and shifted about, keeping the axes of the two sets of curves parallel until the best possible match is found. Once a suitable match has been found, the conductivity and thickness of the upper layer as well as the conductivity of the substratum are determined.

Several electromagnetic depth soundings were made at the Imperial and Eagle coal mines in central Colorado using horizontal coplanar loops situated at the surface and separated by 1000 feet. The results of these soundings are portrayed in Figures 20 and 21; they generally show good agreement with galvanic resistivity data with the average resistivity of the first modeled layer being 20 ohm-meters and that of the second layer 65 ohm-meters. The determined thickness of the first of the two-layer earth model, about 80 meters, corresponds roughly to the present depths of the mine workings in this region.

ELECTROMAGNETIC COUPLING FOR
HORIZONTAL COPLANAR LOOPS

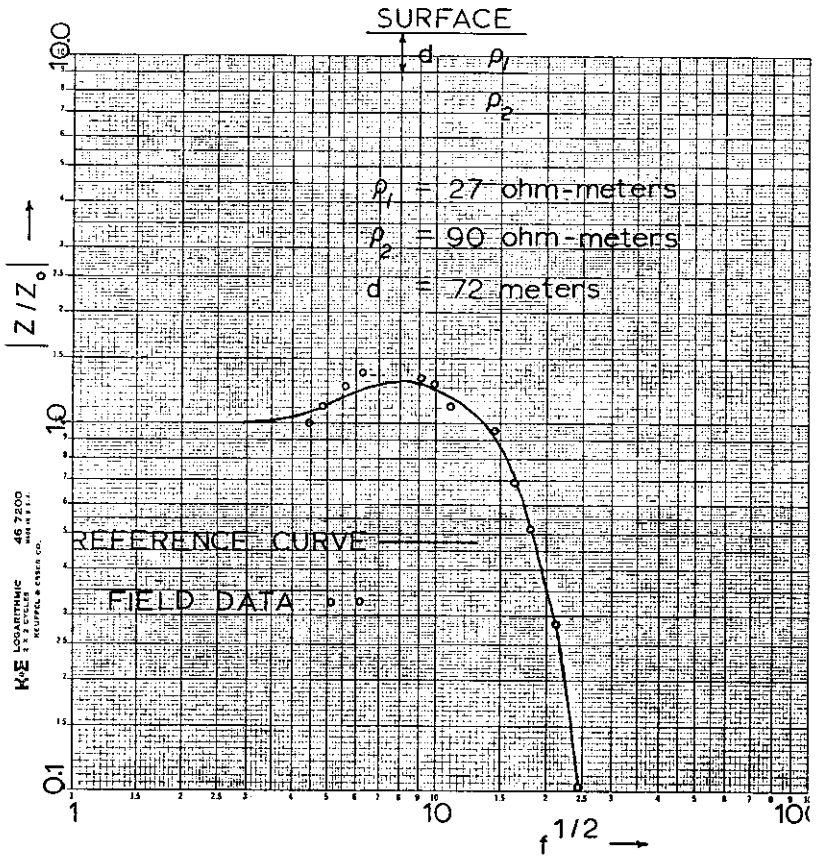

INTERPRETATION OF SOUNDING NO. 1 FROM
IMPERIAL MINE, COLORADO

Fig. 20

ELECTROMAGNETIC COUPLING FOR
HORIZONTAL COPLANAR LOOPS

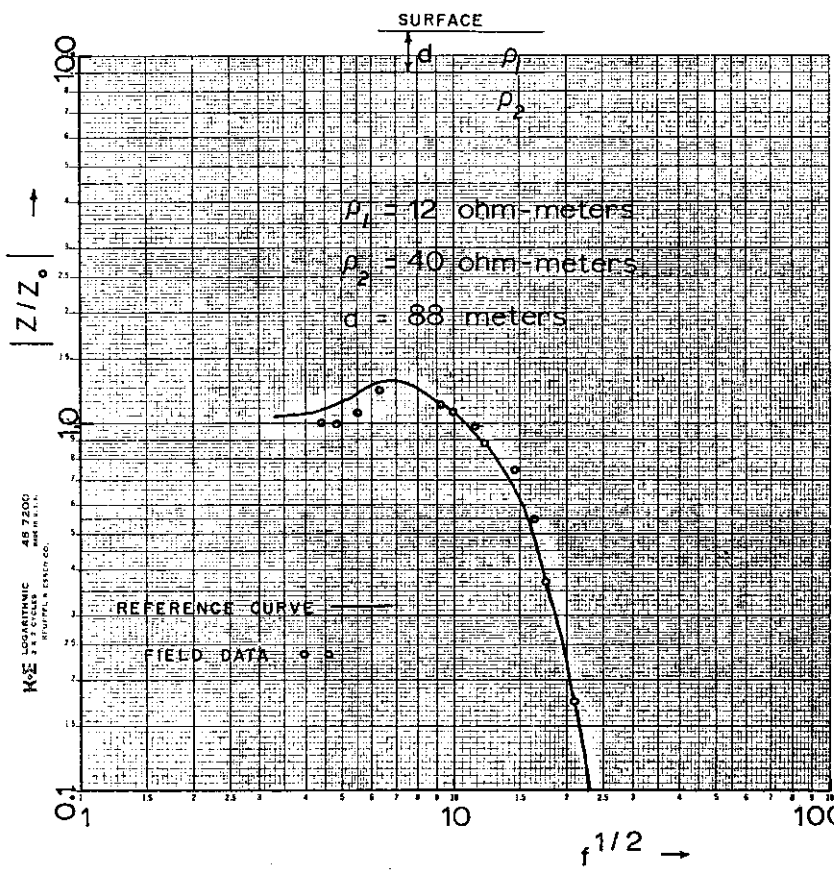

INTERPRETATION OF SOUNDING NO. 2 FROM IMPERIAL MINE,
COLORADO

Fig. 21

NOISE ENVIRONMENT STUDIES

The second main line of effort with respect to research related to the development of an emergency mine communications system has been the development of a technique for characterizing the noise environment at a mine. Such information may be used to specify the minimum source strength required for a communications system and the receiver sensitivity that is useful. In practice, it will probably be found that the upper limit on transmitter strength will be determined by the weight allowed in the source, whereas the maximum receiver sensitivity will be dictated by the ambient noise field levels.

The optimal design of a beacon electromagnetic communications system for use in emergency situations after a mine disaster requires statistical information of ambient electromagnetic noise levels and of the resistivity distribution of rocks overlying coal measures. Analysis of the electromagnetic background noise is important, for it is against this noise background that the transmitting beacon signal must be recognized at the earth's surface. In order to analyze electromagnetic noise statistics, an 8-K Nova 4001 mini-computer (16 bit resolution) combined with an 8 channel analog-to-digital converter (13 bit resolution), multiplexing unit, and teletype for I/O handling was installed in a Dodge A-100 van. A block schematic of the field computer system is shown in Figure 22.

The conventional approach to characterization of noise is through the use of power-density spectrums in which the average level of the noise field over some long term is determined at a series of frequencies. For the present study, the choice was made to use amplitude histograms over relatively broad frequency bands to characterize the noise. In so doing, the signal from an electric field sensor or a magnetic field sensor is first passed through a filter which rejects strongly below some lower frequency limit and above some upper frequency limit. Then, within these frequency bands, the percentage of time the noise from the sensors exceeds specified levels is determined.

The advantage of the noise histogram approach is that it provides information on the design of a high-sensitivity receiver system which is not readily obtainable in the spectral approach. For example, different approaches would have to be used for noise rejection in the case in which the noise amplitude is relatively uniform in time than in the case in which it is impulsive, varying widely with time. In the first case, optimum noise rejection would be obtained by setting a threshold for signal detection just above the noise level. In the second case optimum noise rejection would be obtained by using redundant transmissions, and detecting the signal during quiet periods.

Amplitude density studies of ambient electric and magnetic noise have been made at the Gary No. 14 mine, West Virginia, the Peabody No. 10 mine, Illinois, and at the Imperial and Eagle mines, Colorado. Hourly measurements were made over 8 frequency bands during the course of 24 hours, and for each frequency band, 10,000 samples were taken.

Measurements of the horizontal electric field background noise become important when measurements of electric field beacon signals are used for communication. Similarly, if measurements of wave tilt of the magnetic field are used for location purposes, it will be quite useful to know what percent of the

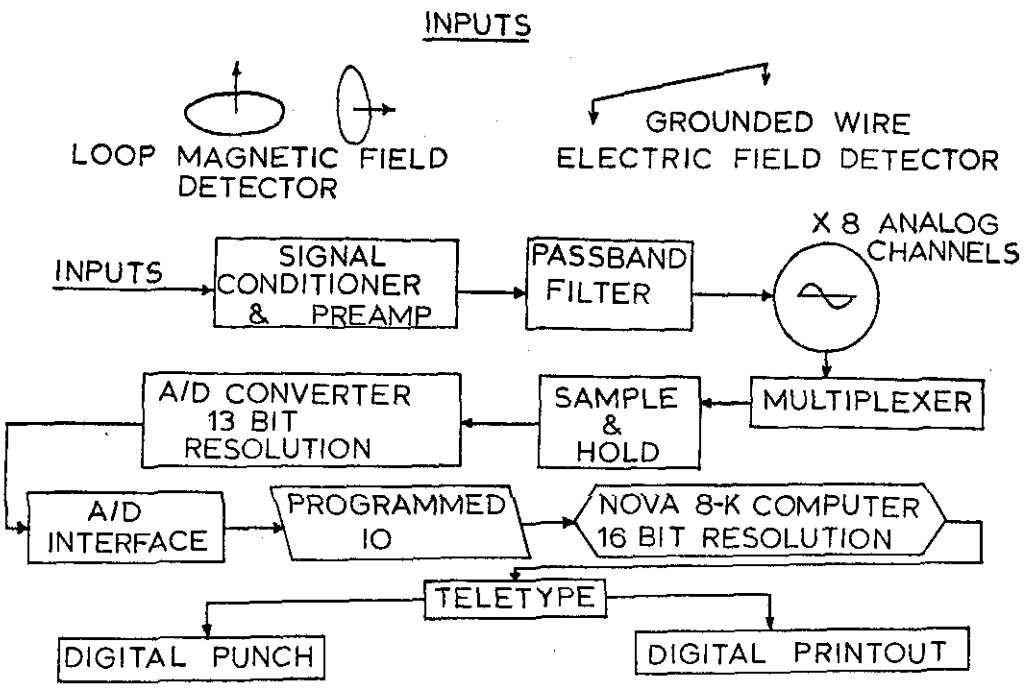

Fig. 22 Block schematic of field computer system.

time certain background magnetic field noise levels are exceeded.

At both the Gary No. 14 mine and the Peabody No. 10 mine measurements were taken at the surface directly above a working face. At the Imperial and Eagle mines measurements were taken about 1200 feet north of a working face. Only surface-based measurements were taken; thus the results described here are applicable for the design of an uplink electromagnetic transmission system.

Gary No. 14 Coal Mine, West Virginia

Ambient surface electromagnetic noise measurements were made at the Gary No. 14 mine approximately 754 feet directly above a working face. The Gary No. 14 mine has a daily capacity of about 6,500 tons and is a D.C. faced mine. Amplitude probability density plots of the surface vertical magnetic field noise and horizontal electric field noise are given in Appendix A (see Figures A-1 through A-16), a typical example of which is shown in Figure 23. Each plot consists of 6 graphs, each of which, in turn, comprise 10,000 data points. The time of day is indicated on each graph, and, for purposes of illustration, only every fourth hour is plotted.

An immediate observation drawn from Figures A-1 through A-16 is that the maximum percent of events ranges from 30 to 55. In addition, it is markedly apparent that there is much more variance of ambient electromagnetic noise with frequency than with time of day. This is an important observation, for it indicates that one may design, in general, his transmitting antenna around the parameter of frequency, irrespective of time of day. Examples of how such summary electromagnetic noise measurements, together with electrical properties studies and knowledge of low-frequency coupling behavior between various source antenna-receiver configurations, may be used for the practical implementation of a beacon electromagnetic communication system will follow shortly.

Peabody No. 10 Coal Mine, Illinois

Ambient surface electromagnetic noise measurements were made at the Peabody No. 10 mine approximately 354 feet directly above a working face. The Peabody No. 10 mine has a daily capacity of about 15,500 tons and is an A.C. faced mine. Amplitude probability density plots of the surface vertical magnetic field noise and horizontal electric field noise are given in Appendix B (See Figures B-1 through B-16). These amplitude probability density plots demonstrate little change of the maximum percent noise with time of day and clearly show the magnitudes of the higher noise levels at the lower frequencies. A 1:5:1 variance is seen at around 2200 and 800 hours, however, which may be attributable to shift changes within the mine. This variance is only apparent at frequencies less than 1000 Hz.

Imperial and Eagle Mines, Colorado

Ambient surface electromagnetic noise measurements were made midway between the nonoperating Imperial mine and the operating Eagle mine approximately 300 feet above a working face but considerably offset ($\sim$1000 feet) from the working face. The Eagle mine has a daily production of about 1800 tons and uses both 440 V.A.C. and 250 V.D.C. Amplitude probability density plots of the surface vertical magnetic field noise and horizontal electric field noise are given in

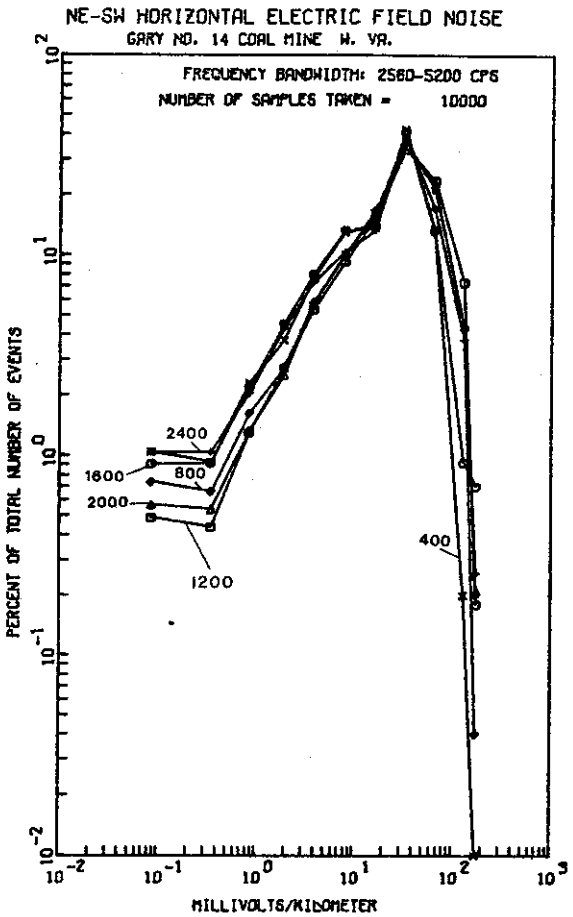
NE-SW HORIZONTAL ELECTRIC FIELD NOISE
GARY NO. 14 COAL MINE W. VA.
FREQUENCY BANDWIDTH: 2560-5200 CPS
NUMBER OF SAMPLES TAKEN = 10000
PERCENT OF TOTAL NUMBER OF EVENTS
MILLIVOLTS/KILOMETER
2400
1600
800
2000
1200
400

Fig. 23

Appendix C (see Figures C-1 through C-16).

From the plots of electric field noise, it is observed that for the 20-80 cps bandwidth, 40% of the total number of events from 10,000 samples (samples were taken with the sampling time chosen such that the aliased frequency was above the upper limit of the frequency of concern) had amplitudes of 1 to 2 millivolts per kilometer, 12% of the total number of events had amplitudes between 2 and 3 millivolts per kilometer and less than 0.1% of all events had magnitudes close to 10 millivolts per kilometer. For higher frequency ranges up to 5200 cps a broadening of the spectrum occurs for events of magnitude less than 1 millivolt per kilometer. Thus, for example, in the frequency range of 320-640 cps, more than 85% of all events had amplitudes less than 1 millivolt per kilometer. For electric field noise frequencies above 5000 cps, however, a distinct narrowing of the spectrum again occurs with approximately 52% of all measured events having magnitudes in excess of 2 millivolts per kilometer.

From the vertical magnetic field amplitude histogram plots, on the other hand, it is observed that for the 20-80 cps frequency range, most of the events occurring have magnitudes of 5 gammas per second (actually, the histograms are for the time derivative of the magnetic field, for which any induction coil receiving sensor will be sensitive) or greater; i.e., over 70% of all events have amplitudes of at least 5 gammas per second. For frequencies greater than 80 cps two phenomena are apparent. The first is similar to that observed for the N-S component of the horizontal electric field; namely, that of a broadening of the spectrum of the number of events occurring over a larger domain of amplitudes. For example, in the 640-1280 cps bandwidth 80% of all the measured events have magnitudes between 2.5×10^{-2} gammas per second and 6×10^{-1} gammas per second as opposed to only 49% of all measured events over the same amplitude range for the 160-320 cps bandwidth. The second phenomenon to be noted is a shift in the maximum percent of the total number of events to an order of magnitude lesser amplitude; i.e., the maximum percent of the total number of events in the 20-80 cps frequency bandwidth is on the order of 10 gammas per second, whereas the maximum percent for the 5200-10,400 cps frequency bandwidth is on the order of 1 gamma per second.

In summary, the amplitude histogram plots of both the horizontal electric field and vertical magnetic field noise events illustrate more change with frequency (100:1 for frequencies ranging from 1000 Hz to 40 Hz) than with time of day. The maximum percent of the horizontal electric field noise does display some variance with time of day at frequencies above 200 Hz; however, the magnitudes of the events occurring with greatest probability are so small that they do not seem to represent any communications problem, even at very low frequencies.

Because of the surface offset distance relative to the working face at the Eagle mine, the summary noise tabulations do not represent the "worst-type" noise environment in this case. They do give information on ambient noise background levels for communications purposes at a considerable distance away from a working face, however.

APPLICATION OF FIELD STUDIES

Vertical-Axis Loop Transmitter

As an example of how Appendices A, B, and C, together with measured resistivity values, might be used for the practical implementation of a beacon electromagnetic communications system in which the transmitter is a buried vertical magnetic dipole, consider the following. Suppose it is desired to communicate from a mine working to the surface where the overburden has a thickness of 250 meters and a mean resistivity of 20 ohm-meters. A frequency which would give adequate penetration to the surface may be determined by the relation,

$$f = \rho/\pi\mu d^2 \tag{7}$$

where ρ is the resistivity in ohm-meters, μ the magnetic permeability in henries/meter (approximately equal to $4\pi \times 10^{-7}$ henries/meter), and d the depth in meters to the mine working. As Wait (personal communication) notes, equation (7), which is based on the attenuation of a plane wave in a conducting medium, gives an overly pessimistic upper limit for an operating frequency; however, such a frequency would be adequate provided a communications system is designed around noise constraints and the overburden resistivity distribution.

With the above parameter values,

$$f = \frac{20}{3.14 \cdot 12.56 \cdot 10^{-7} \cdot 250^2}$$

$$\cong 80 \text{ Hz}$$

Let the operating frequency, then, be 80 Hz and assume that the turns-area of the receiving coil is 1000 square meters (this is typical of geophysical-type coil receivers operating at this frequency). Impose a design constraint on the dipole transmitter-receiver system that the signal-to-noise ratio at the surface directly over the transmitter be 3:1. The question then becomes: what must the source transmitter moment be in order to ensure signal levels which are 10 db above ambient noise levels most of the time. Suppose the noise statistics are similar to those measured at the Imperial and Eagle coal mines, Colorado. Then, from Figure C-1, it is noted that 70% of the vertical magnetic field noise levels (actually the time derivative of the magnetic field, to which an induction coil is sensitive) at the surface range between 3 gammas per second and 10 gammas per second (2.4×10^{-3} amp-turns per meter-second and 8×10^{-3} amp-turns per meter-second) and appear relatively independent of time of day.

Now the e.m.f. induced in a loop receiver at the earth's surface due to a time-varying magnetic field is given by

$$V_{\text{Receiver}} = 8 \cdot 10^{-4} \mu \left(\frac{\Delta H}{\Delta t}\right)_{\text{Receiver}} \{\text{Effective Area}\}_{\text{Receiver}} \tag{8}$$

where V_{Receiver} is the induced e.m.f. in volts, $\Delta H/\Delta t$ is the time rate of change

in the magnetic field in gammas/second, and the effective area of the receiver is given in square meters. Therefore, the probability is 70% that the e.m.f. induced in the receiving loop just from noise at the surface will be

$$V_{Receiver} = 8 \times 10^{-4} \cdot 12.56 \cdot 10^{-7} \cdot 10 \cdot 10^{3}$$

$$= 10^{-5} \text{ volts}$$

that is, noise background will probably generate 10μv in the receiving coil at 80 Hz for a coal mining province whose noise statistics are similar to those at Eagle and Imperial mines. Since a signal level is desired which is at least 10 db above this noise background, transmitter signal strengths must be about 30 μv at the receiver. Now, for sufficiently low frequencies, the moment of the underground coil transmitter is related to the voltage seen at the surface receiver loop placed immediately above the transmitter by

$$M = h^{3}V/(\{\text{Effective Area}\}_{Receiver} f \cdot 12.56 \cdot 10^{-7}) \qquad (9)$$

where h is the depth in meters to the transmitter coil from a receiver loop placed immediately over the transmitter, f is the transmitting frequency in Hz, V is the signal voltage desired at the receiver, and M is the required source moment of the transmitter. For signal strengths of 30μv directly above the transmitter as seen with a receiver loop with an effective area of 1000 square meters, the moment required at 80 Hz would be

$$M = 250^{3} \cdot 3.0 \cdot 10^{-5}/(10^{3} \cdot 8.0 \cdot 10 \cdot 12.56 \cdot 10^{-7})$$

$$= 4.68 \times 10^{3} \text{ ampere-m}^{2}$$

This source moment could be obtained by a coil which consists of 290 turns of wire and which is laid out in a loop with dimensions of 2.0 meters by 2.0 meters (to conform to the shape of a mine opening). A current of 4 amperes would then be required to provide this moment.

This example was chosen to illustrate the manner in which resistivity data may be used with ambient electromagnetic noise data for a specific communications application (using a loop source antenna and a loop receiving antenna) in a mine. For the above example, the required source moment could be decreased by increasing the effective area of the receiving sensor.

Grounded Horizontal Electric Line Transmitter

At this point it would be appropriate to consider how horizontal electric field noise amplitude probability density plots may be used in the systems engineering design of an alternative underground antenna. An alternative underground antenna might be an insulated piece of wire which is grounded at distant ends (in which use of rails or possibly telephone lines within a mine working might be made). Such a system is shown in Figure 24.

The current "bipole" transmitting antenna could be tied into roof bolts at A and B with a typical separation, L, say on the order of 10 meters. Or the line source antenna in the mine could simply be tied into two grounded electrodes at A and B.

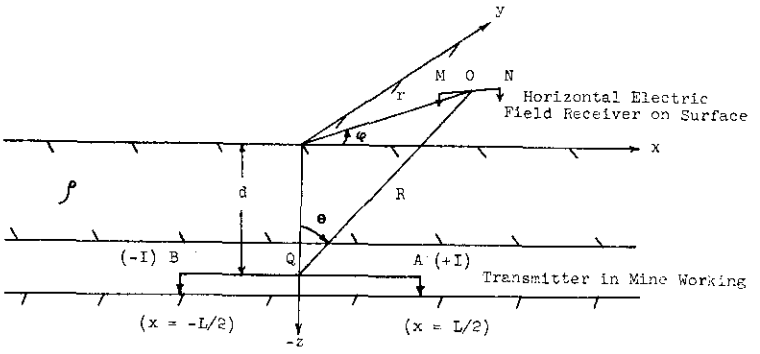

Fig. 24 Three-dimensional configuration of a line source antenna in a mine working and an arbitrarily located surface horizontal electric-field sensing receiver. Q is the midpoint of the current bipole, and O is the midpoint of the measuring dipole on the surface. The distance $\overline{MN}$ is sufficiently small such that the potential difference across $\overline{MN}$ is a good measure of the electric field at the point O. $r = (x^2 + y^2)^{\frac{1}{2}}$; $R = (x^2 + y^2 + d^2)^{\frac{1}{2}}$. The electrical resistivity of the overburden is denoted by ρ.

In most mining provinces the distance $\overline{AB}$ will be considerably smaller than the separation distance R between the midpoints of the buried transmitter and surface receiver (since a practical value of d is usually on the order of 100m). In this case we shall examine the static voltage response at the receiver point 0 since it is largest for this antenna-receiver configuration and since it will afford us immediate insight into the behavior of extremely low frequency electric fields around a buried horizontal electric line beacon transmitter. Thus, let us first consider the potential (voltage) that would be measurable at 0 due to a buried line source antenna of length L by which current of strength I is put into ground of resistivity ρ. For mathematical convenience we have oriented our reference coordinate system such that the x-axis is in the same direction as the transmitting antenna.

The potential at 0 due to the current element AB is given by

$$V = \frac{I\rho}{2\pi}\left\{\frac{1}{\overline{AO}} - \frac{1}{\overline{BO}}\right\} \tag{10}$$

where

$$\overline{AO} = \{r^2+(L/2)^2 - 2r(L/2)\cos\phi + d^2\}^{\frac{1}{2}}$$

$$\overline{BO} = \{r^2+(L/2)^2 + 2r(L/2)\cos\phi + d^2\}^{\frac{1}{2}}$$

so that

$$V(r,\phi) = \frac{I\rho}{2\pi}\left\{\frac{1}{(r^2 + (L/2)^2 - 2r(L/2)\cos\phi + d^2)^{\frac{1}{2}}} - \frac{1}{(r^2 + (L/2)^2 + 2r(L/2)\cos\phi + d^2)^{\frac{1}{2}}}\right\}$$

or

$$V(r,\phi) = \frac{I\rho}{2\pi r}\{(1+(L/2r)^2 - L\cos\phi/r + (d/r)^2)^{-\frac{1}{2}} - (1+(L/2r)^2 + L\cos\phi/r + (d/r)^2)^{-\frac{1}{2}}\}$$

Consider now the various bipole-bipole arrangements as shown in plan view in Figure 25. The two configurations which are relevant to the mine communications problem are the parallel and perpendicular, i.e.,

$$E_x(x,y;d) = -\frac{I\rho}{2\pi}\frac{\partial}{\partial x}\left\{\frac{1}{(x^2+y^2+L^2/4-Lx+d^2)^{\frac{1}{2}}} - \frac{1}{(x^2+y^2+L^2/4+Lx+d^2)^{\frac{1}{2}}}\right\}$$

$$E_x(x,y;d) = \frac{I\rho}{4\pi r^3}\left\{\frac{2x - L}{(1+(L/2r)^2-Lx/r^2+(d/r)^2)^{3/2}} - \frac{2x + L}{(1+(L/2r)^2+Lx/r^2+(d/r)^2)^{3/2}}\right\}$$

or

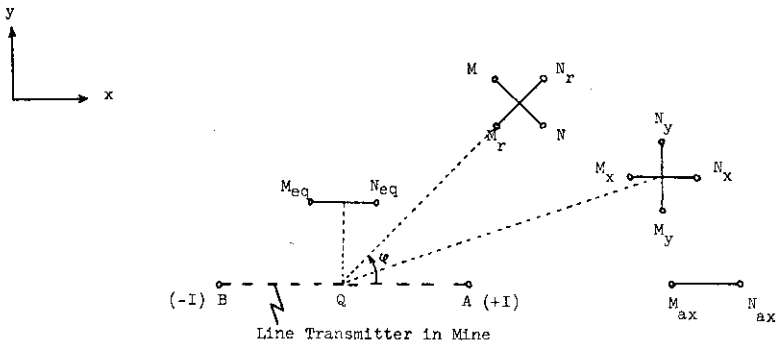

Fig. 25 Various buried transmitter and surface receiver configurations shown in plan view.

$M_{ax}\ N_{ax}$ ~ axial configuration

$M_x\ N_x$ ~ parallel configuration

$M_y\ N_y$ ~ perpendicular configuration

$M_r\ N_r$ ~ radial configuration

$M_\varphi\ N_\varphi$ ~ azimuthal configuration

$M_{eq}N_{eq}$ ~ equatorial configuration

$$V_{\substack{\text{Receiver,}\\ \text{Parallel}}}(x,y;d) = \frac{I\rho\ell L}{4\pi d^3}\left\{\frac{2x/L - 1}{(1+(r/d)^2+(L/2d)^2-Lx/d^2)^{3/2}} - \frac{2x/L + 1}{(1+(r/d)^2+(L/2d)^2+Lx/d^2)^{3/2}}\right\}$$

PARALLEL CONFIGURATION (11)

where ℓ is the length of the receiving electric field sensor. We note that for $\phi = 0$,

$$V_{\substack{\text{Receiver,}\\ \text{Parallel}}}(x,o;d) = \frac{I\rho\ell L}{4\pi d^3}\left\{\frac{2x/L - 1}{(1+(x/d -L/2d)^2)^{3/2}} - \frac{2x/L + 1}{(1+(x/d +L/2d)^2)^{3/2}}\right\}$$

AXIAL CONFIGURATION (12)

We also note that for $\phi = \pi/2$,

$$V_{\substack{\text{Receiver,}\\ \text{Parallel}}}(o,y;d) = \frac{I\rho\ell L}{2\pi d^3}\ \frac{1}{(1+(y/d)^2+(L/2d)^2)^{3/2}}$$

EQUATORIAL CONFIGURATION (13)

Similarly,

$$E_y(x,y;d) = -\frac{I\rho}{2\pi}\frac{\partial}{\partial y}\left\{(x^2+y^2+(L/2)^2-Lx+d^2)^{-\frac{1}{2}} - (x^2+y^2+(L/2)^2+Lx+d^2)^{-\frac{1}{2}}\right\}$$

so that

$$V_{\substack{\text{Receiver,}\\ \text{Perpendicular}}}(x,y;d) = \frac{I\rho\ell y}{2\pi d^3}\left\{\frac{1}{(1+(r/d)^2+(L/2d)^2-Lx/d^2)^{3/2}} - \frac{1}{(1+(r/d)^2+(L/2d)^2+Lx/d^2)^{3/2}}\right\}$$

PERPENDICULAR CONFIGURATION (14)

We observe that <u>when x = 0 or when y = 0 we are along null lines for the perpendicular electric field, a phenomenon which could be used for location purposes</u>!

Let us now consider another example in systems design in which an electrical field is generated underground by passing current through a wire of length L. The voltage measured at the surface of the earth (in the <u>axial configuration</u>) arising from this wire can then be calculated from formula (12) where ρ is the resistivity of the overburden and x is the horizontal offset of the receiver from the transmitter site (in the axial direction of the transmitter). When the receiver is directly above the buried line transmitter ($x = 0$) the magnitude of the received voltage is

$$\left|V_{\text{Receiver}}\right| = \frac{\rho I L \ell}{2\pi d^3} \frac{1}{(1 + L^2/4d^2)^{3/2}} \tag{15}$$

Suppose now that it is desired to communicate from a mine working to the surface where the overburden has a thickness of about 100 meters and an average resistivity of 24 ohm-meters; i.e., the same parameter problem as that at Peabody No. 10 coal mine, Illinois. A frequency which would give adequate penetration to the surface may be determined by equation (7) so that an operating frequency of

$$f = 24/(3.14 \cdot 12.56 \cdot 10^{-7} \cdot 10^{4}) \simeq 610 \text{ Hz}$$

may be taken. It should be noted at this juncture that we are already in violation of the assumed static behavior of the electric field, upon which formulas (10) through (14) are based, when we choose an operating frequency of 610 Hz (ELF region). It would still be useful, however, to proceed with the static derivations to illustrate how one may gain ready insight into design parameters.

Assume the length of the surface wire receiver is about 10 meters, and impose a design constraint on the buried line transmitter-receiver system that the signal levels at the surface directly above the transmitting line are 10 db greater than maximum ambient noise levels. The question then becomes: what must the source transmitter moment (product of current, I, and length L) be in order to ensure a signal-to-noise ratio of 3:1 at the surface directly above the transmitting antenna most of the time? Suppose also that the noise statistics for the horizontal electric field are similar to those measured at the Peabody No. 10 coal mine, Illinois. Then from Figure B-12 it is noted that most of the time ambient horizontal electric field noise levels at the surface are about 10μv/m at f = 610 Hz.

Now the e.m.f. induced in a wire receiver at the surface whose length is about 10 m just from noise is 0.1 millivolt. Therefore transmitter signal strengths must be about 0.3 millivolts at the receiver. From equation (15) an adequate source moment may be approximately determined on the basis of whether the length of the transmitter wire is large or small relative to the depth of burial. If the length of the transmitter wire, L, is considerably smaller than the depth of burial, an adequate source moment in this case would be about 7 amp-meters. If the length of the insulated grounded transmitter wire in the mine is 30.5 meters, the current required would be about 0.2 amperes.

This example was chosen to illustrate the manner in which resistivity data may be used with ambient electromagnetic noise data and theoretical considerations for a specific communications application in a mine. For the above example, the required current could be decreased by increasing the length of the transmitter wire. Similarly, if the resistivity of the overburden were larger with the use of the same operating frequency, a smaller source moment would be required by roughly the factor $1/\rho$.

A more exact analysis using the nonstatic solution for a buried grounded insulated current element could be made with the results recently obtained in research carried out by Hill (1973a). Hill considers the electromagnetic surface fields for an inclined buried cable of finite length and evaluates the magnetic field components at the surface for various tilts of the transmitting line. It would be a ready extension to evaluate the surface electric field

produced (in general) by an inclined buried current element and to perform the above system design analysis making use of available electrical properties data and ambient background noise data.

THROUGH-THE-EARTH TRANSMISSION TESTS

Numerous through-the-earth electromagnetic transmission tests, both of the pulse and continuous wave type, employing either an electric line source or a vertical-axis loop source were made in several mining provinces (Peabody No. 10 coal mine in southern Illinois, U.S. Bureau of Mines Experimental Mine in Pennsylvania, and the Robena No. 4 coal mine in Pennsylvania). The results of these field transmission tests enable one to examine the limitations of various source-receiver antenna configuration under the constraints of everyday mining operations. The results also help one to draw inferences as to the relative merits of possible location schemes which could be used to locate underground workers at beacon antenna transmitting sites. Location schemes would be of two types. For example, the transmitting antenna might be located on the surface above the mine workings, be either a loop antenna (whose axis is oriented vertically or horizontally) or a grounded insulated line antenna, and be excited either with continuous wave or pulse current. The underground worker may then wish to position himself relative to the surface antenna for location or possible evacuation. A perhaps more expedient location scheme, however, would not be a downlink one, as suggested above, but an uplink one; namely, the situation where the transmitting beacon antenna is underground and carried by the miner (or immediately accessible to him) and where the receiver site(s) is (are) on the surface.

Inferences to Location

One approach already mentioned for a through-the-earth beacon location scheme is the detection of (extremely low frequency) nulls at the surface in the electric field normal to the orientation of a buried line source antenna. By noting such null lines one can ascertain the location of the transmitter within the mine working.

Another technique, which makes use of the magnetic field produced at the surface from a buried vertical-axis loop antenna, is to detect the null in the horizontal magnetic field directly above the transmitting loop (which exists at all frequencies). The null in the vertical magnetic field is at a surface horizontal offset distance from the transmitter axis of 1.4 times the transmitter depth of burial (null becomes sharper as frequency decreases). The maximum in the vertical magnetic field is directly over the transmitting loop antenna or the maximum in the horizontal magnetic field is at a horizontal offset of approximately half the transmitter burial depth. These approaches to location have been discussed theoretically by Wait (1970) and, during the summers of 1971 and 1972, were field tested, both at the Peabody No. 10 mine in Illinois and at the U.S. Bureau of Mines Experimental Mine in Bruceton, Pennsylvania.

An electromagnetic beacon propagation feasibility test was conducted at the Peabody No. 10 coal mine on June 11, 1971. The Peabody No. 10 mine is located near Pawnee in Ellis and Christian counties, Illinois, and lies under relatively flat topography. The Illinois No. 6 coal seam is being mined, and Peabody No. 10 mine has an approximate annual production of 7,000,000 tons. During the time when measurements were taken, the Peabody No. 10 mine was operating. Because the mine was in full operation, and ambient electromagnetic noise levels were large, the feasibility of an electromagnetic subsurface-surface

beacon communication link was rigorously examined. Noise levels during the test, which were described in an earlier section of this report, were probably representative of a "worst-type" situation insofar as a disaster situation is concerned.

The average resistivity of the surface rocks through which electromagnetic propagation took place was 24 ohm-meters. A beacon loop transmitter with an effective area of 230 square meters was installed in the vicinity of the Main South Tunnel (see Figure 26) at a depth from the surface of 108 meters. The buried vertical magnetic dipole source carried a current of 3 amperes at a frequency of 310 Hertz and was driven by a General Radio power oscillator (200 watts maximum, 5 amperes maximum current). At the Peabody No. 10 mine a frequency not exceeding 310 Hertz would be desirable since one skin depth, δ, or the distance by which the electromagnetic fields would be severely attenuated by propagation through the overburden, is

$$\delta \triangleq \frac{\rho}{f\mu\pi} = \frac{24}{310 \cdot 3.14 \cdot 12.56 \cdot 10^{-7}} \simeq 106 \text{ meters}$$

This depth corresponds approximately to the depth of burial of the source transmitter.

The vertical and horizontal magnetic field components produced on the surface were measured at three sites, one directly over the source transmitter and two offset from the buried antenna (see Figure 26 for location of surface sites). The horizontal magnetic field components at the surface were measured in this case with a high mumetal induction coil whose effective area, impedance, and coil sensitivity were calibrated before the field test (see Figures 27 and 28); the vertical magnetic field at the surface was measured with a loop laid out on the surface with a 1000-foot length of 26-turn cable whose impedance versus frequency was also measured before the field test (see Table II). Impedance versus frequency measurements were made so as also to ascertain the resonant frequency of the mumetal coil and the required input impedance of the measuring equipment.

The results of the field transmission tests are illustrated in Figure 29 where the behavior of the measured magnetic field components produced on the surface as a function of offset distance is plotted. In Figure 29 the measured magnetic field components are normalized by $|H_{z_o}|$, the magnitude of the produced vertical magnetic field directly over the buried transmitter.

It is noted that the vertical magnetic field produced at the surface remains essentially constant out to an offset distance of $\delta/5$, where δ is one (plane-wave) skin depth ($\sqrt{\rho/f\pi\mu}$). At an offset distance of one skin depth the magnitude of the vertical magnetic field is down by only 3 db. The horizontal magnetic field produced at the surface, on the other hand, exhibits a sharp null directly over the beacon and reaches a maximum at an offset distance roughly equivalent to one skin depth away from the source.

These results indicate that measurements of the horizontal magnetic field produced at the surface from the buried magnetic dipole antenna could be used to locate the buried dipole source by determining the null directly over the subsurface antenna and the maximum at one skin depth offset distance from the

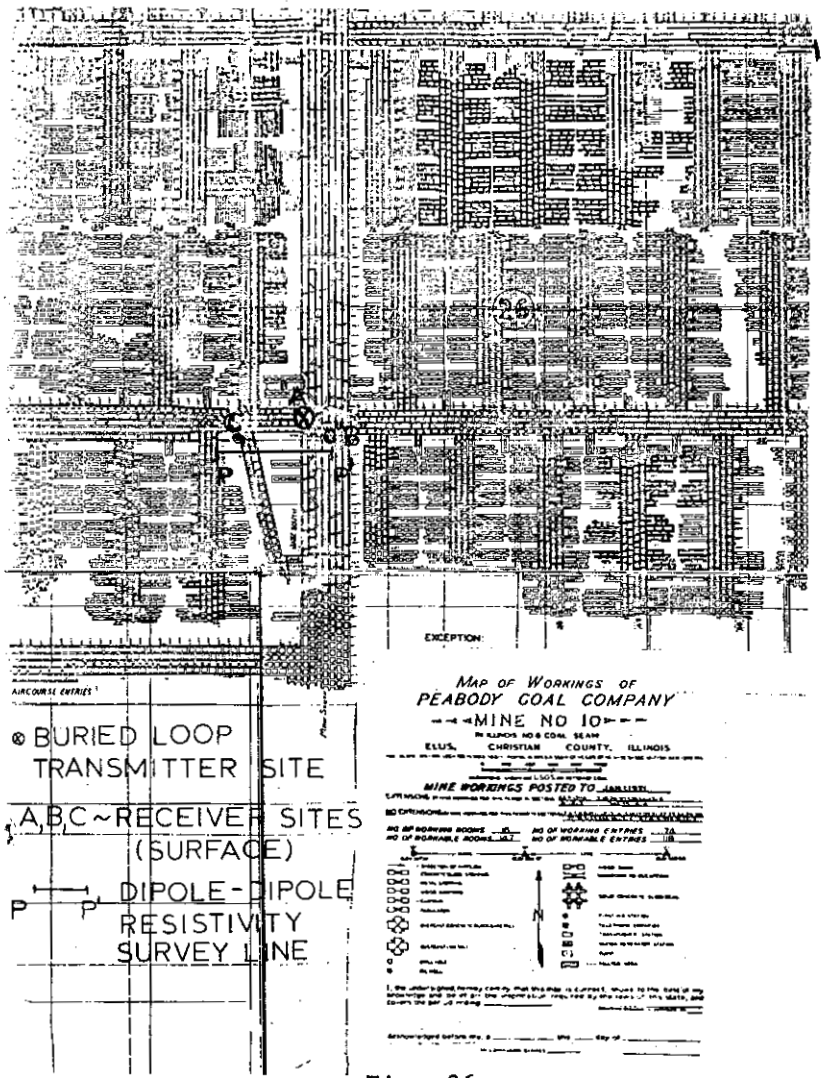

Fig. 26

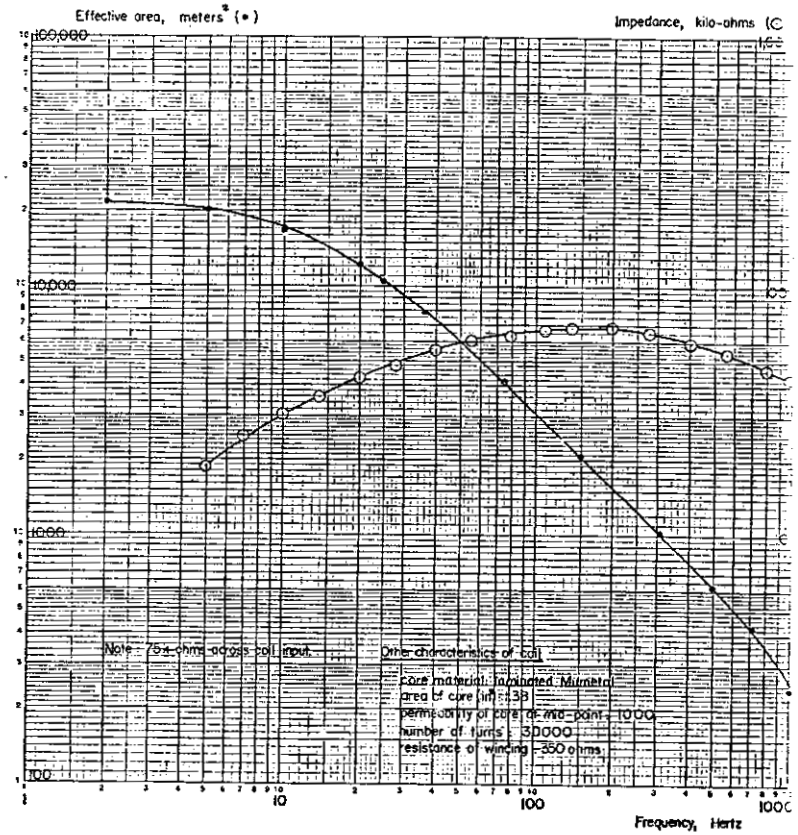

Effective area and impedance of "U. of Texas" coil vs frequency.

Fig. 27

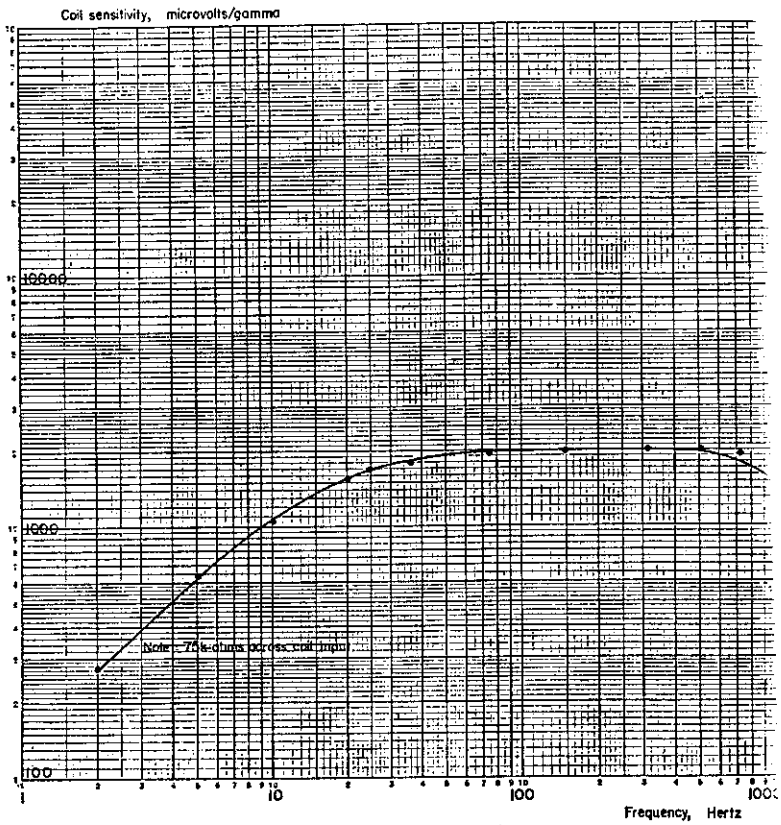

Sensitivity of "U. of Texas" coil vs frequency.

Fig. 28

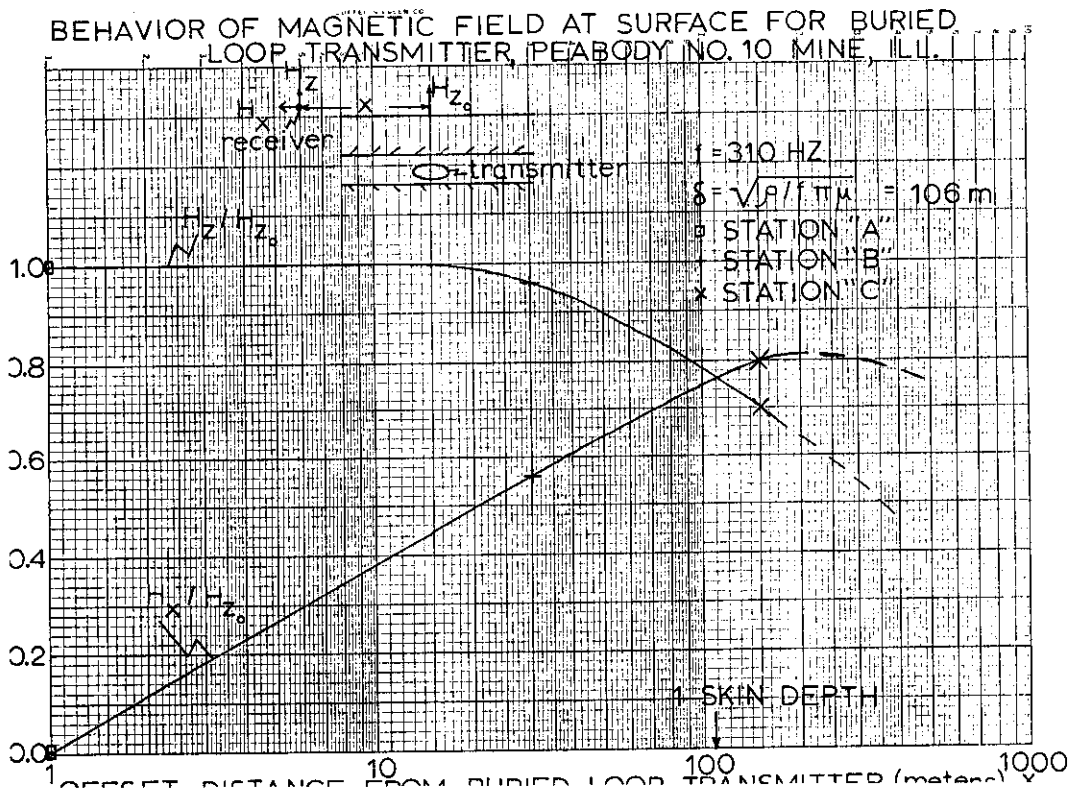

Fig. 29

TABLE II

Frequency	Impedance x 10^{-3}
5	1.72
7	1.82
10	1.82
14	1.71
20	1.80
28	1.76
40	1.73
56	1.73
80	1.71
100	1.71
140	1.76
200	1.79
280	1.86
400	1.98
560	2.20
800	2.30
1000	2.15
1400	1.60
2000	1.11
2800	.81
4000	.61
5600	.46
8000	.36

Impedance of seismic cable used for surface measurements in the electromagnetic subsurface-surface beacon communication test at Peabody No. 10 coal mine, Illinois. Impedance (ohms) is given as a function of frequency.

antenna. In addition, the propagation test results demonstrate that for downlink communications, it would not be too critical where a surface loop transmitter were positioned relative to a receiver in a mine working. If it is known that the receiver (vertical-axis induction coil) in the mine is not offset greater than one skin depth from the surface dipole transmitter, signal strengths within the mine at the receiver site should not be significantly affected.

It is interesting to compare the field results obtained at the Peabody No. 10 mine to the theoretical considerations employed by Wait (1969, 1970) and Banõs (1966). Wait shows that when the earth may be represented as an electrically and magnetically homogeneous halfspace of conductivity σ and permeability μ, and for the situation illustrated in Figure 30 where the earth's surface is the plane $z = 0$ and the loop is located at $z = -h$, the horizontal and vertical magnetic field components produced at the surface are, respectively,

$$H_x = \frac{IA}{2\pi} \int_0^\infty \frac{\lambda^3}{\lambda+u} e^{-uh} J_1(\lambda x) d\lambda \tag{16}$$

and

$$H_z = \frac{IA}{2\pi} \int_0^\infty \frac{\lambda^3}{\lambda+u} e^{-uh} J_0(\lambda x) d\lambda \tag{17}$$

where the buried magnetic dipole of area A carries current I and where $u = (\lambda^2+i\omega\mu\sigma)^{\frac{1}{2}}$. Upon numerical evaluation of the integrals in equations (16) and (17) above, Wait observes that $|H_x|$ has a sharp null for $D \triangleq x/h = 0$ and rises to a maximum for $D \simeq 0.6$. This observation was closely verified in the field in the test at Peabody No. 10 mine. In addition, the behavior of the magnitude of the vertical magnetic field in the Peabody test substantiates Wait's results. At the Peabody No. 10 mine,

$$H = (\sigma\mu\omega)^{\frac{1}{2}}h$$

$$= (12.56\cdot10^{-12}\cdot6.28\cdot3.1\cdot10^2/24)^{\frac{1}{2}}\ 10^2$$

$$\simeq 0.003 << 1$$

so that when the receiver site is located at an offset distance 'x' equivalent to the depth to the transmitter h, the normalized field strength H_z/H_{z_o} should fall to approximately 75% of its peak value. This behavior is illustrated in Figure 29.

Passive Detection of a Buried Loop from the Surface

Several investigators (Parkinson, Powell, Wait, 1972) have suggested that one possible method of locating a trapped miner would be to passively excite a closed insulated loop of wire from the surface. The miner would have the target loop which could be any closed conductor, such as a single turn loop of AWG #10 wire of radius on the order of 1 meter. Both the source antenna and receiver loops would be at the surface (Figure 31). One distinct advantage of such a scheme is in the simplicity for the underground miner; namely, he would

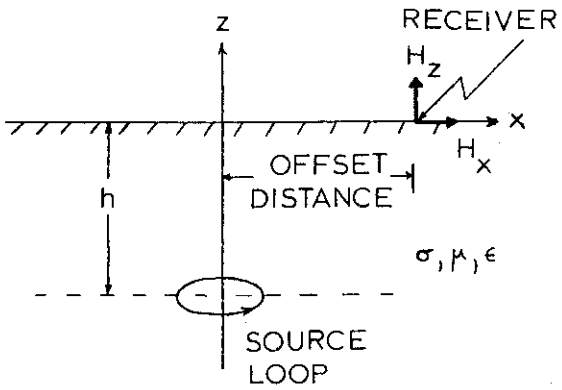

Fig. 30 Oscillating magnetic dipole buried in the earth.

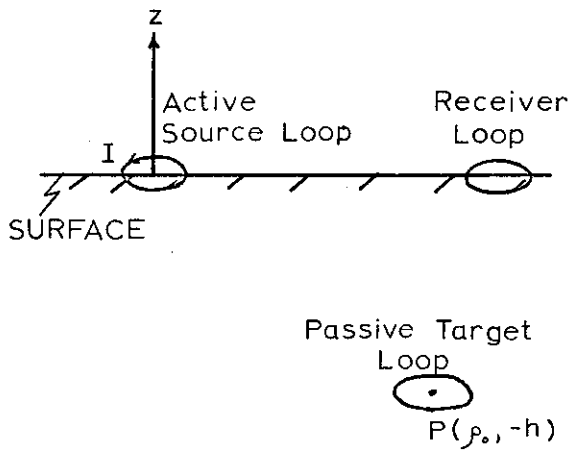

Fig. 31 Geometrical configuration for passive loop detection scheme. Source antenna has radius a with n turns. Passive target loop has radius a_t with n_t turns.

not have to possess (either within a mine working or on his person) any power source and all that he would need to do in a disaster situation is lay out a closed loop of insulated wire of maximum area. In this part of the report we discuss the practicality of such a scheme. In the sequel, reference is made to Figure 31.

The transmitting loop antenna is located at the surface at the origin of our reference coordinate system and has a radius "a" with "n" turns. The passive target loop is buried at a depth -h, is offset a horizontal distance of ρ_o, and has a radius "a_t" with "n_t" turns. The active transmitter loop will carry some current I and will induce a current in the buried target loop which will be denoted by I_t. This target loop, then, will act as a secondary, passively excited source which will generate a back e.m.f. in the transmitting, active antenna. This back e.m.f. will cause a current of smaller magnitude I_s to flow in the active loop at the surface. We now examine the ratio of the secondary current, I_s, due to the presence of the buried target loop to the primary current, I, for it is against both the primary source field and the ambient noise background that I_s must be detected.

Wait and Spies (1971a) give the expression for the vertical magnetic field at the target observation point P at a depth h and offset distance ρ_o from the source antenna:

$$H_z(\rho_o - h) = \frac{\pi a^2 I}{2\pi h^3} \hat{Q} \tag{18}$$

where

$$\hat{Q} = \int_o^\infty \frac{J_1(Ax)}{(Ax/2)} \frac{x^3 e^{-Zx} e^{-(x^2+iH^2)^{1/2}}}{(x^2+iH^2)^{1/2} + x} J_o(Dx)\,dx \tag{19}$$

and where $A = a/h$, $Z = h_o/h$, $D = \rho/h$, $H = (\sigma\mu_o\omega)^{1/2}h$. (Note that the only difference between equations (19) and (17) is that the fact that the loop antenna may not be a dipole antenna is accounted for; i.e., it may be a finite loop which is taken into account by the factor $J_1(Ax)/(Ax/2)$. Note that $\lim_{a\to o} J_1(Ax)/(Ax/2) = 1$.) In the above formulas Wait allows the source loop antenna to be elevated at a distance h_o above the ground and also allows for a finite size of the transmitting loop instead of treating the source antenna as a vertical magnetic dipole in the strict sense. The symbol σ denotes the conductivity (assumed uniform and isotropic) of the overburden, ω ($= 2\pi f$) denotes the radian frequency of the transmitter, and μ denotes the magnetic permeability of the overburden ($= 4\pi \cdot 10^{-7}$ henries/meter).

In our case, the source loop antenna is on the surface so that $Z = 0$. We now wish to calculate the current induced in the passive loop, I_t. This is accomplished by first considering the e.m.f. generated in the target loop, E_t, due to the time rate-of-change of magnetic flux through it and then dividing that e.m.f. by the resistance R_t of the target loop wire. The e.m.f. generated in the target loop is found by a straightforward application of Faraday's law and Stoke's Theorem; namely,

$$\nabla \times \vec{E} = -\,\partial\vec{B}/\partial t = -\mu_o \partial\vec{H}/\partial t \tag{20}$$

and

$$\iint_S \nabla \times \vec{E}\cdot\vec{n}\, dS = \vec{E}\cdot\vec{} = -\mu_o \iint_S \frac{\partial \vec{H}}{\partial t}\vec{n}dS \tag{21}$$

where the surface integral is over the effective area of the target loop and where the line integral is the total e.m.f. generated in the target loop. Equation (21) yields

$$2\pi a_t n_t E_t = -\mu_o n_t \pi a_t^2 \frac{\partial H_z}{\partial t}(\rho_o - h)$$

so that

$$E_t = -\frac{\mu_o a_t}{2}\frac{\partial H_z}{\partial t}(\rho_o - h) \tag{22}$$

and

$$I_t = E_t/R_t = -\frac{\mu_o a_t}{2R_t}\frac{\pi a^2}{2\pi h^3}\hat{Q}\frac{dI}{dt} \tag{23}$$

from (18) above. Since $I(\omega)$ in the source loop varies sinusoidally with time, equation (23) may be written as

$$I_t \equiv I_{target} = -\frac{\mu_o a_t a^2 \omega}{4R_t h^3} I\,\hat{Q} \tag{24}$$

The next step is to compute the magnetic field $H_{z,s}$ at the point (0,0) due to the current I_t induced in the small passive loop. This secondary magnetic field may be found from (Wait, 1970):

$$H_{z,s} = \frac{n_t a_t^2 I_t}{2h^3} Q \tag{25}$$

where

$$Q = \int_o^\infty \frac{x^3 e^{-(x^2+iH^2)^{1/2}}}{x+(x^2+iH^2)^{1/2}} J_o(Dx)dx$$

or, by making use of equation (24),

$$H_{z,s} = -\frac{\mu_o n_t a_t^3 a^2 \omega I}{8R_t h^6} Q\,\hat{Q} \tag{26}$$

If I_s is the induced current in the active source loop on the surface due to the current flow I_t in the passive loop and if R is the resistance per unit length of the active source loop, then

$$I_s = -\frac{\mu_o a}{2R}\,\partial H_{z,s}/\partial t = \frac{\pi^2 \mu_o^2 n_t a_t^3 a^3 f^2 Q\hat{Q} I}{4R_t Rh^6} \tag{27}$$

Thus

$$\frac{I_s}{I} = \frac{\pi^2 \mu_o^2 n_t a_t^3 a^3 f^2 Q\hat{Q}}{4R_t Rh^6} \tag{28}$$

The maximum value for Q or $\hat{Q}$ is where the offset distance ρ_o is zero; this maximum value for Q and $\hat{Q}$ is unity so that

$$\left(\frac{I_s}{I}\right)_{\text{, maximum}} = \frac{4\pi^4 n_t a_t^3 a^3 f^2}{R_t Rh^6} \cdot 10^{-14} \tag{29}$$

where R and R_t are given in ohms; a, a_t, and h in meters; and f in cycles per second.

Equation (29) demonstrates that the secondary fields radiated by the passive loop antenna are quite small unless: (1) the radii a and/or a_t are made quite large relative to the depth of burial h, (2) the transmitting frequency f is markedly increased, or (3) the resistance R of the source loop and/or the resistance R_t of the passive loop is made small. Generally, weight is not a severe limitation for the source loop antenna at the surface so that a loop transmitting antenna might typically consist of one turn of AWG #1 insulated copper wire with a circular radius of 50 meters (requiring about 1000 feet of wire). This loop antenna would have a resistance of about 0.10 ohm. If one were willing to double the weight of wire, he could approximately halve the resistance.

Because the secondary fields radiated by the passive loop are proportional to the third power of radii whereas they are in inverse proportion to only the first power of the resistances of the loops, it follows that it would be better to increase the area(s), even if in order to keep the weight of the passive loop low, R_t increases. As Wait and Spies (1971a) show, however, the maximum value chosen for Q and $\hat{Q}$ occurs at low frequencies, at a zero offset distance from the transmitter loop, and where the radii of the source loop and passive loop are much smaller than the overburden thickness. Thus, as a and/or a_t are increased in relation to h, a finite loop evaluation, not a dipolar one, must be made. For example, when the radius a of the source antenna is half the depth of burial to the passive loop, the coaxial vertical magnetic field at the passive loop (i.e., $\hat{Q}$) falls from a value of unity to 0.72, a drop of 28%. This finite loop evaluation, when the areas of the loops become large relative to the overburden thickness, is not a severe limitation, although it must be kept in mind when considering actual coupling magnitudes.

Another consideration is that the target passive loop and/or the receiving loop at the surface (here chosen to be at the same position as the surface transmitting loop) may be designed so as to have a resonant peak in the effective area at the transmitting frequency (which is judiciously chosen for

adequate penetration and lower power spectrum noise levels). An example of such a peak in effective area (number of turns times area) of a typical air-core loop used for transmission tests at the U.S. Bureau of Mines Experimental Mine is illustrated in Figure 32 (this loop weighs about 4 lb and is about 1 meter in diameter).

Still another possibility for increasing the ratio of $|I_s/I|_{,maximum}$ is to increase the transmitting frequency of the source loop. As stated above, however, this may be done efficiently only to a certain limit in order to obtain adequate penetration within the earth. An illustration of the attenuation of the subsurface vertical magnetic field of a surface vertical-axis loop antenna is given in Figure 33. In Figure 33 the attenuation in decibels is plotted as a function of the dimensionless depth ratio $h/\delta = h\sqrt{\pi f\mu\sigma}$, where δ is a skin depth in the earth equal to $1/\sqrt{\pi f\mu\sigma}$, σ being the conductivity of the overburden and μ being the magnetic permeability ($= 4\pi\cdot 10^{-7}$ henries/meter). On the basis of electrical properties measurements of the overburden made thus far (Geyer and Keller, 1971b) an average value of σ for the overburden of most coal mines would be about 10^{-2} mhos/m and, at most, h would be 400 m (an overburden thickness of about 1350 feet). In this case

$$h\sqrt{\pi\mu f\sigma} = 4\cdot 10^{2}\cdot 2\pi\cdot 10^{-4}\ \sqrt{f/10}$$

A typical transmitting frequency would be 1000 Hz so that $h/\delta = h\sqrt{\pi\mu f\sigma} \approx 2.5$. Thus, referring to Figure 33, for most practical purposes the attenuation of the vertical magnetic field at 1000 Hz would be less than 10 db for even the deepest mine. However, if we increase the transmitter frequency, attenuation becomes greater so that in order to keep the same signal levels at the passive loop site, the power output of the transmitter would have to be increased. In addition, as Wait and Spies (1971d) note, the values of Q and $\hat{Q}$ above become less than unity with increase of the transmitter frequency.

In Tables III-VIII below, the maximum value of the ratio of the secondary to primary current at the source transmitter location due to passive excitation of a buried loop is given at a number of frequencies and depths of burial and under the constraint that the passive loop weight is to be kept to about 2 lb. Tables IX-XI give the same ratio as a function of frequency if an increased weight to about 6 lb for the passive loop would be acceptable. (It should be noted that the values given for $|I_s/I|$ are maximum possible values, particularly for the higher frequencies since the values of Q and $\hat{Q}$ were taken to be unity. At higher frequencies Q and $\hat{Q}$ would actually be less than unity. For example, at 10,000 Hz, an overburden resistivity of 100 ohm-meters, and an overburden thickness of 100 m, the value of Q and $\hat{Q}$ would be closer to 0.9.)

The above analysis has been based on a C.W. type transmission. Recently, Wait and Hill (1972a) have considered the electromagnetic transient response of a small wire loop buried in a homogeneous conducting earth for impulsive excitation and have observed that the time delay and difference in wave shape of the target response offers some hope for detection and direction-finding. However, on the basis of experimental field transmission tests (downlink and uplink) performed at the U.S. Bureau of Mines Experimental Coal Research Mine as well as on the basis of ambient noise measurements taken at a number of large operating coal mines (Geyer and Keller, 1971b) it seems that it would be more

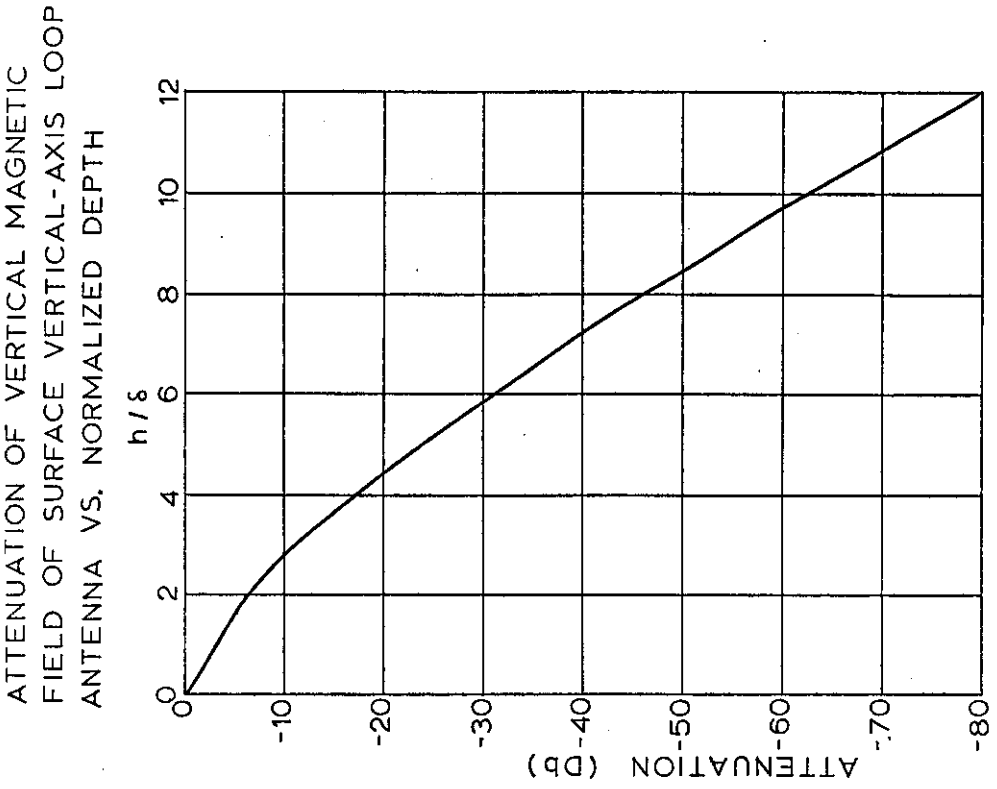
ATTENUATION OF VERTICAL MAGNETIC FIELD OF SURFACE VERTICAL-AXIS LOOP ANTENNA VS. NORMALIZED DEPTH
h / δ
0
2
4
6
8
10
12
ATTENUATION (Db)
0
-10
-20
-30
-40
-50
-60
-70
-80

Fig. 33

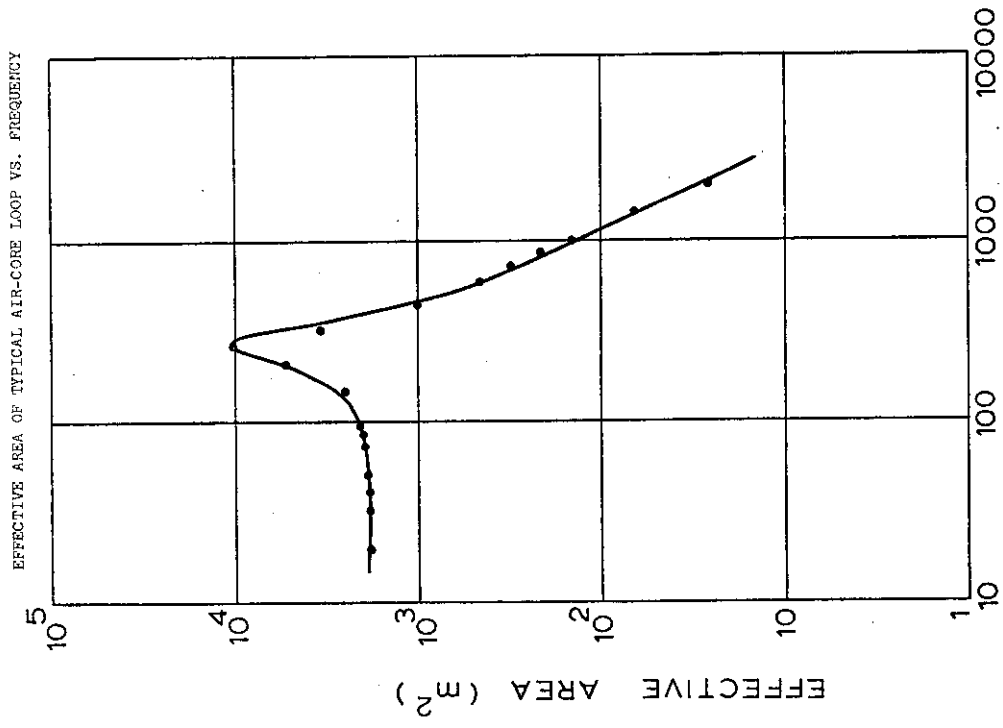
EFFECTIVE AREA OF TYPICAL AIR-CORE LOOP VS. FREQUENCY
EFFECTIVE AREA (m²)
10^5
10^4
10^3
10^2
10
1
FREQUENCY (Hz)
10
100
1000
10000

Fig. 32

TABLE III. Ratio of Secondary to Primary Current at Source Transmitter Location Due to Passive Excitation of Buried Loop.

f (Hz)	$\left\|I_s/I\right\|$, maximum
10	$8.12 \cdot 10^{-15}$
100	$8.12 \cdot 10^{-13}$
1000	$8.12 \cdot 10^{-11}$
10,000	$8.12 \cdot 10^{-9}$
100,000	$8.12 \cdot 10^{-7}$
1,000,000	$8.12 \cdot 10^{-5}$

Passive loop buried 100 m and consists of 1 turn of AWG #5 insulated copper wire with circular radius of 1 m. Passive loop weighs 2 lb and has a resistance R_t of 0.006 ohm. Source loop at surface consists of 1 turn of AWG #1 insulated copper wire and has a circular radius of 50 m and resistance R of 0.10 ohm.

TABLE IV. Ratio of Secondary to Primary Current at Source Transmitter Location Due to Passive Excitation of Buried Loop.

f (Hz)	$\left\|I_s/I\right\|$, maximum
10	$1.27 \cdot 10^{-16}$
100	$1.27 \cdot 10^{-14}$
1000	$1.27 \cdot 10^{-12}$
10,000	$1.27 \cdot 10^{-10}$
100,000	$1.27 \cdot 10^{-8}$
1,000,000	$1.27 \cdot 10^{-6}$

Passive loop buried 200 m and consists of 1 turn of AWG #5 insulated copper wire with circular radius of 1 m. Passive loop weighs 2 lb and has a resistance R_t of 0.006 ohm. Source loop at surface consists of 1 turn of AWG #1 insulated copper wire and has a circular radius of 50 m and resistance R of 0.10 ohm.

TABLE V. Ratio of Secondary to Primary Current at Source Transmitter Location Due to Passive Excitation of Buried Loop.

f (Hz)	$\left\|I_s/I\right\|$, maximum
10	$1.11 \cdot 10^{-17}$
100	$1.11 \cdot 10^{-15}$
1000	$1.11 \cdot 10^{-13}$
10,000	$1.11 \cdot 10^{-11}$
100,000	$1.11 \cdot 10^{-9}$
1,000,000	$1.11 \cdot 10^{-7}$

Passive loop buried 300 m and consists of 1 turn of AWG #5 insulated copper wire with circular radius of 1 m. Passive loop weighs 2 lb and has a resistance R_t of 0.006 ohm. Source loop at surface consists of 1 turn of AWG #1 insulated copper wire and has a circular radius of 50 m and resistance R of 0.10 ohm.

TABLE VI. Ratio of Secondary to Primary Current at Source Transmitter Location Due to Passive Excitation of Buried Loop.

f (Hz)	$\left\|I_s/I\right\|$, maximum
10	$9.74 \cdot 10^{-13}$
100	$9.74 \cdot 10^{-11}$
1000	$9.74 \cdot 10^{-9}$
10,000	$9.74 \cdot 10^{-7}$
100,000	$9.74 \cdot 10^{-5}$
1,000,000	$9.74 \cdot 10^{-3}$

Passive loop buried 100 m and consists of 1 turn of AWG #14 insulated copper wire with circular radius of 10 m. Passive loop weighs 2 lb and has a resistance R_t of 0.50 ohm. Source loop at surface consists of 1 turn of AWG #1 insulated copper wire and has a circular radius of 50 m and resistance R of 0.10 ohm.

TABLE VII. Ratio of Secondary to Primary Current at Source Transmitter Location Due to Passive Excitation of Buried Loop.

f (Hz)	$\left\|I_s/I\right\|$, maximum
10	$1.52 \cdot 10^{-14}$
100	$1.52 \cdot 10^{-12}$
1000	$1.52 \cdot 10^{-10}$
10,000	$1.52 \cdot 10^{-8}$
100,000	$1.52 \cdot 10^{-6}$
1,000,000	$1.52 \cdot 10^{-4}$

Passive loop buried 200 m and consists of 1 turn of AWG #14 insulated copper wire with circular radius of 10 m. Passive loop weighs 2 lb and has a resistance R_t of 0.50 ohm. Source loop at surface consists of 1 turn of AWG #1 insulated copper wire and has a circular radius of 50 m and resistance of 0.10 ohm.

TABLE VIII. Ratio of Secondary to Primary Current at Source Transmitter Location Due to Passive Excitation of Buried Loop.

f (Hz)	$\left\|I_s/I\right\|$, maximum
10	$1.34 \cdot 10^{-15}$
100	$1.34 \cdot 10^{-13}$
1000	$1.34 \cdot 10^{-11}$
10,000	$1.34 \cdot 10^{-9}$
100,000	$1.34 \cdot 10^{-7}$
1,000,000	$1.34 \cdot 10^{-5}$

Passive loop buried 300 m and consists of 1 turn of AWG #14 insulated copper wire with circular radius of 10 m. Passive loop weighs 2 lb and has a resistance R_t of 0.50 ohm. Source loop at surface consists of 1 turn of AWG #1 insulated copper wire and has a circular radius of 50 m and resistance of 0.10 ohm.

TABLE IX. Ratio of Secondary to Primary Current at Source Transmitter Location Due to Passive Excitation of Buried Loop.

f (Hz)	$\left\|I_s/I\right\|$, maximum
10	$2.44 \cdot 10^{-12}$
100	$2.44 \cdot 10^{-10}$
1000	$2.44 \cdot 10^{-8}$
10,000	$2.44 \cdot 10^{-6}$
100,000	$2.44 \cdot 10^{-4}$
1,000,000	$2.44 \cdot 10^{-2}$

Passive loop buried 100 m and consists of 1 turn of AWG #10 insulated copper wire with circular radius of 10 m. Passive loop weighs 6 lb and has a resistance R_t of 0.20 ohm. Source loop at surface consists of 1 turn of AWG #1 insulated copper wire and has a circular radius of 50 m and resistance of 0.10 ohm.

TABLE X. Ratio of Secondary to Primary Current at Source Transmitter Location Due to Passive Excitation of Buried Loop.

f (Hz)	$\left\|I_s/I\right\|$, maximum
10	$3.81 \cdot 10^{-14}$
100	$3.81 \cdot 10^{-12}$
1000	$3.81 \cdot 10^{-10}$
10,000	$3.81 \cdot 10^{-8}$
100,000	$3.81 \cdot 10^{-6}$
1,000,000	$3.81 \cdot 10^{-4}$

Passive loop buried 200 m and consists of 1 turn of AWG #10 insulated copper wire with circular radius of 10 m. Passive loop weighs 6 lb and has a resistance R_t of 0.20 ohm. Source loop at surface consists of 1 turn of AWG #1 insulated copper wire and has a circular radius of 50 m and resistance of 0.10 ohm.

TABLE XI. Ratio of Secondary to Primary Current at Source Transmitter Location Due to Passive Excitation of Buried Loop.

f (Hz)	$\left\|I_s/I\right\|_{,maximum}$
10	$3.34 \cdot 10^{-15}$
100	$3.34 \cdot 10^{-13}$
1000	$3.34 \cdot 10^{-11}$
10,000	$3.34 \cdot 10^{-9}$
100,000	$3.34 \cdot 10^{-7}$
1,000,000	$3.34 \cdot 10^{-5}$

Passive loop buried 300 m and consists of 1 turn of AWG #10 insulated copper wire with circular radius of 10 m. Passive loop weighs 6 lb and has a resistance R_t of 0.20 ohm. Source loop at surface consists of 1 turn of AWG #1 insulated copper wire and has a circular radius of 50 m and resistance of 0.10 ohm.

expedient, if possible, to use an active source at depth for direction-finding and only to consider passive detection as a backup method of location. It is because ambient noise levels at the surface of most operating coal mines are in excess of the secondary fields radiated by a buried passive loop.

Downlink Pulse Signalling to Underground Mine Working

Theoretical Considerations

Another approach for through-the-earth communications, in this case downlink from the surface to an arbitrary subsurface position within a mine working, may be effected by a long insulated wire surface antenna excited by an impulsive or step current. This insulated wire at the surface is grounded at distant ends (see Figure 34), and with this type of antenna at the surface, a number of different source-receiver sensor configurations are possible (see Figure 35). In a previous report (Geyer, 1972a) the mutual coupling (voltage induced in the receiving antenna normalized by the current in the source antenna) for impulsive excitation of the line source at the surface and for a vertical loop receiver was found to be

$$
\begin{aligned}
Z_{\substack{\text{Vertical}\\ \text{Loop}}}(x_o,z_o;t) = \frac{\mu_o}{2\pi t^2}\Big\{&\Big(\frac{1}{2}\Big(1-\frac{\mu_o z_o^2}{2\rho t}\Big)\exp\Big(\frac{-\mu_o x_o^2}{4\rho t}\Big)\\
&-\frac{\mu_o x_o z_o}{2\sqrt{\pi}\,\rho t}\,K\exp\,(-\mu_o x_o^2/4\rho t)\\
&+\Big(\frac{\mu_o}{\pi\rho t}\Big)^{\frac{1}{2}}\frac{z_o}{2}\Big)\,\frac{\mu_o z_o}{2\rho t}\exp(-\mu_o z_o^2/4\rho t)\\
&+\Big(\frac{\mu_o z_o}{2\rho t}\exp(-\mu_o x_o^2/4\rho t)+\frac{\mu_o x_o}{2\sqrt{\pi}\,\rho t}\,K\exp\Big(-\frac{\mu_o x_o^2}{4\rho t}\Big)\\
&-\frac{1}{2}\Big(\frac{\mu_o}{\pi\rho t}\Big)^{\frac{1}{2}}\Big)\exp\,(-\mu_o z_o^2/4\rho t)\Big\}
\end{aligned}
\tag{30}
$$

where the receiving sensor is at (x_o,z_o), ρ is the resistivity of the overburden, μ_o the magnetic permeability ($= 4\pi \times 10^{-7}$ henries/m), and where K is known as Dawson's integral or

$$
K = \int_0^{(\mu_o/\rho t)^{\frac{1}{2}}x_o/2} \exp(\alpha^2)\,d\alpha \tag{31}
$$

Similarly, the mutual coupling for a horizontal loop was found to be,

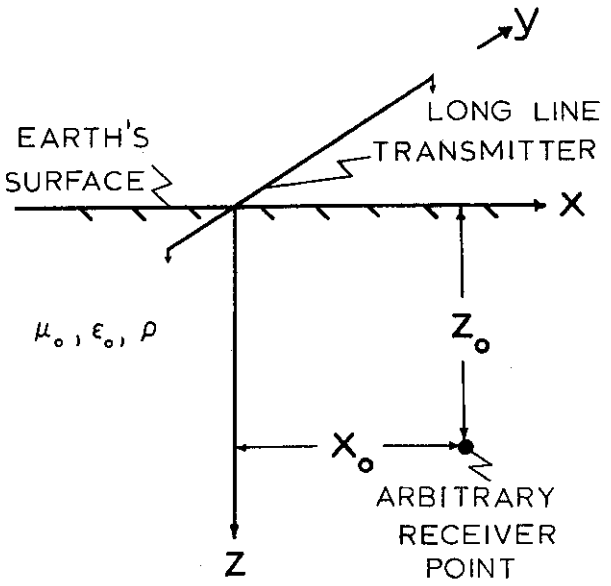

Fig. 34 Geometry of a long insulated grounded wire at the earth's surface and an arbitrarily located broadside receiver position.

DOWNLINK SOURCE - RECEIVER SENSOR CONFIGURATIONS

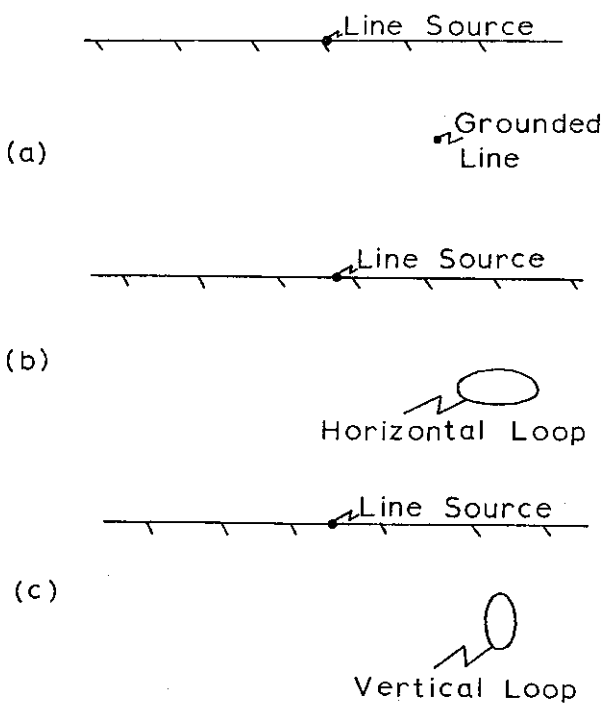

Fig. 35

$$Z_{\substack{\text{Horizontal}\\ \text{Loop}}}(x_o,z_o;t) = -\frac{\mu_o}{2\pi t^2}\left\{\frac{\mu_o x_o}{2\rho t}\left(\frac{1}{2}\left(1-\frac{\mu_o z_o^2}{2\rho t}\right)\right.\right.$$

$$+\frac{z_o}{2\sqrt{\pi}}\left(\frac{\mu_o}{\rho t}\right)^{\frac{1}{2}}\exp\left(\left(\frac{\mu_o}{\rho t}\right)^{\frac{1}{2}}\frac{x_o}{z}\right)$$

$$\left.\left.+K\frac{\mu_o z_o}{2\sqrt{\pi}\,\rho t}\left(1-x_o\left(\frac{\mu_o x_o}{2\rho t}\right)\right)\right\}\exp\left(-\frac{\mu_o}{4\rho t}\left(x_o^2+z_o^2\right)\right) \qquad (32)$$

and the electric field measured with a grounded line receiver,

$$E_y(x_o,z_o;t) = \frac{\mu_o I_o}{2\rho t^2}\left\{\frac{1}{2}\left(1-\frac{\mu_o z_o^2}{2\rho t}\right)\exp\left(-\mu_o x_o^2/4\rho t\right)\right.$$

$$-\frac{\mu_o x_o z_o}{2\sqrt{\pi}\,\rho t}\exp\left(-\mu_o x_o^2/4\rho t\right)K$$

$$\left.+\left(\frac{\mu_o}{\pi\rho t}\right)^{\frac{1}{2}}\frac{z_o}{z}\right\}\exp\left(-\mu_o z_o^2/4\rho t\right) \qquad (33)$$

Numerous theoretical coupling curves for any of the above receiving sensors at a number of different depths of burial and offset distances and for several resistivity distributions of the overburden were calculated under the assumption that the source line antenna was impulsively excited. These results were extensively discussed in a previous communication (Geyer, 1972). Several typical transient coupling responses for the propagated electric and magnetic field components are given in Figures 36, 37, 38, 39, 40, and 41.

As noted earlier, the evaluated transient mutual coupling responses at a buried receiver site for impulsive input to the source antenna suffer no loss in generality and may be put to use for any type of current input to the source antenna. This fact is an important one, for the practical use of the time-domain electromagnetic method frequently requires the transmission of a step current (as distinct from an impulsive current) into the ground and the corresponding recording of a transient at the receiver location. If the harmonic function $\mathbf{F}(i\omega)$ corresponding to an impulsive input $\delta(t)$ is known for all frequencies, then the response for other inputs can also be determined. Consider, for example, a unit impulse into the earth as a linear system:

$$\delta(t) \qquad \text{EARTH} \qquad f(t)$$

where $f(t)$ is the impulse response of the earth linear system. Next, consider a step function $u(t)$ as input into the same earth:

$$u(t) \qquad \text{EARTH} \qquad f(t) * u(t)$$

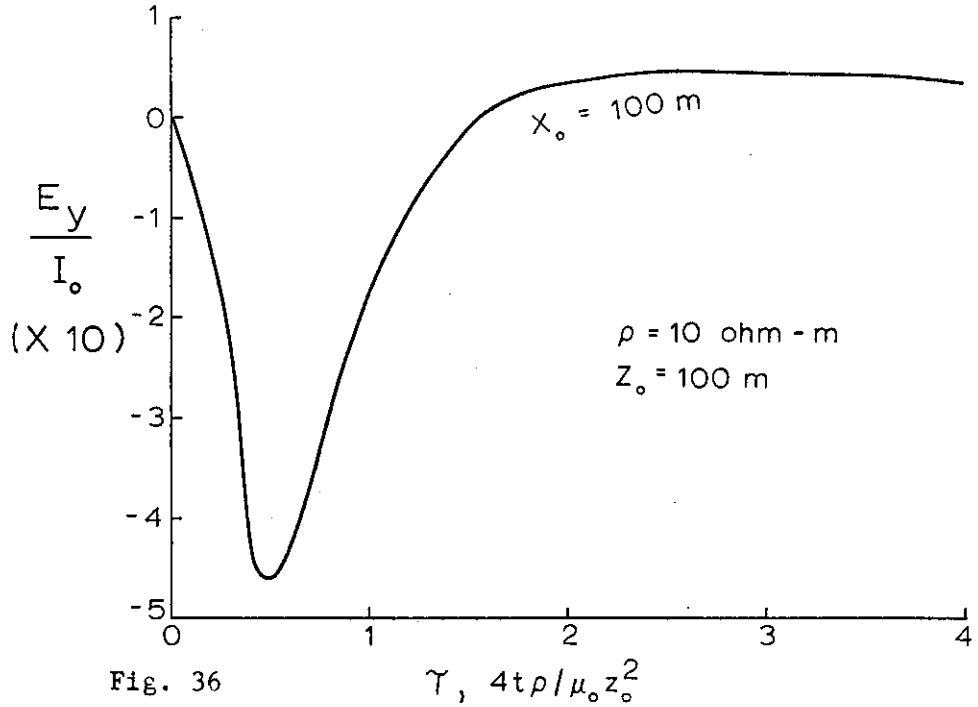
$\frac{E_y}{I_o}$
(X 10)
X_o = 100 m
ρ = 10 ohm - m
Z_o = 100 m
τ, $4t\rho/\mu_o z_o^2$

Fig. 36

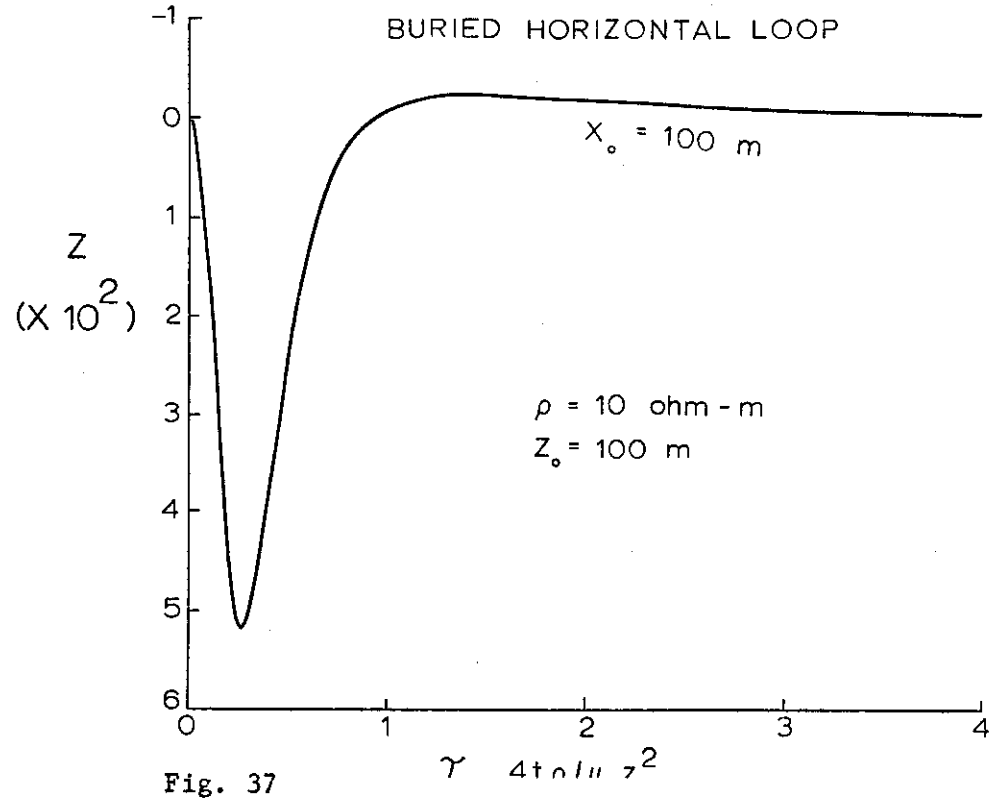
BURIED HORIZONTAL LOOP
Z
(X 10^2)
X_o = 100 m
ρ = 10 ohm - m
Z_o = 100 m
τ $4t\rho/\mu_o z^2$

Fig. 37

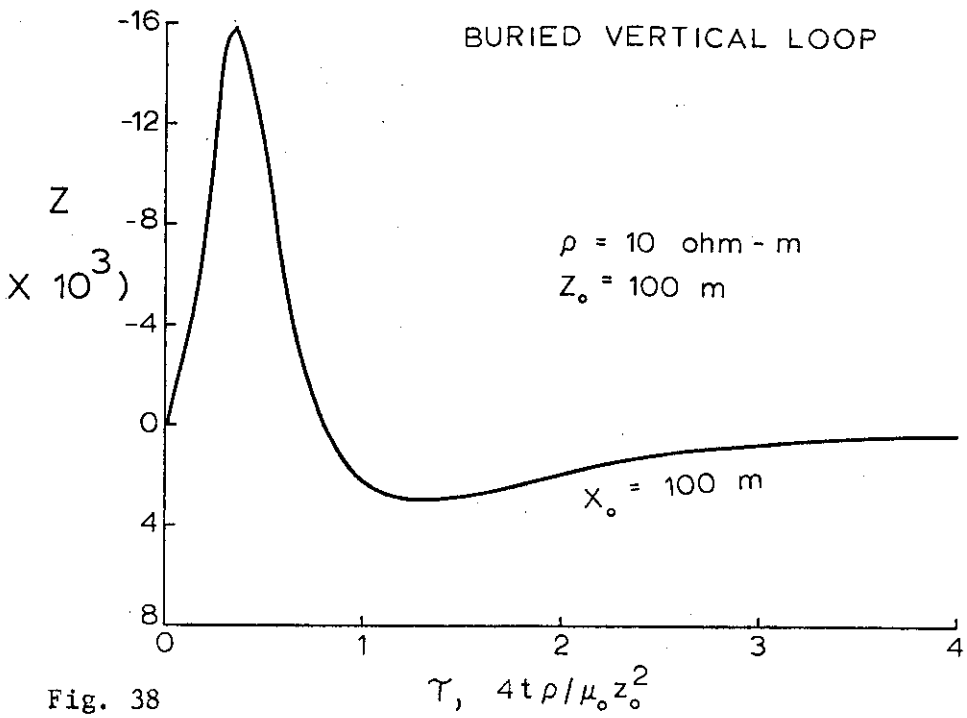
BURIED VERTICAL LOOP
ρ = 10 ohm - m
Z₀ = 100 m
X₀ = 100 m
Z
X 10³)
-16
-12
-8
-4
0
4
8
0
1
2
3
4
τ, 4tρ/μ₀z₀²

Fig. 38

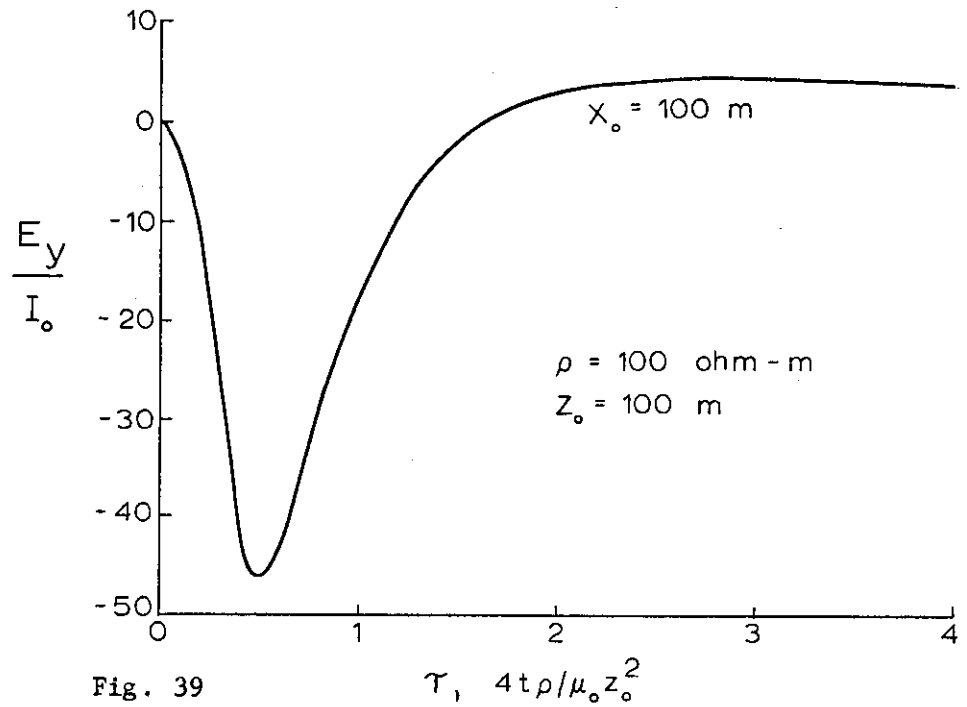
ρ = 100 ohm - m
Z₀ = 100 m
X₀ = 100 m
E_y / I₀
10
0
-10
-20
-30
-40
-50
0
1
2
3
4
τ, 4tρ/μ₀z₀²

Fig. 39

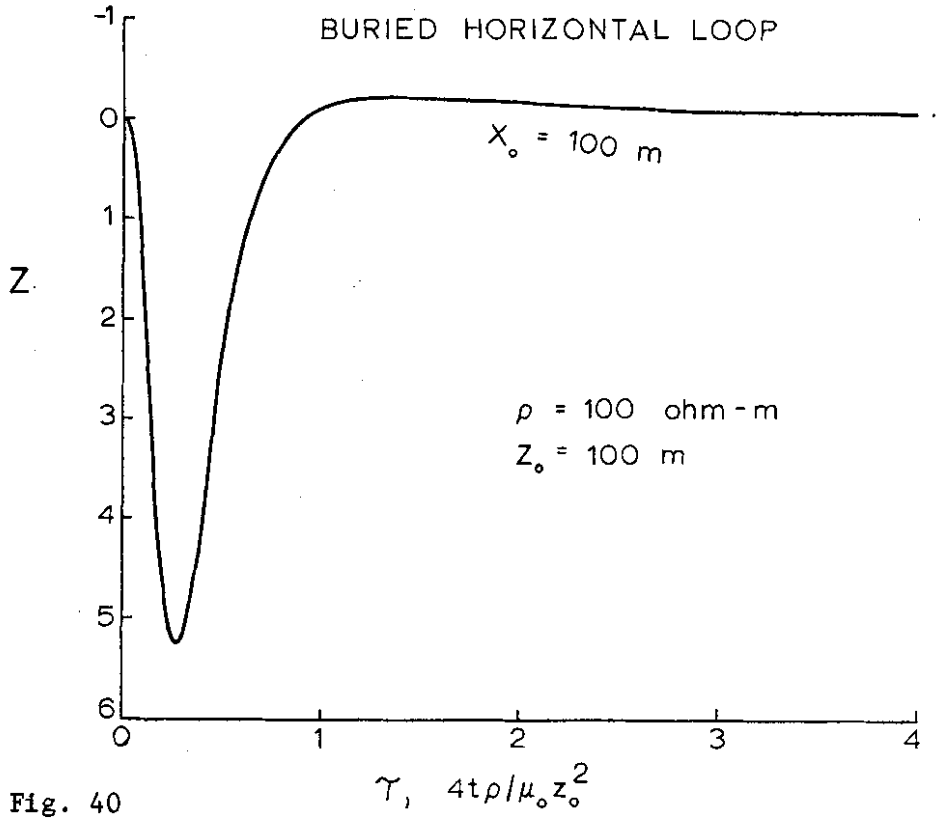
BURIED HORIZONTAL LOOP
X_o = 100 m
ρ = 100 ohm-m
Z_o = 100 m
Z
-1
0
1
2
3
4
5
6
0
1
2
3
4
τ, $4t\rho/\mu_o z_o^2$

Fig. 40

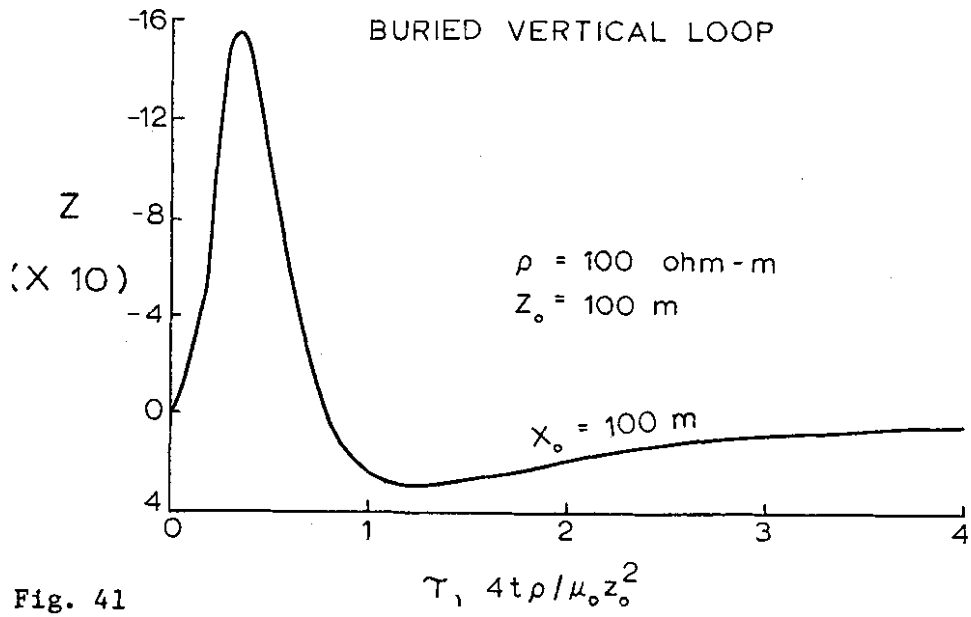
BURIED VERTICAL LOOP
ρ = 100 ohm-m
Z_o = 100 m
X_o = 100 m
Z
(X 10)
-16
-12
-8
-4
0
4
0
1
2
3
4
τ, $4t\rho/\mu_o z_o^2$

Fig. 41

where $f(t) * u(t)$ is the impulse response of the earth convolved with the step input function. In the frequency domain this mathematical operation can be written as $F(i\omega)/i\omega$ where $F(i\omega)$ represents the system function of the earth and $1/i\omega$ is the operator that will transform $F(i\omega)$ into the response for a step input function. Thus, if one uses a current input to the source antenna which is different from a sharp impulse $\delta(t)$, all he need do is to convolve that current input with the transient coupling response evaluated for impulsive excitation to analyze the resultant waveforms.

Several important points are deduced from theoretical considerations for downlink pulse signalling using a long insulated line transmitter grounded at the surface (Geyer, 1972a). For example, analysis of a variety of depths of burial and horizontal offsets of the receiving sensor from the surface line antenna indicates that doubling the depth to an electric field sensor reduces the coupling transient peak by approximately one order of magnitude, whereas the same increase in depth to a vertical loop receiver changes the magnitude of the coupling response by about two orders of magnitude. As the horizontal source-receiver offset distance becomes larger, the coupling transients for all field components decay less rapidly and positive signal peaks for the electric field occur later in time. All coupling transient responses increase as the square of the resistivity of the earth. Finally, all of these phenomena, as well as distinctions in amplitude and shape of the coupling transient responses, may be ascertained with a recorder which has a relatively fast rise time.

Experimental Downlink Pulse Signalling

The above theoretical considerations and calculations were made so that they could be used in the design and interpretation of an actual field transmission test. Prior to a downlink pulse transmission experiment performed at the U.S. Bureau of Mines Experimental Coal Mine, a study was made of the resistivity distribution of the overburden. This study was made so as to ensure proper interpretation of experimental coupling data with calculated theoretical coupling curves. A typical resistivity profile of the overburden at the Experimental Coal Mine is given in Figure 42. From this figure we may ascertain that the electrical properties of the overburden are relatively homogeneous and uniform, a situation not unexpected in light of the nature of the geology of the overburden which consists primarily of highly weathered shale with some silty laminae of sandstone. The average resistivity of the section shown in Profile Line 1NW-SE is about 177 ohm-meters.

In the pulse transmission experiment the line antenna at the surface was excited with a step current and the transient signal at the receiver location was sensed with a grounded insulated line receiver, amplified, displayed on a small Tektronix oscilloscope, and photographed with a camera. The length of the surface antenna was approximately 223 m, and the magnitude of the exciting step current 1 ampere. In this test the horizontal electrical field at zero offset distance was measured. The source antenna, which was separated from the buried receiver by approximately 23 m, was excited by driving a General Ratio 1308-A Power Amplifier (200 watts, 5 amperes maximum output) with a square-wave function generator.

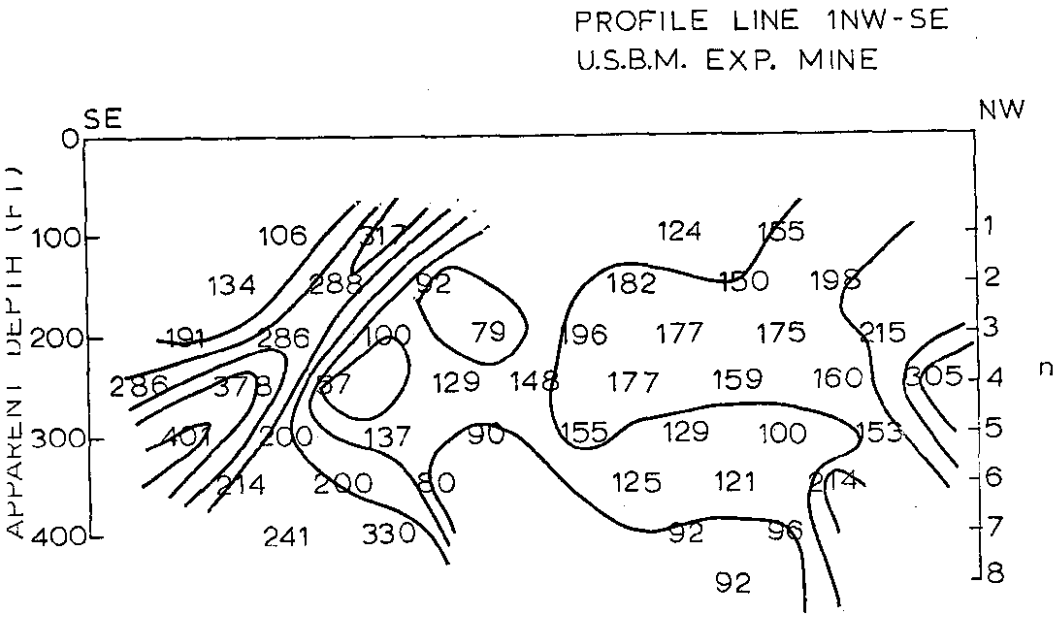

Fig. 42 Typical resistivity profile (in ohm-meters) of overburden at U. S. Bureau of Mines Experimental Coal Mine, Bruceton, Pennsylvania. Eltran galvanic array used in resistivity determination.

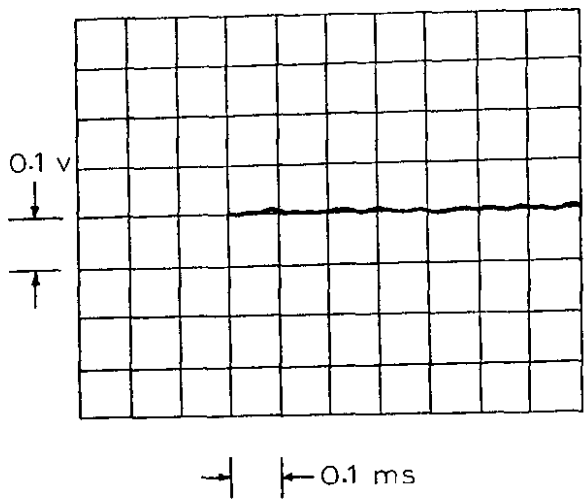

Fig. 43 Transient coupling for horizontal electric field without excitation of the line surface antenna as traced from a photograph of oscilloscope face. Gain is 30 db.

The transient coupling for the horizontal electric field without excitation of the line surface antenna is shown in Figure 43 (traced from a photograph of the coupling signal on the oscilloscope). The received transient coupling signal with excitation of the line surface antenna is shown in Figures 44 and 45, where Figure 45 displays the signal corrected for the gain of the amplifier and length of the receiver sensor. Figure 45 also illustrates the theoretical step response at the receiver location and shows reasonably close agreement with the field data. The differences evident in the theoretical step response and the actual response measured are interpreted to be the result of some factors; i.e. (1) the theoretical coupling curve used for comparison was that calculated assuming an infinitely long surface antenna rather than a finite horizontal electric dipole and (2) the system response of the amplifier system was not deconvolved out of the data illustrated in Figures 44 and 45.

At any rate, the results of the downlink pulse-type communication test (as opposed to C.W. tests) demonstrate the feasibility of a transient technique for through-the-earth signalling. One obvious advantage to a pulse-type technique is that a relatively large amount of frequency information is inherent in one pulse. However, a distinct disadvantage of a pulse-type communication system for signalling between the surface and a mine working is that ambient noise backgrounds, particularly in the "late-time" part of the transient coupling response, will lead to reduced signal/noise ratios at practical transmitter power output levels (between 10 and 100 watts). At the U.S. Bureau of Mines Experimental Mine, this constraint was not a serious limitation; however, in a large operating coal mine, measured electrical noise environment levels (Geyer, et al, 1971b) suggest that a receiver system for a pulse-type system would have to be designed so as to account for decreased signal-to-noise ratios in the late-time (after the zero crossings) part of the transient response.

Continuous Wave Field Transmission Tests

The implications of the use of either a short line source or a loop source buried at depth within a mine working have already been discussed with regard to possible location schemes. In this part of the report we examine in greater detail uplink communication techniques and actual tests from a mine working to the surface so that we may be able to gain insight into which source-receiver configuration might be best to use under a given set of circumstances. It was examined that how well the coupling signals correspond to what theory predicts, how many distortion effects (due to sources of noise and secondary scattering; i.e. power lines, buried pipes and rails, mine machinery, etc.) are seen which affect communications, and how one may avoid distorting structures by a judicious choice of the type of measurements he will make. In addition, we will be able to observe in first-hand fashion what the effect of large transmitting loops (i.e., finite loops) have on the nature of propagated electromagnetic fields measured at the earth's surface; thus something can be said about wavetilt, actual magnitudes of the measured field components, and maxima and null phenomena in the surface field components as they relate to the size of the transmitting antenna loop.

One technique, then, for communications from a mine working to the surface would involve the excitation of an insulated loop of wire with continuous wave audio-frequency current, where the loop of wire might be that which is wound about a mine pillar. One would then measure the produced electromagnetic field at the earth's surface. For example, the produced magnetic field could be

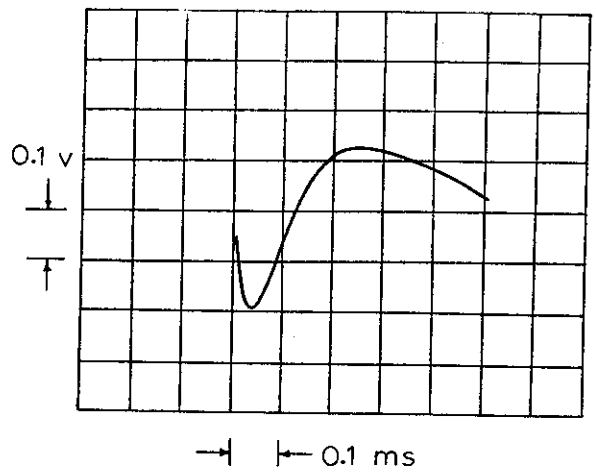

Fig. 44 Transient coupling for horizontal electric field with excitation of the line surface antenna as traced from a photograph of oscilloscope face. Gain is 30 db.

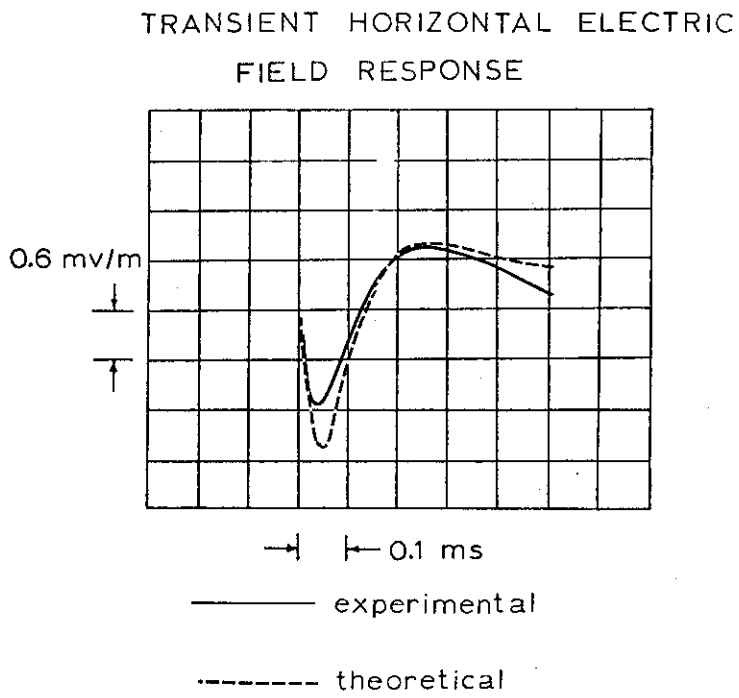

Fig. 45 Transient horizontal electric field signal corrected for gain of amplifier system and length of receiver sensor.

measured by using two small induction loops; by noting spatial changes in the amplitude voltage response through either induction loop, one can, in addition to establishing a communications link, triangulate on the position of the buried transmitter. Actual field tests were made using this source-receiver configuration, which is illustrated in Figure 46.

The other alternative for through-the-earth uplink or downlink voice transmission involves the use of an insulated wire which is grounded at both ends and which is excited with C.W. audio-frequency current or with a strong impulsive current. Excitation of a line source with a strong impulsive current together with experimental results has already been discussed. Here the first mode of antenna excitation -- that of C.W. audio-frequency current -- is discussed.

During the summer months of 1972 (June - September) numerous transmission tests, both uplink and downlink, were made at the United States Bureau of Mines Experimental Coal REsearch Mine in Bruceton, Pennsylvania, and the U.S. Steel Rubina No. 4 Coal Mine in Uniontown, Pennsylvania, using various source-receiver configurations. This section of the report discusses the results of several of those transmission tests in which a line current source was used as the transmitting antenna. Such a configuration is shown in Figure 47. The transmission tests were made over a relatively broad band of frequencies and at a number of different geographic setups.

Horizontal Electric Field Measurements - Buried Line Source Transmitter - U.S. Bureau of Mines Experimental Coal Research Mine, Bruceton, Pennsylvania

In Figures 48, 49, 50, 51, and 52 are summarized typical C.W. mutual coupling transmission data taken at the U.S. Bureau of Mines Experimental Coal Research Mine at Bruceton, Pennsylvania, where measurements of the horizontal electric field at the surface over a broad range in audio frequency were made. In these transmission tests only the component of the surface horizontal electric field which is parallel to the direction of the buried line transmitting antenna was measured. These data are corrected for the calibration response of a 60 Hertz filter-amplifier system and are normalized by the source strength moment of the line transmitter (i.e., the product of the current output to the transmitting antenna and the length of the transmitting antenna). Note that the normalization is by the current output (rather than by the power output) since the amount of current with which one is able to power the transmitter changes with frequency, normally decreasing with frequency. Because the strength of the source transmitter is proportional to the current (the current may often decrease while driving voltages increase, thus keeping the output power levels constant), it is probably best that mutual coupling data be presented in this fashion.

The location of the buried line source transmitter, which consisted of a 45 meter length of AWG #18 gauge insulated copper wire grounded at distant ends with copper-clad steel stakes driven into the ground (roof bolts could also be used for the ground return electrodes, but in this case care should be taken to reduce the contact resistance of the roof bolts by either filing of the normally accumulated layers of rust or by using screw-set clamps), is shown in Figure 53. The line source transmitter was powered by a General Ratio Model 1308-A Power Oscillator (200 watt, 5 ampere maximum output). Output current levels from the

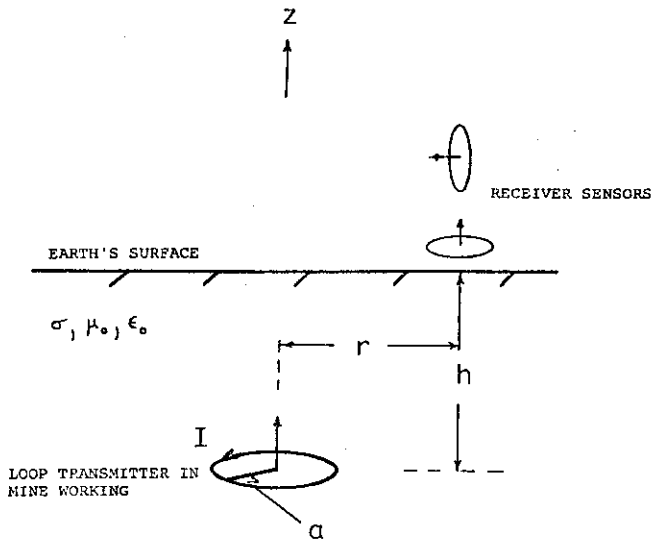

Fig. 46 Vertical-axis loop transmitter antenna and induction loop receiving sensors for uplink C.W. transmission.

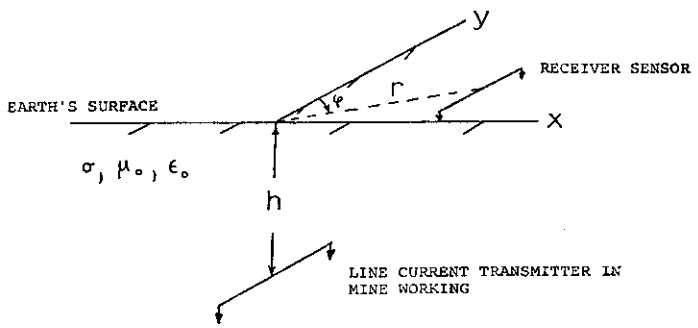

Fig. 47 Three-dimensional view of transmitter antenna and receiver sensor under consideration for uplink C.W. transmission.

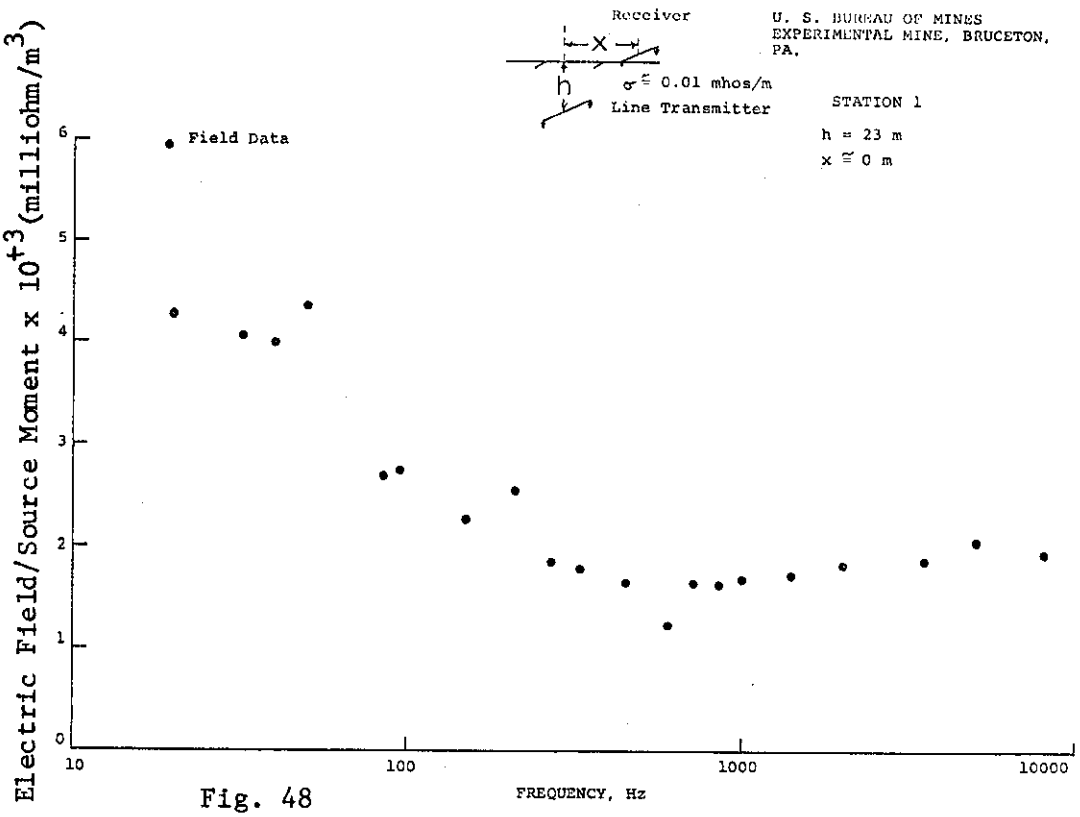
Receiver
X
h
σ ≅ 0.01 mhos/m
Line Transmitter
U. S. BUREAU OF MINES
EXPERIMENTAL MINE, BRUCETON,
PA.
STATION 1
h = 23 m
x ≅ 0 m
Field Data
Electric Field/Source Moment x 10+3 (milliohm/m3)
FREQUENCY, Hz
0
1
2
3
4
5
6
10
100
1000
10000

Fig. 48

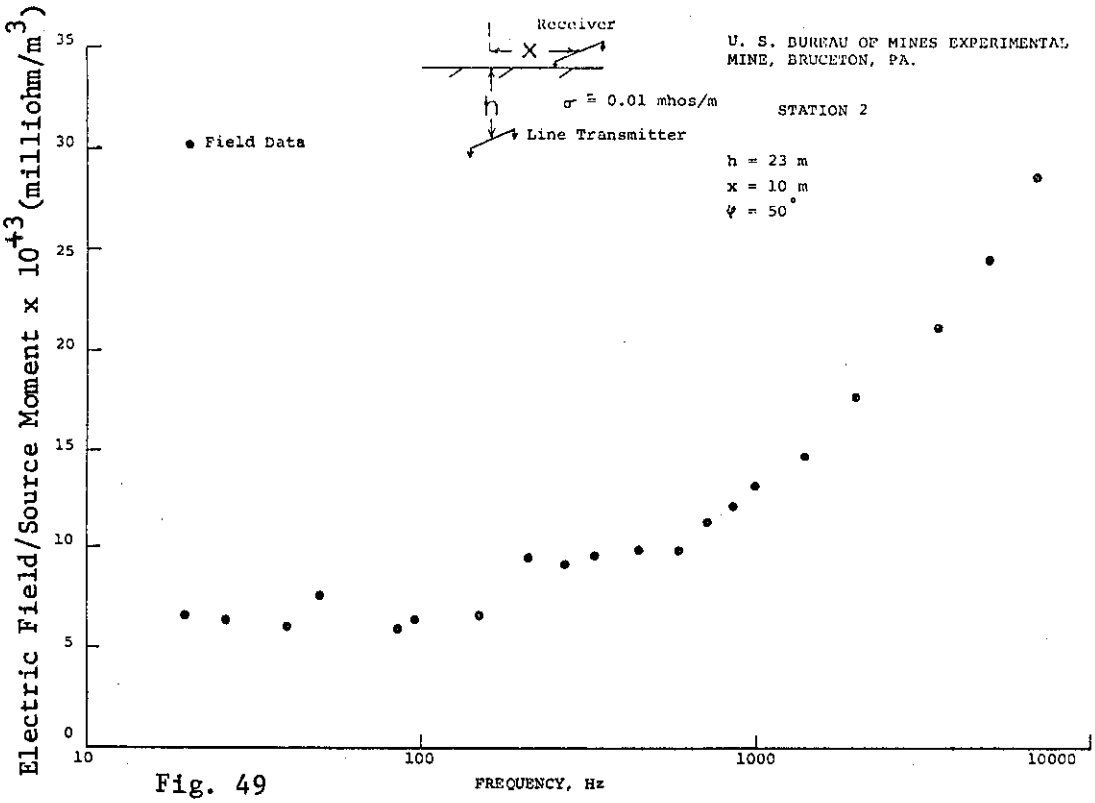
Receiver
X
h
σ ≅ 0.01 mhos/m
Line Transmitter
U. S. BUREAU OF MINES EXPERIMENTAL
MINE, BRUCETON, PA.
STATION 2
h = 23 m
x = 10 m
φ = 50°
Field Data
Electric Field/Source Moment x 10+3 (milliohm/m3)
FREQUENCY, Hz
0
5
10
15
20
25
30
35
10
100
1000
10000

Fig. 49

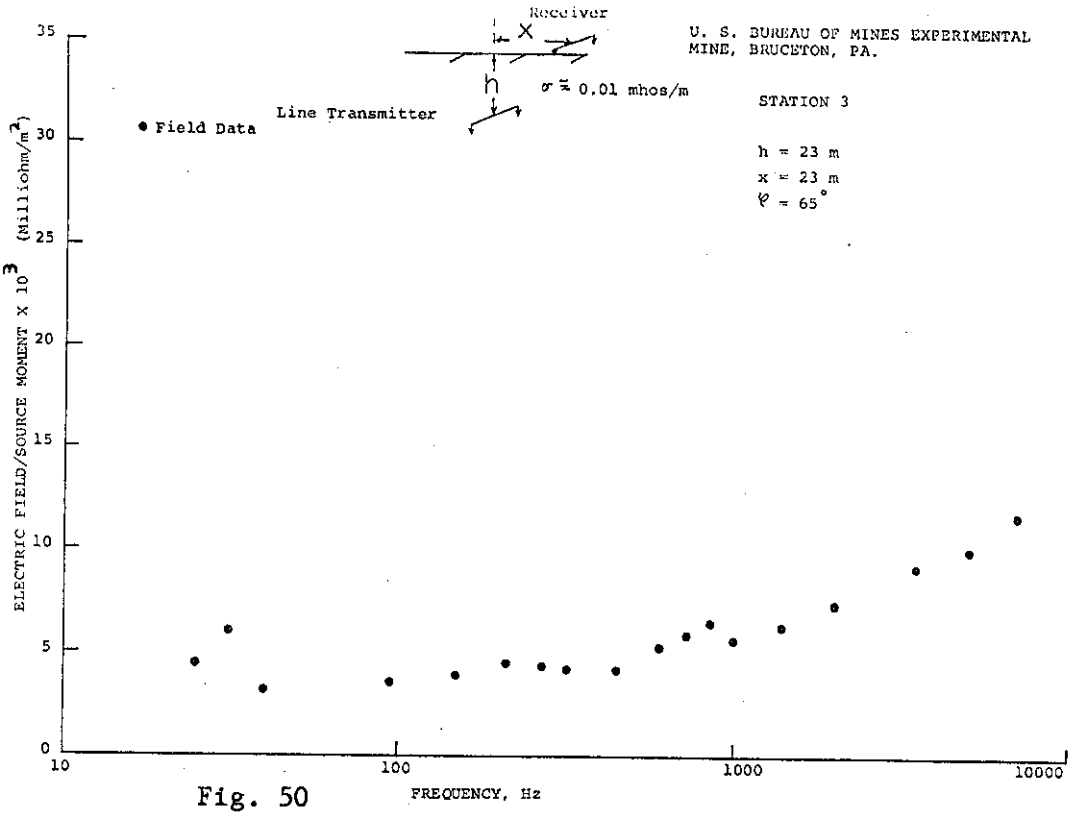
Receiver
U. S. BUREAU OF MINES EXPERIMENTAL MINE, BRUCETON, PA.
h
σ ≅ 0.01 mhos/m
Line Transmitter
STATION 3
● Field Data
h = 23 m
x = 23 m
φ = 65°
ELECTRIC FIELD/SOURCE MOMENT X 10³ (Milliohm/m²)
35
30
25
20
15
10
5
0
10
100
1000
10000
FREQUENCY, Hz

Fig. 50

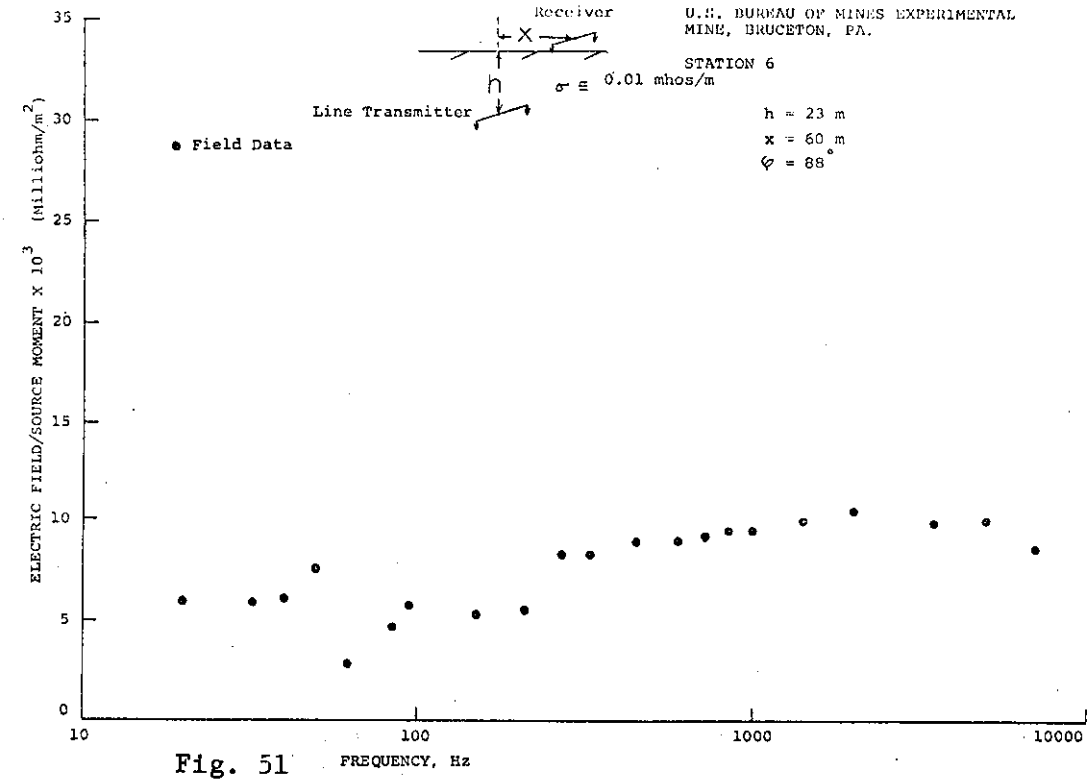
Receiver
U.S. BUREAU OF MINES EXPERIMENTAL MINE, BRUCETON, PA.
STATION 6
h
σ ≅ 0.01 mhos/m
Line Transmitter
● Field Data
h = 23 m
x = 60 m
φ = 88°
ELECTRIC FIELD/SOURCE MOMENT X 10³ (Milliohm/m²)
35
30
25
20
15
10
5
0
10
100
1000
10000
FREQUENCY, Hz

Fig. 51

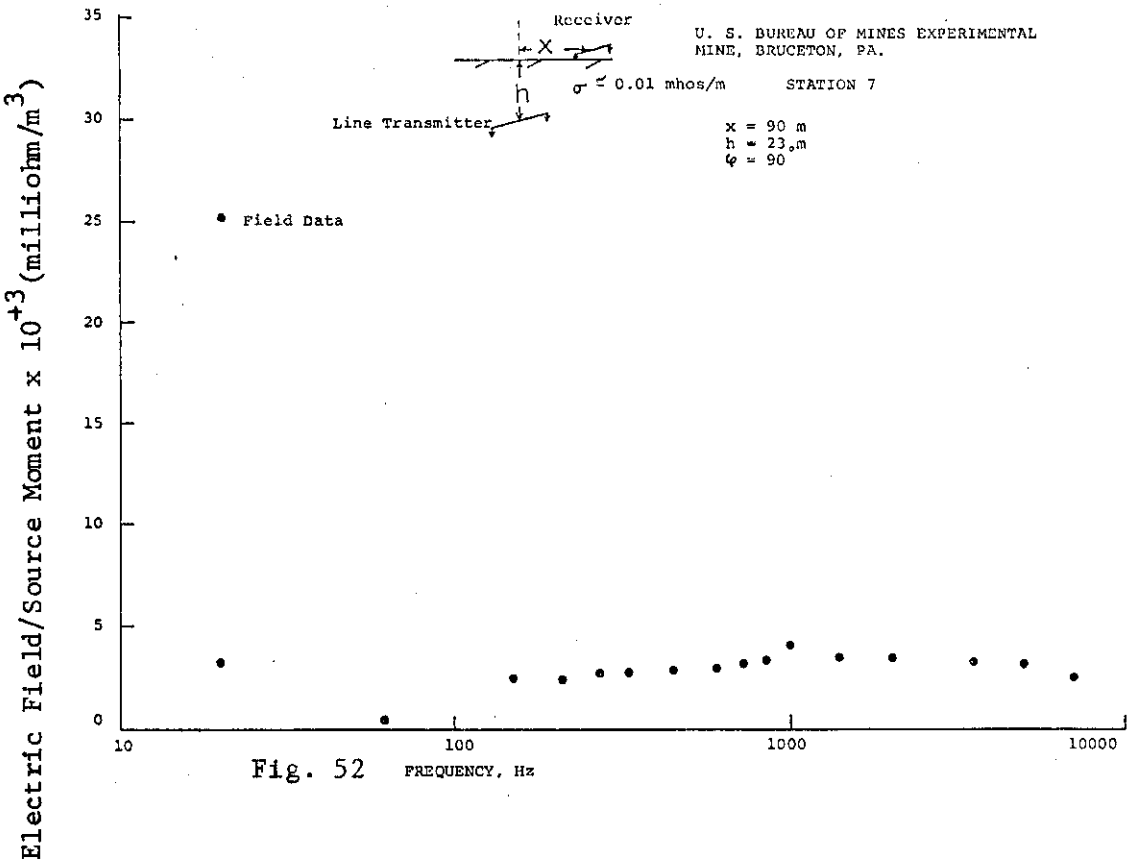
Receiver
X
h
Line Transmitter
U. S. BUREAU OF MINES EXPERIMENTAL MINE, BRUCETON, PA.
σ ≃ 0.01 mhos/m
STATION 7
x = 90 m
h = 23 m
φ = 90
Field Data
Electric Field/Source Moment x 10+3 (milliohm/m3)
35
30
25
20
15
10
5
0
10
100
1000
10000
FREQUENCY, Hz

Fig. 52

line transmitter into the ground varied from about 0.8 ampere at 20 Hertz to about 0.2 ampere at 20,000 Hertz. The surface locations of the various receiver sites are also shown in Figure 53, where the angles between the center of the surface projection of the line transmitter and the centers of the various electric-field receiving electrode setups are indicated.

Surface electric field measurements were made with non-polarizing electrodes (metal immersed in a solution of one of its salts) oriented in a direction parallel to the buried line transmitter. Such stable, non-polarizing electrodes were used so that electrolytic potentials would not be built up between the electrodes and the solutions in soil pores. The potential difference between the surface receiver electrodes was measured with a Hewlett-Packard Model 3410A Tunable Phase-Lock Microvoltmeter; this microvoltmeter has an input impedance of 10 megohms and is capable of measuring coherent signal levels 10 db below random ambient electromagnetic noise levels (white noise). A typical cross-section of field-collected electrical resistivity data over the U.S. Bureau of Mines Bruceton Mine was illustrated in Figure 42.

The C.W. coupling transmission data given in Figures 48-52 show, in general, good agreement with what might be predicted theoretically for an average resistivity of the overburden of about 100 ohm-meters. Namely, two features of the field data clearly stand out, as illustrated in Figure 54: (1) the parallel electric field strengths decay exponentially with increasing offset from the buried line transmitter, and (2) parallel electric field signals produced at the earth's surface per unit source moment are larger at lower frequencies.

A peculiar feature not predicted by any theoretical considerations which is particularly evident in the nature of the received electric field signals at station setups 2 and 3 is the observation that the coupling transmission signals (normalized by the strength of the source antenna) actually increased with increasing frequency. Moreover, there is almost negligible scatter in this data! The exact reason for this field result (which is opposite to what would be predicted by theory) is not known. However, it is thought that the power line which ran directly overhead parallel to the buried transmitter (NE-SW), as well as the surface pipe lines which were present, could have acted as secondary noise and scattering sources with efficiency of signal coupling in this case increasing with frequency.

Vertical Magnetic Field Measurements - Buried Vertical-Axis Loop Transmitter - U.S. Bureau of Mines Experimental Coal Research Mine, Bruceton, Pennsylvania

According to theoretical considerations (Wait, 1970; Wait and Spies, 1971d) the amplitudes of the vertical and horizontal magnetic field components, respectively, produced at the earth's surface by a buried vertical-axis insulated loop carrying alternating current are given by the following expressions:

$$|H_z| = \frac{a^2 I}{2h^3} |Q| \tag{34}$$

and

$$|H_\rho| = \frac{a^2 I}{2h^3} |M| \tag{35}$$

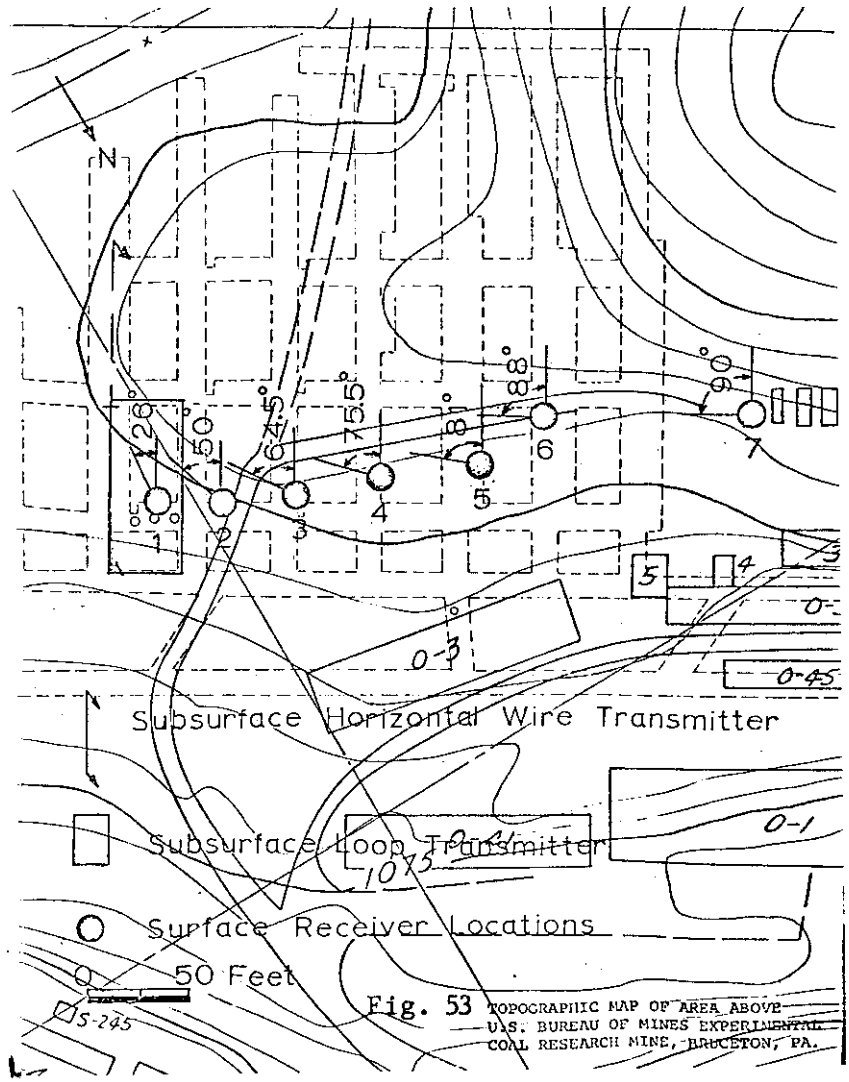

Fig. 53 TOPOGRAPHIC MAP OF AREA ABOVE U.S. BUREAU OF MINES EXPERIMENTAL COAL RESEARCH MINE, BRUCETON, PA.

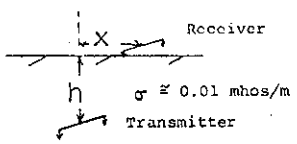

U. S. BUREAU OF MINES EXPERIMENTAL MINE, BRUCETON, PA.

h ≅ 23 m

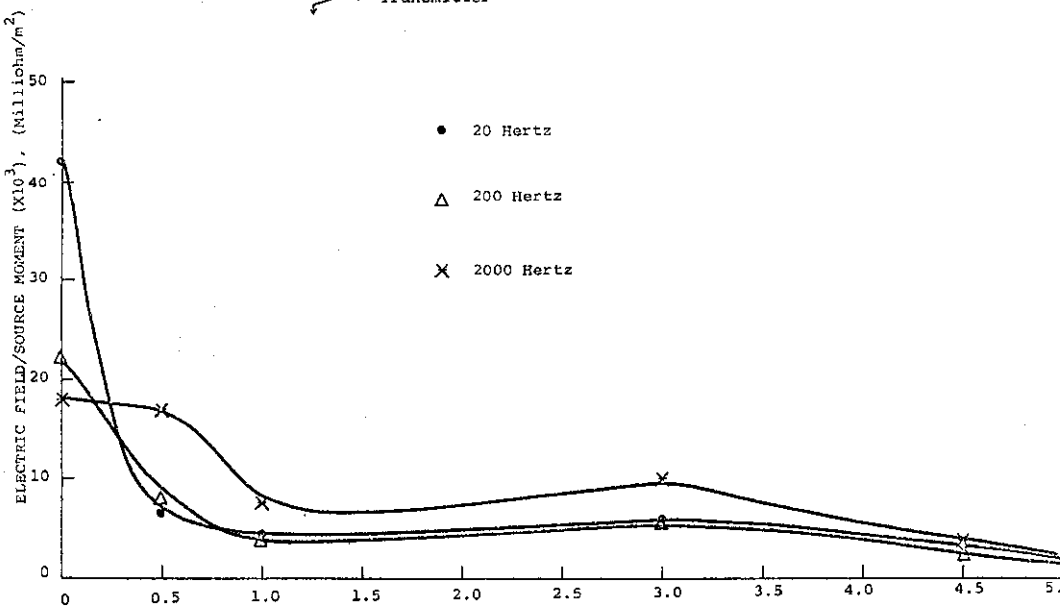

Fig. 54 NORMALIZED OFFSET FROM BURIED LINE TRANSMITTER, x/h

where the attenuation factors $|Q|$ and $|M|$ are not simply exponential functions of the separation between the source antenna and receiving sensor, but are rather given by the dimensionless expressions,

$$|Q| = \left| \int_0^\infty \frac{J_1(Ax)}{(Ax/2)} \frac{x^3 e^{-Zx} e^{-(x^2+iH^2)^{\frac{1}{2}}}}{(x^2+iH^2)^{\frac{1}{2}} + x} J_o(Dx)dx \right| \tag{36}$$

$$|M| = \left| \int_0^\infty \frac{J_1(Ax)}{(Ax/2)} \frac{x^2(x^2+iH^2)^{\frac{1}{2}} e^{-Zx} e^{-(x^2+iH^2)^{\frac{1}{2}}}}{(x^2+iH^2)^{\frac{1}{2}} + x} J_1(Dx)dx \right| \tag{37}$$

Here J_o and J_1 are Bessel functions, D is the horizontal offset distance ρ divided by the depth of burial h, and H is the product $h(2\pi f\sigma\mu_o)^{\frac{1}{2}}$. The symbol A represents the ratio of the radius of the source loop to the depth of burial of the source loop; as noted previously (Wait and Spies, 1971d; Geyer, et al, 1972b) the theoretical offset positions of the amplitude nulls in the surface vertical magnetic field as well as the peak in the surface horizontal magnetic field depend on the parameter A. For example, as the radius of the source loop transmitter becomes large relative to its depth of burial (say twice as large), the offset null position in the vertical magnetic field can shift by approximately 70% at near static conditions to about 100% at higher frequencies (see Figure 55). In addition, the actual magnitude of $|Q|$ directly over the source antenna decreases as $A \triangleq a/h$ increases. Figure 56 illustrates percent changes in $|Q|$ relative to static coupling directly over the buried vertical-axis loop transmitter as the radius of the transmitting loop becomes equal to the depth of burial (a/h = 1) or becomes equal to twice the depth of burial (a/h = 2). These phenomena in themselves are not detrimental to a communications scheme. They must be recognized, however, if one wishes to map the nulls in the surface vertical magnetic field and use them as location criteria.

For static conditions the size of the loop does not affect the sharpness of the null in the vertical magnetic field (which for a very small loop ($a/h \simeq 0$) occurs at an offset distance from the transmitter equal to about 1.4 times the depth of burial of the transmitter), ambient electromagnetic noise factors being equal. The effect of increasing the frequency of transmission tends to blur or make less distinct these nulls. For field purposes, however, the offset positioning of these nulls (though less distinct) is not significantly affected. In a similar fashion, an increase in the electrical conductivity σ of the overburden tends to blur the distinctness of these nulls while not significantly affecting the offset position of the null. This phenomenon is to be expected, since for a given depth of burial h to the transmitter and a given size A = a/h of the transmitter, it is really the product $(\sigma f)^{\frac{1}{2}}$ which determines the sharpness of the null.

The above discussion leads to several deductions. For one, if an attempt is made to measure absolute amplitudes of the vertical magnetic field with a vertical-axis induction loop as a means for locating a buried transmitter in a mine working, there is a necessity for knowing quite accurately both the effective electrical conductivity of the overburden as well as the size of the transmitting loop antenna. Generally, a priori knowledge is at hand on the depth of burial and frequency of transmission, but it may not always be practical to know what the effective size of the transmitting antenna is unless a standard is

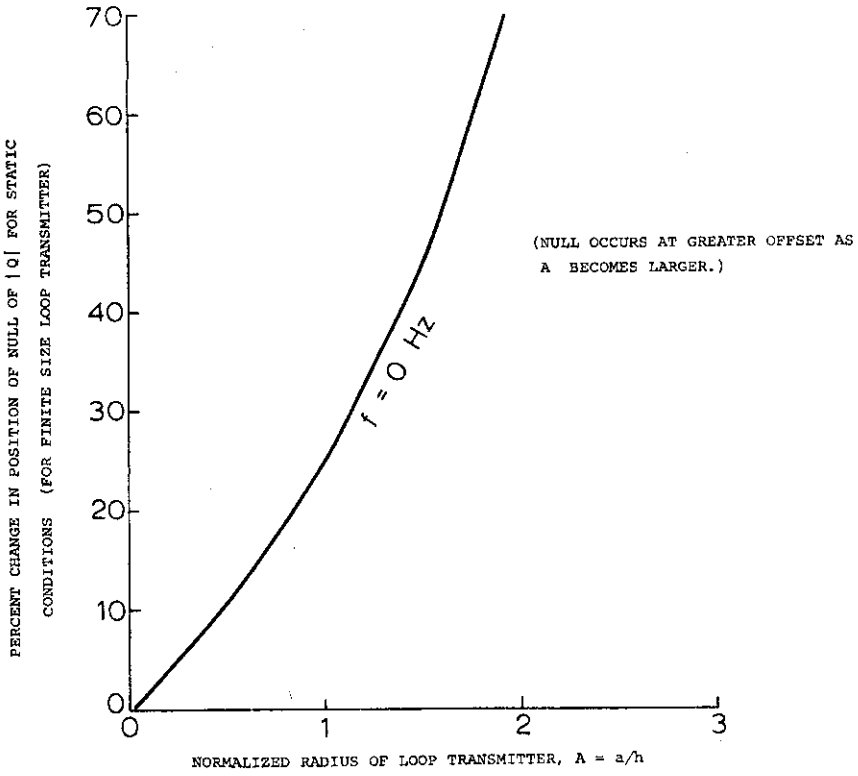
PERCENT CHANGE IN POSITION OF NULL OF |Q| FOR STATIC CONDITIONS (FOR FINITE SIZE LOOP TRANSMITTER)
70
60
50
40
30
20
10
0
0
1
2
3
f = 0 Hz
(NULL OCCURS AT GREATER OFFSET AS A BECOMES LARGER.)
NORMALIZED RADIUS OF LOOP TRANSMITTER, A = a/h

Fig. 55

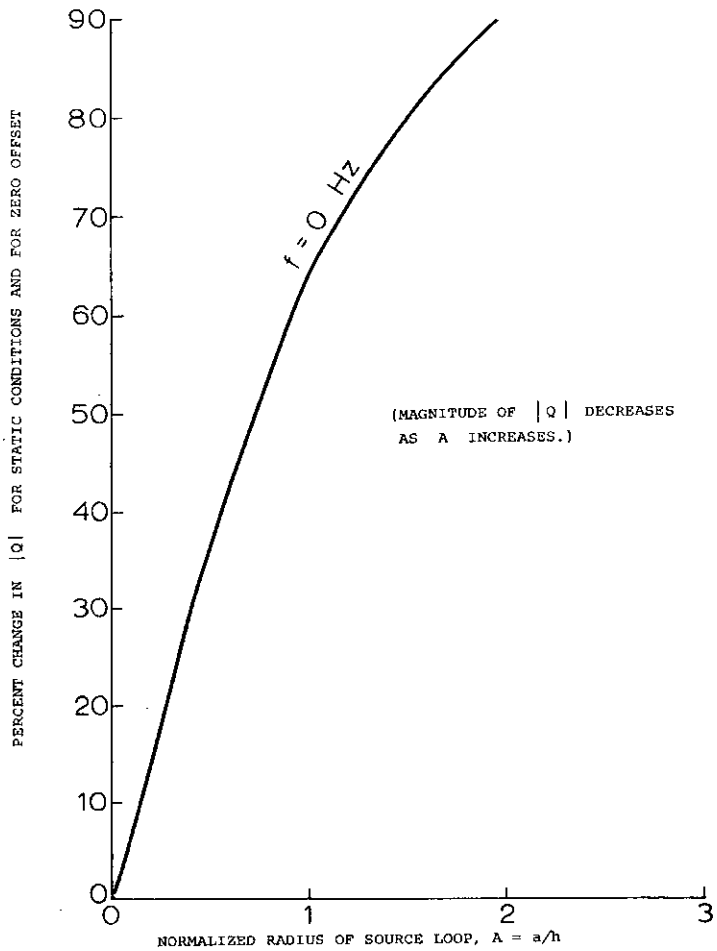
PERCENT CHANGE IN |Q| FOR STATIC CONDITIONS AND FOR ZERO OFFSET
90
80
70
60
50
40
30
20
10
0
0
1
2
3
f = 0 Hz
(MAGNITUDE OF |Q| DECREASES AS A INCREASES.)
NORMALIZED RADIUS OF SOURCE LOOP, A = a/h

Fig. 56

both set and implemented. As a general rule (Geyer and Keller, 1971b) it was found that electrical conductivities within any given coal mining district do not change by more than 10:1. Changes in electrical conductivity of the overburden from one coal mining region to another (e.g., from eastern Colorado to West Virginia), however, can vary as much as 100:1. Of course, exceptions to the above rule-of-thumb exist, and the generalizations made above would probably not hold in metal mine districts, metal mine regions being usually quite inhomogeneous electrically. At this juncture, a trade-off exists: namely, the effect of electrical inhomogeneities on the field behavior may be minimized by decreasing the frequency of transmission; however, by using lower frequencies and keeping output transmitter power constraints the same, one generally has lower signal/noise ratios. The latter effect often overshadows any effects of electrical inhomogeneities.

In Figures 57-61 are summarized typical C.W. mutual coupling data taken at the U.S. Bureau of Mines Experimental Coal Research Mine at Bruceton, Pennsylvania, where measurements of the vertical magnetic field at the surface over a broad range in audio frequency were made. These data are corrected for the calibration response of a 60 Hertz filter-amplifier system, for change in effective area of the receiving loop sensor (e.m.f. induced in loop = effective area X magnetic permeability of freespace X $2\pi f$ X vertical magnetic field) and by the current output to the transmitting antenna since the amount of current with which one is able to power the transmitter changes with frequency (normally decreasing with increasing frequency as noted earlier). Because the strength of the source transmitter is proportional to the current, it is probably best that mutual coupling data be presented in this fashion. Moreover, the form of presentation of the empirical data (attenuation function $|Q|$ in Figures 57-61 also corresponds to that used by Wait (1971a) and thus provides for ready comparison with theoretical calculations over prespecified models.

The location of the buried vertical-axis loop transmitter, which consisted of 5 turns of AWG #18 gauge insulated copper wire wound around a pillar beneath station 1 and powered by a General Radio Model 1308-A power oscillator (200 watt, 5 ampere maximum output), is shown in Figure 53. Surface measurements were made with an air-core loop sensor whose effective area and impedance were measured in the laboratory (see Figure 62) and whose diameter is 1 meter. E.m.f.'s induced in the induction loop sensor were measured with a Hewlett-Packard Model 3410-A Phase-Lock Microvoltmeter which could measure coherent signal levels 10 db below ambient electromagnetic noise levels. The effective radius of the source loop antenna in this case for uplink transmissions was approximately 0.39 the depth of burial. An average conductivity of 0.01 mhos/meter was taken for the overburden for theoretical comparisons. This choice was made from the field resistivity data collected on the surface (Geyer and Keller, 1972b); a typical profile over the mine workings at the U.S. Bureau of Mines Bruceton Mine is shown in Figure 42.

The mutual coupling curve for the vertical magnetic field at station 1 is shown in Figure 57 as a function of frequency from 20 Hertz to 10,000 Hertz. At this station the offset distance ρ was approximately zero so that $D \triangleq \rho/h \simeq 0$. The field data demonstrate close agreement with the theoretical considerations of Wait and Spies (1971a) except at 32 Hertz and 330 Hertz, where large noise levels were noted. Another observation which should be noted from Figures 57-61

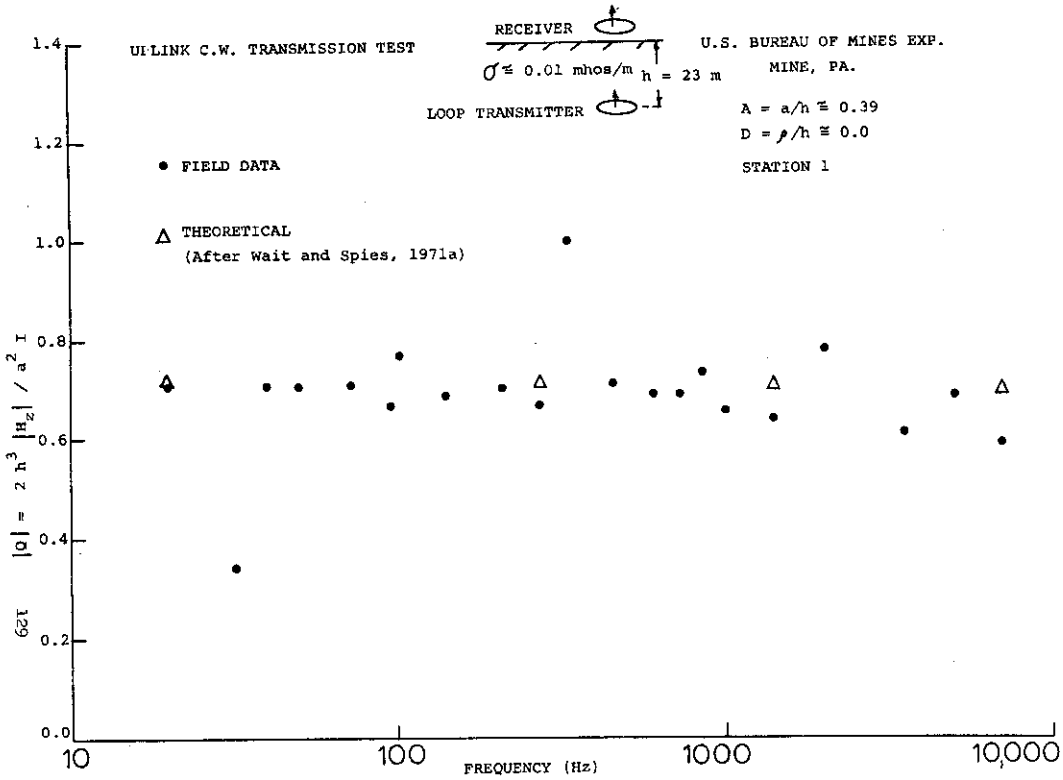
UPLINK C.W. TRANSMISSION TEST
RECEIVER
σ ≅ 0.01 mhos/m
h = 23 m
LOOP TRANSMITTER
U.S. BUREAU OF MINES EXP. MINE, PA.
A = a/h ≅ 0.39
D = ρ/h ≅ 0.0
STATION 1
• FIELD DATA
Δ THEORETICAL
(After Wait and Spies, 1971a)
|Q| = 2 h³ |Hz| / a² I29
FREQUENCY (Hz)
1.4
1.2
1.0
0.8
0.6
0.4
0.2
0.0
10
100
1000
10,000

Fig. 57

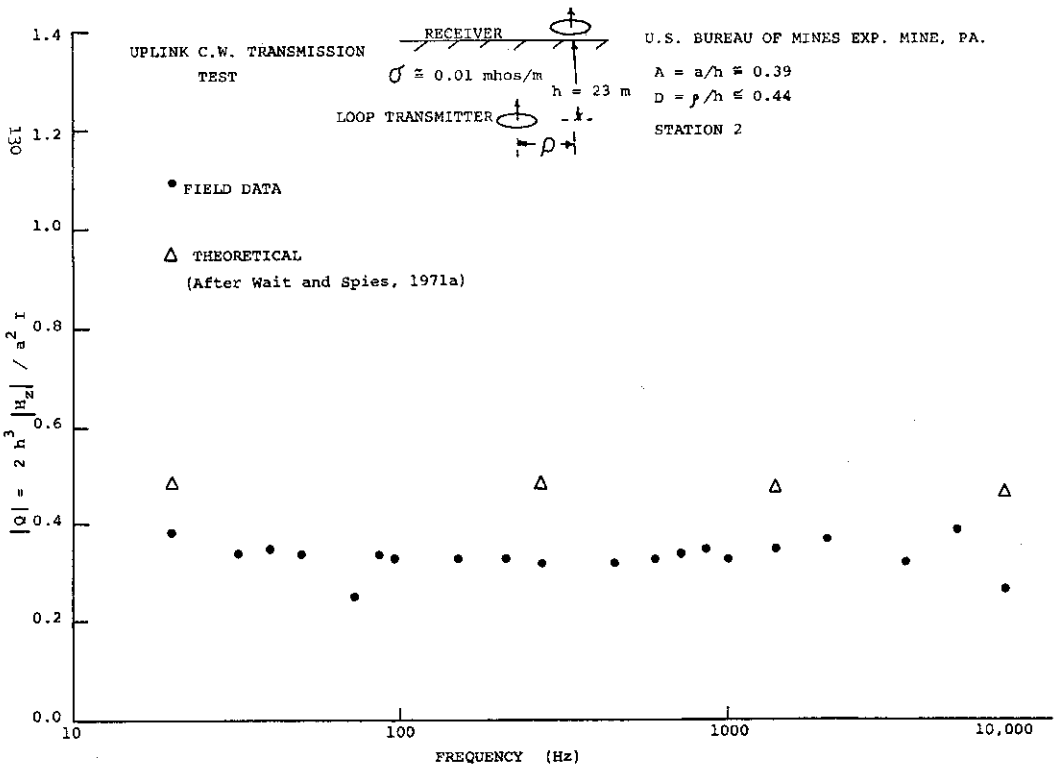
UPLINK C.W. TRANSMISSION TEST
RECEIVER
σ ≅ 0.01 mhos/m
h = 23 m
LOOP TRANSMITTER
ρ
U.S. BUREAU OF MINES EXP. MINE, PA.
A = a/h ≅ 0.39
D = ρ/h ≅ 0.44
STATION 2
• FIELD DATA
Δ THEORETICAL
(After Wait and Spies, 1971a)
|Q| = 2 h³ |Hz| / a² I30
FREQUENCY (Hz)
1.4
1.2
1.0
0.8
0.6
0.4
0.2
0.0
10
100
1000
10,000

Fig. 58

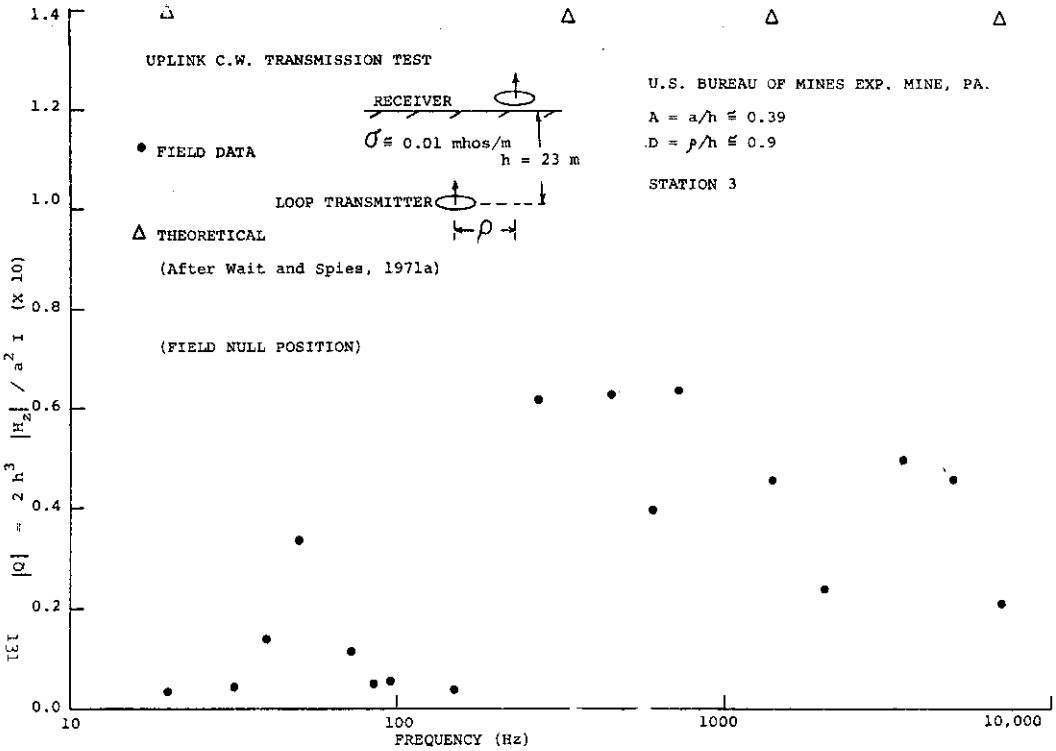
UPLINK C.W. TRANSMISSION TEST
RECEIVER
σ ≅ 0.01 mhos/m
h = 23 m
LOOP TRANSMITTER
ρ
U.S. BUREAU OF MINES EXP. MINE, PA.
A = a/h ≅ 0.39
D = ρ/h ≅ 0.9
STATION 3
FIELD DATA
THEORETICAL
(After Wait and Spies, 1971a)
(FIELD NULL POSITION)
|Q| = 2h³ |Hz| / a² I (X 10)
131
FREQUENCY (Hz)
1.4
1.2
1.0
0.8
0.6
0.4
0.2
0.0
10
100
1000
10,000

Fig. 59

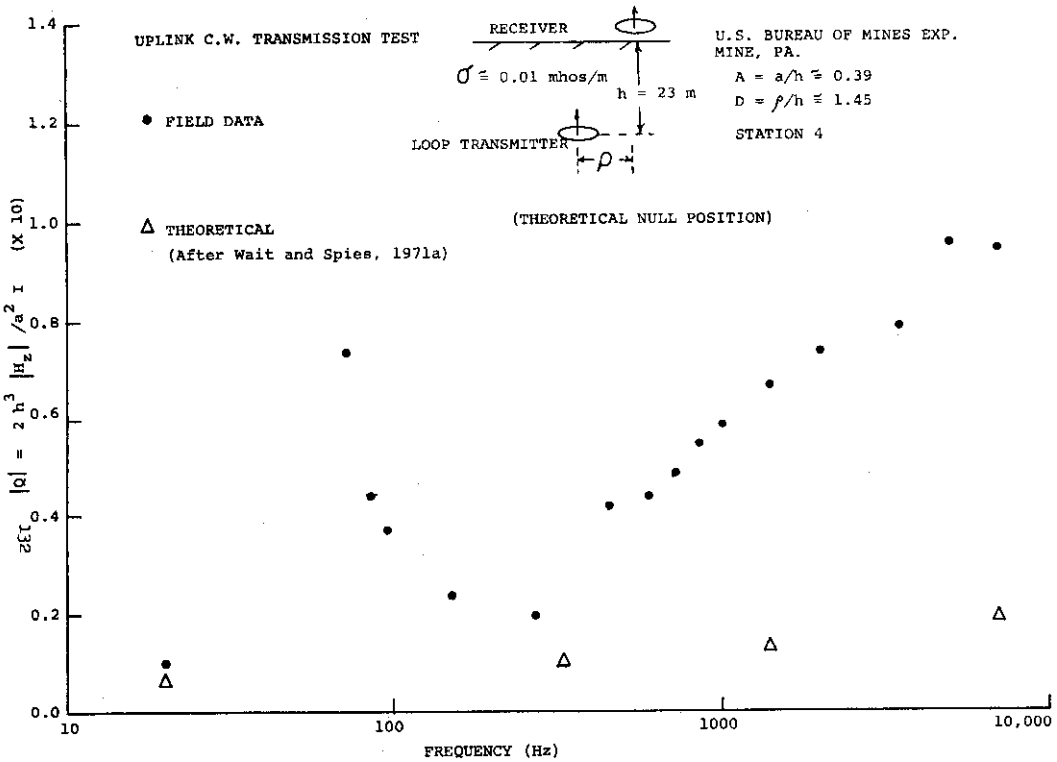
UPLINK C.W. TRANSMISSION TEST
RECEIVER
σ ≅ 0.01 mhos/m
h = 23 m
LOOP TRANSMITTER
ρ
U.S. BUREAU OF MINES EXP. MINE, PA.
A = a/h ≅ 0.39
D = ρ/h ≅ 1.45
STATION 4
FIELD DATA
THEORETICAL
(After Wait and Spies, 1971a)
(THEORETICAL NULL POSITION)
|Q| = 2h³ |Hz| /a² I (X 10)
132
FREQUENCY (Hz)
1.4
1.2
1.0
0.8
0.6
0.4
0.2
0.0
10
100
1000
10,000

Fig. 60

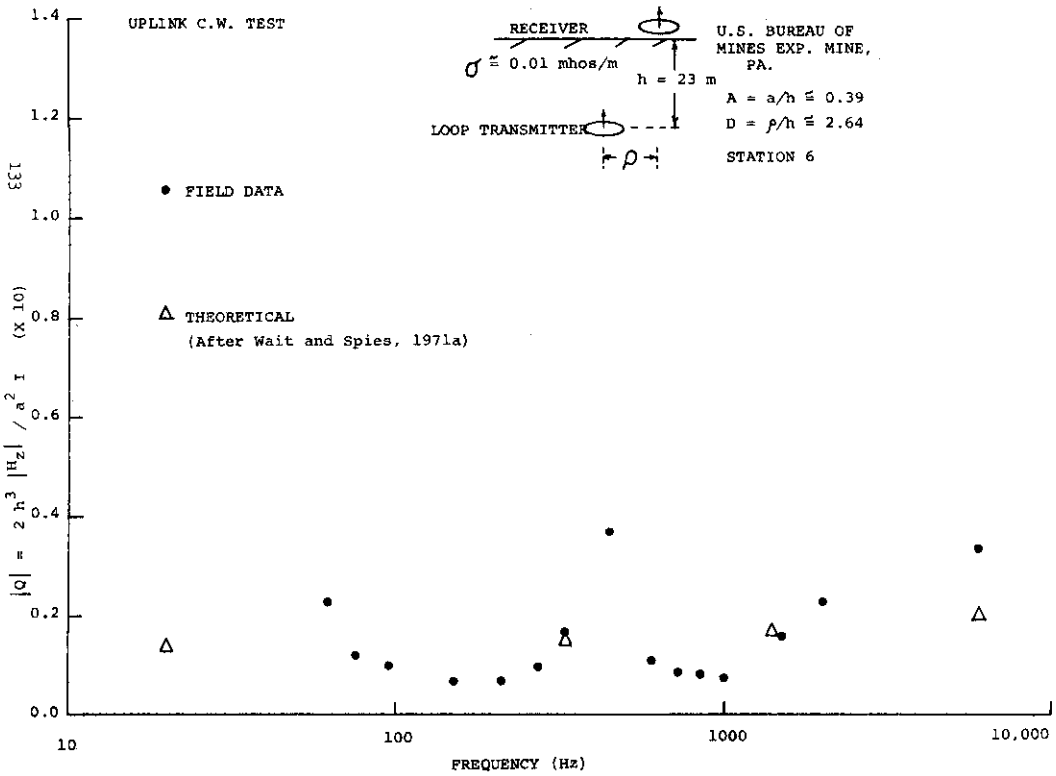
UPLINK C.W. TEST
RECEIVER
U.S. BUREAU OF MINES EXP. MINE, PA.
σ ≅ 0.01 mhos/m
h = 23 m
A = a/h ≅ 0.39
D = ρ/h ≅ 2.64
LOOP TRANSMITTER
ρ
STATION 6
FIELD DATA
THEORETICAL
(After Wait and Spies, 1971a)
|Q| = 2 h³ |Hz| / a² I (X 10)
1.4
1.2
1.0
0.8
0.6
0.4
0.2
0.0
10
100
1000
10,000
FREQUENCY (Hz)

Fig. 61

is that for any given geographic setup the response is essentially constant; that is, there is very little attenuation in the vertical magnetic field over the 10-10,000 Hertz frequency range when propagating through the overburden at the Bruceton Mine. Another way to say this is that the attenuation function Q does not decrease with the parameter $|(\pi f \mu_o \sigma)^{\frac{1}{2}} R|$ as quickly as the function $e^{-|(\pi f \mu_o \sigma)^{\frac{1}{2}} R|}$ (which function describes the attenuation dependence for a plane wave in a lossy medium).

At an offset distance equal to about four-tenths of the source antenna depth of burial (see Figure 58), good agreement with theoretical considerations was also attained, little scatter being present in the data. The mutual coupling responses measured at stations 3 and 4 (see Figures 59 and 60), however, show considerable scatter from theoretical calculations. I.e., a field null position in $|H_z|$ was detected at $D \simeq 1$ rather than the theoretical (static) $D \simeq 1.4$. This observed scatter may be explained in the following way. Close to stations 3 and 4 (see Figure 62) were located both surface pipelines and overhead NE-SW powerlines. The effect of the overhead powerlines and/or the surface pipelines may have been responsible for shifting the null position in $|H_z|$; i.e., either the powerline or the pipelines or both may have been excited by the buried loop antenna which, in turn, acted as secondary scattering sources and led to distortion of the profile of the attenuation function $|Q|$ as measurements were taken close to them. The reason why such scatter was not present in measurements taken at station setup 2 is that the signal/noise ratio was higher (instrumentation used was capable of measuring signal levels which were 10 db less than ambient electromagnetic random noise levels).

Such an explanation seems quite reasonable when the theoretical effects of conductive rails and pipes are considered. Wait (1971f) and Howard (1972) have considered the effect of cylindrical conductors buried in the earth when they are excited by a long uniform line source of current on the surface and have shown the shift in the subsurface vertical magnetic field null directly under the surface line antenna in a direction away from the cylindrical scattering conductor. Although this model is not that which was present in the actual field tests, it does provide an intuitive feel and answer for the behavior of electromagnetic fields excited by other sources in the presence of such scattering conductors. It perhaps should be emphasized that such scattering effects (noise factors aside) can be limitations in schemes which attempt to map nulls for location purposes. The scattering problem of conductive bodies under excitation by dipolar sources is not at all trivial, and recently some notable progress has been made in gaining insight into such distorting effects (Wait and Hill, 1973a; Hill and Wait, 1973b; Hill and Wait, 1973c).

At an offset distance from the subsurface antenna axis of 60 meters (station setup 6) close agreement with theory again was attained. As predicted by theory the vertical magnetic field produced at the surface is at a maximum directly over the vertical-axis loop antenna, drops to a null position at an offset distance of about 1.5 times the depth of burial of the source antenna, builds up to a second maximum (which is about 20 db lower than that directly over the source), and then continues to fall off with increasing distance. These phenomena are summarized in Figure 63 at four different transmission frequencies (20 Hz, 100 Hz, 1000 Hz, and 7000 Hz). Figure 63 shows that the measured field null at these frequencies did not coincide with that expected

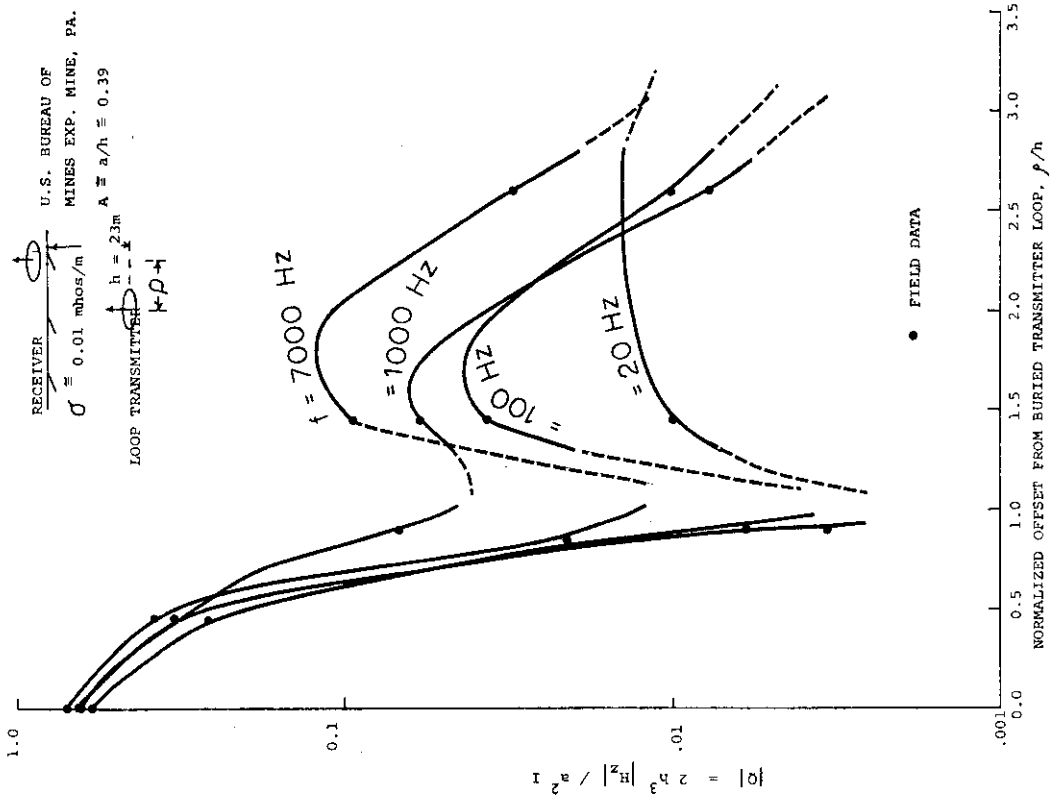
RECEIVER
σ ≅ 0.01 mhos/m
U.S. BUREAU OF
MINES EXP. MINE, PA.
A ≅ a/h ≅ 0.39
LOOP TRANSMITTER
h = 23m
f = 7000 HZ
= 1000 HZ
= 100 HZ
= 20 HZ
• FIELD DATA
|Q| = 2 h³ |Hz| / a² I
NORMALIZED OFFSET FROM BURIED TRANSMITTER LOOP, ρ/h

Fig. 63

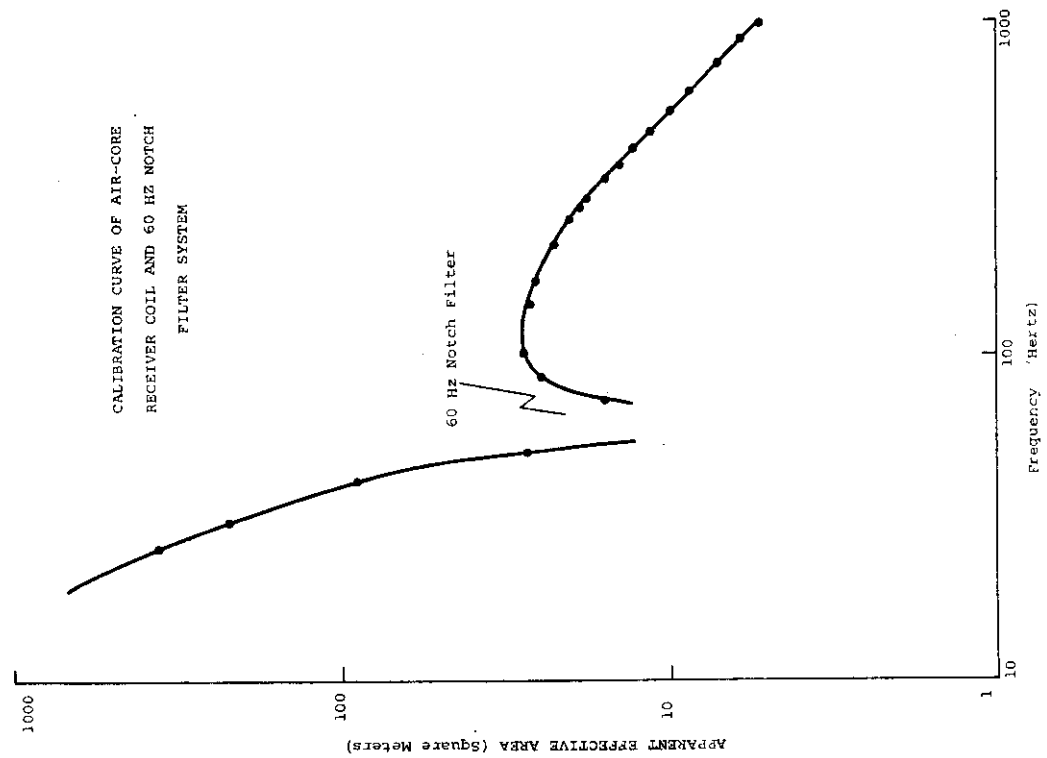
CALIBRATION CURVE OF AIR-CORE
RECEIVER COIL AND 60 HZ NOTCH
FILTER SYSTEM
60 Hz Notch Filter
APPARENT EFFECTIVE AREA (Square Meters)
Frequency (Hertz)

Fig. 62

theoretically, being slightly skewed to smaller offset distances. These data also show a shift in the null toward greater offsets as frequency (or "H") increases; this shift is similar to that predicted by theory (Wait and Spies, 1971a).

The supposition might also be advanced on the basis of field experience that it is probably better to base location schemes, not on absolute field strength measurements, but on relative field strength behavior. Further, although the data gathered at separations of 65-90 meters don't show too much scatter at frequencies less than 1000 Hz, good lock-in on signals in the frequency range 1000-2000 Hz seemed to be attained most quickly. The latter statement is demonstrated by field measurements taken at the U.S. Steel Rubina No. 4 Mine, Uniontown, Pennsylvania, which are described below.

Vertical Magnetic Field Measurements - Surface Vertical-Axis Loop Transmitter - U.S. Steel Robena No. 4 Coal Mine, Uniontown, Pennsylvania

A downlink C.W. transmission test was made at the U.S. Steel Robena No. 4 mine, Uniontown, Pennsylvania, on September 6, 1972. In this transmission test a vertical-axis single-turn loop antenna was set up at the surface with an area of 2200 square meters. An induction loop sensor to measure the amplitude of the subsurface vertical magnetic field was set up underground around a mine pillar with a separation between the centers of the source antenna and receiving sensor of about 194 meters. The source antenna was powered with 5 amperes of current and transmissions were made at 20 Hz, 50 Hz, 95 Hz, 160 Hz, 210 Hz, 270 Hz, 330 Hz, 450 Hz, 600 Hz, 720 Hz, 850 Hz, 1000 Hz, 1400 Hz, 2000 Hz, 5000 Hz, and 7000 Hz. The loop source antenna was set up in the immediate vicinity of the 3-phase INA rectifier system which was used to drive fans for mine ventilation and the receiving sensor loop was placed at a depth of 194 meters beneath in a mine working so that the loops were roughly coaxial.

The immediate presence of the rectifier system presented perhaps the worst situation insofar as ambient background electromagnetic noise is concerned. The results of this transmission test are portrayed in Figure 64. These mutual coupling data show that most scatter occurs below 1000 Hertz, a fact not unexpected in light of a priori knowledge of noise sources at the mine. Above 1000 Hertz the coupling decreases with increasing frequency. With the above constraints an optimal transmission frequency in this case might be between 1 and 2 kHz. Time did not allow any surface-based resistivity measurements to be taken at the Rubina No. 4 Mine. Therefore, in order to have some comparison of the empirical data with computed theoretical models an average effective resistivity of about 100 ohm-meters was assumed. It is perhaps because this choice for an average effective overburden resistivity is too high that a more rapid fall-off of coupling at frequencies greater than 1 kHz than that predicted by theory for a uniform earth having a resistivity of 100 ohm-meters is observed. In general, however, the transmission tests are considered quite successful so far as demonstrating through-the-earth communication capabilities.

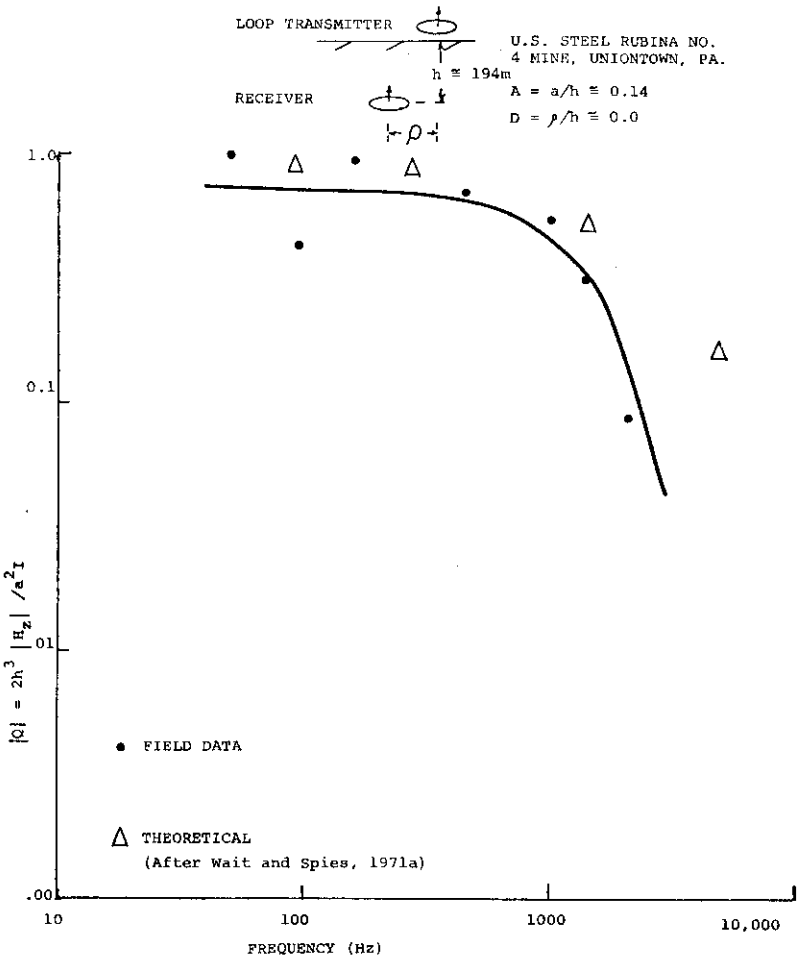

Fig. 64 Downlink C.W. transmission test.

Horizontal Magnetic Field Measurements - Buried Vertical-Axis Loop Transmitter - U.S. Bureau of Mines Experimental Coal Research Mine, Bruceton, Pennsylvania

Measurements of the surface horizontal magnetic field produced by a vertical-axis loop were made in actual field transmission tests at the U.S. Bureau of Mines Experimental Mine, as well as the vertical magnetic field (discussed above). The source antenna-receiver sensor configuration in this case is also illustrated in Figure 46, with the receiving sensor loop axis being horizontal. In the above discussion the attenuation function M for the horizontal (radial) magnetic field at the surface was given by the expression:

$$M = \int_0^\infty \frac{J_1(Ax)}{(Ax/2)} \frac{x^2(x^2+iH^2)^{\frac{1}{2}}}{(x^2+iH^2)+x} e^{-Zx} e^{-(x^2+iH^2)^{\frac{1}{2}}} J_1(Dx)dx \qquad (38)$$

where the integrand factor $J_1(Ax)/(Ax/2)$ takes into account field behavior departures from a dipolar source condition when the source antenna loop becomes large relative to separation distances from the receiving sensor.

Several features of the behavior of the attenuation function M (or the horizontal magnetic field $H\rho$) at the surface are noted. First, directly over the vertical-axis buried loop transmitter there is a sharp null present. Then the value $|M|$ builds up to a maximum value at very low frequencies at a horizontal offset distance of about 1/2 the depth of burial of the source antenna after which the amplitude smoothly falls off with increasing distance from the source. At an offset distance of twice the source depth of burial the horizontal magnetic field has fallen by about 20 db from its maximum.

Thus two phenomena in the horizontal magnetic field behavior could be used as location criteria. One of these would involve the detection of the null in the horizontal magnetic field directly over the buried transmitter. The other would involve the determination of the maximum in the horizontal magnetic field at a surface offset distance equal to half the source depth of burial. A cautionary note should probably be given here. If one maps just the amplitude $|H\rho|$ at the surface, he must be certain that what is measured as a relative null is in fact a null which is on a radial line through the axis of the transmitter loop. Therefore one of two procedures is required: (1) systematic grid mapping is performed or (2) the horizontal-axis receiving loop sensor is rotated 360 degrees around a vertical to the earth's surface!

As in the case for vertical magnetic field null measurements, the size of the loop relative to the overburden thickness can change the position of the maximum in the horizontal magnetic field, although the size of the loop transmitter never affects the presence of the null in the horizontal magnetic field directly over the transmitting loop. As the effective radius of the source loop becomes larger the maximum in $|M|$ or $|H\rho|$ occurs at a greater offset distance ($>D = \rho/h \approx 0.5$). The percent change in position of this maximum for very low frequencies is shown in Figure 65 as a function of size of the loop transmitter. Comparison of Figures 55 and 65 shows that the position of the maximum in $|H\rho|$ changes much more rapidly with increase in the size of the transmitter loop than the position of the null in $|H_z|$, although in both cases the position of

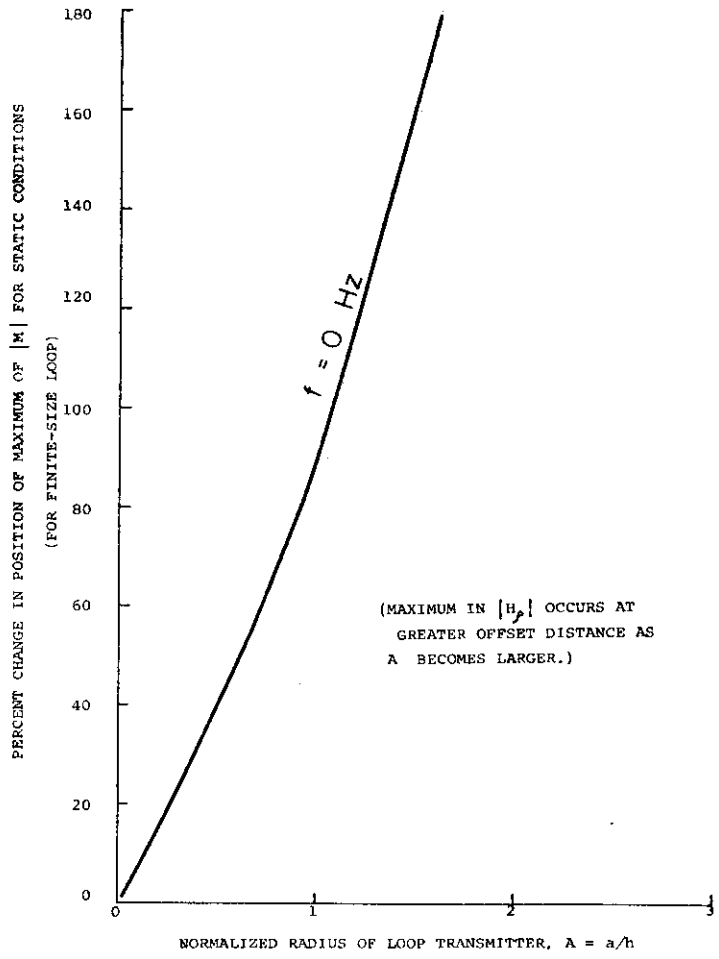
PERCENT CHANGE IN POSITION OF MAXIMUM OF |M| FOR STATIC CONDITIONS
(FOR FINITE-SIZE LOOP)
180
160
140
120
100
80
60
40
20
0
f = 0 Hz
(MAXIMUM IN |Hρ| OCCURS AT
GREATER OFFSET DISTANCE AS
A BECOMES LARGER.)
0
1
2
3
NORMALIZED RADIUS OF LOOP TRANSMITTER, A = a/h

Fig. 65

the maximum and null, respectively, occur at greater offset distances with increasing A. Similarly, the magnitude of the maximum value of $|M|$ decreases as A increases (see Figure 66).

The effect of markedly increasing frequency to the order of magnitude of 10 kHz leads to the introduction of secondary surface nulls and maximums in $|H_\rho|$ (see Figure 66, which, for the sake of simplicity, should probably be avoided in the field. As a general rule, these secondary surface nulls and maximums only occur when the depth of burial h (meters) of the source transmitter is greater than the factor $750/\sqrt{f\sigma}$, σ being the conductivity of the overburden in mhos/m and f being the frequency in Hertz; i.e.,

$$h \geq 750/\sqrt{f\sigma} \tag{39}$$

A typical overburden conductivity in a coal mining province might be 10^{-2} mhos/m so that if a transmission beacon frequency on the order of 100 Hz were chosen, the overburden thickness would have to be at least 750 meters thick in order for the secondary surface nulls and maximums in $|H_\rho|$ to be present. On the other hand, if a transmission frequency of 10 kHz were chosen, the overburden thickness would have to be greater than or equal to 75 meters for the above secondary phenomena to be present.

Unlike the maximum in the vertical magnetic field directly over the buried loop transmitter, the presence of the null in the horizontal magnetic field is not affected by a change in conductivity of the overburden provided that the overburden is relatively homogeneous and uniform electrically and no scattering sources are present. The influence of the presence of a scattering object (such as a pipeline on the surface or an overhead power line) on the fields of a radiating buried dipole antenna has not been analyzed but is being investigated (Wait, 1973), and as mentioned earlier, is far from being a trivial problem.

The results of several uplink C.W. transmissions involving the measurement of the surface horizontal magnetic field produced by a buried vertical-axis loop transmitter are shown in Figures 67-71 over a suite of frequencies in the audio range and for horizontal offsets which range from zero to about three times the transmitter depth of burial. These field data are reduced and presented in a form analogous to that used by Wait and Spies (1971a) so that a direct comparison may be made with their theoretical results.

These field data generally illustrate close agreement with theoretical considerations. A null in $|M|$, for instance, was observed at station 1 (see Figure 67) where $D = \rho/h \simeq 0$ and a maximum detected at station 2 (see Figure 68) where $D \simeq 0.5$. As in measurements of $|Q|$, a fair amount of scatter was present in the data at station 3 (see Figure 69), particularly at frequencies less than 100 Hz, although at station 4 ($D = \rho/h \simeq 1.45$) very little scatter was observed at frequencies above 500 Hz (see Figure 70).

Figure 72 shows the general field behavior of $|M|$ as a function of horizontal surface offset from the underground beacon transmitter at frequencies of 20 Hz and 1000 Hz. Both of these graphs show good agreement with theory in that the null and maximum in $|M|$ could be used conjunctively for location of the transmitting beacon. If the depth h to the mine working, for instance, were

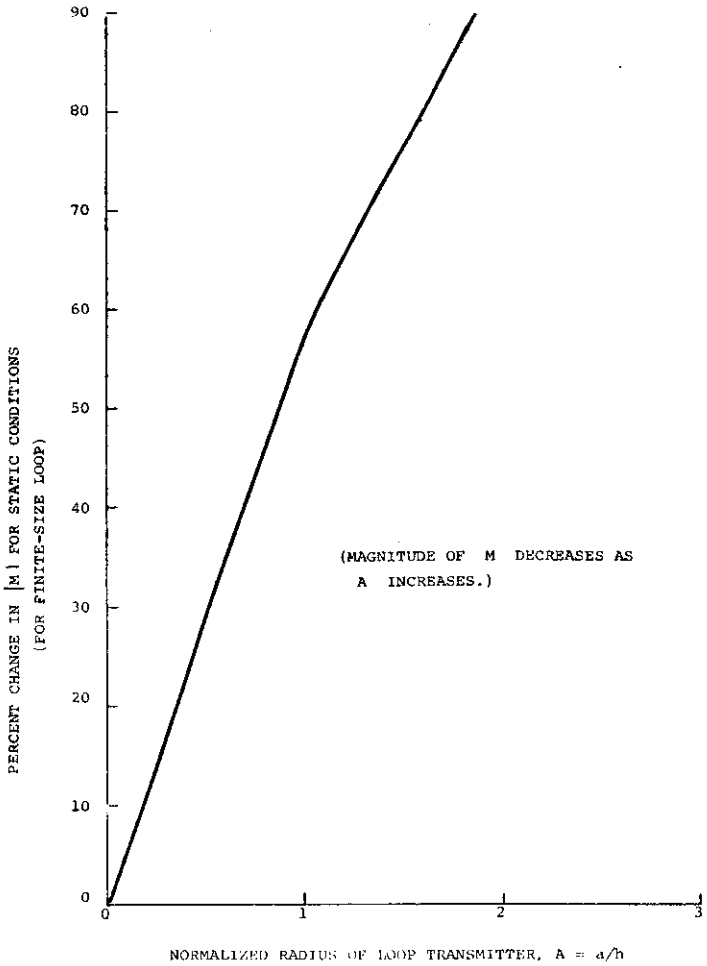
PERCENT CHANGE IN |M| FOR STATIC CONDITIONS
(FOR FINITE-SIZE LOOP)
(MAGNITUDE OF M DECREASES AS
A INCREASES.)
NORMALIZED RADIUS OF LOOP TRANSMITTER, A = a/h

Fig. 66

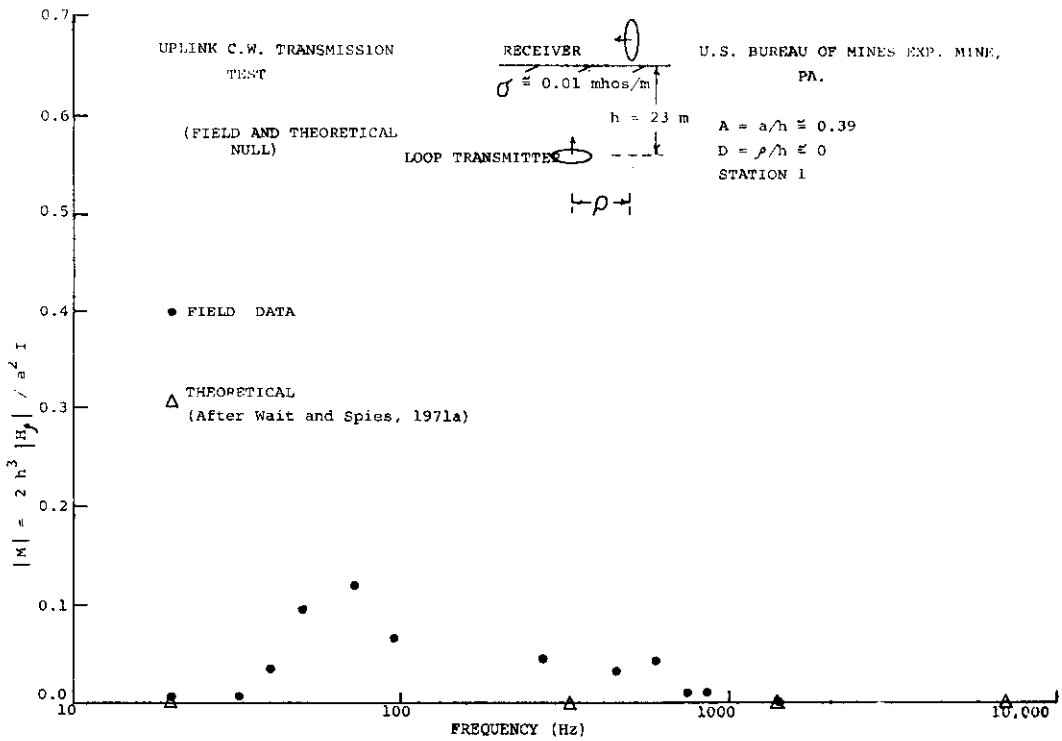
UPLINK C.W. TRANSMISSION
TEST
(FIELD AND THEORETICAL
NULL)
RECEIVER
σ ≅ 0.01 mhos/m
h = 23 m
LOOP TRANSMITTER
ρ
U.S. BUREAU OF MINES EXP. MINE,
PA.
A = a/h ≅ 0.39
D = ρ/h ≅ 0
STATION 1
• FIELD DATA
Δ THEORETICAL
(After Wait and Spies, 1971a)
|M| = 2 h³ |Hz| / a² I
FREQUENCY (Hz)

Fig. 67

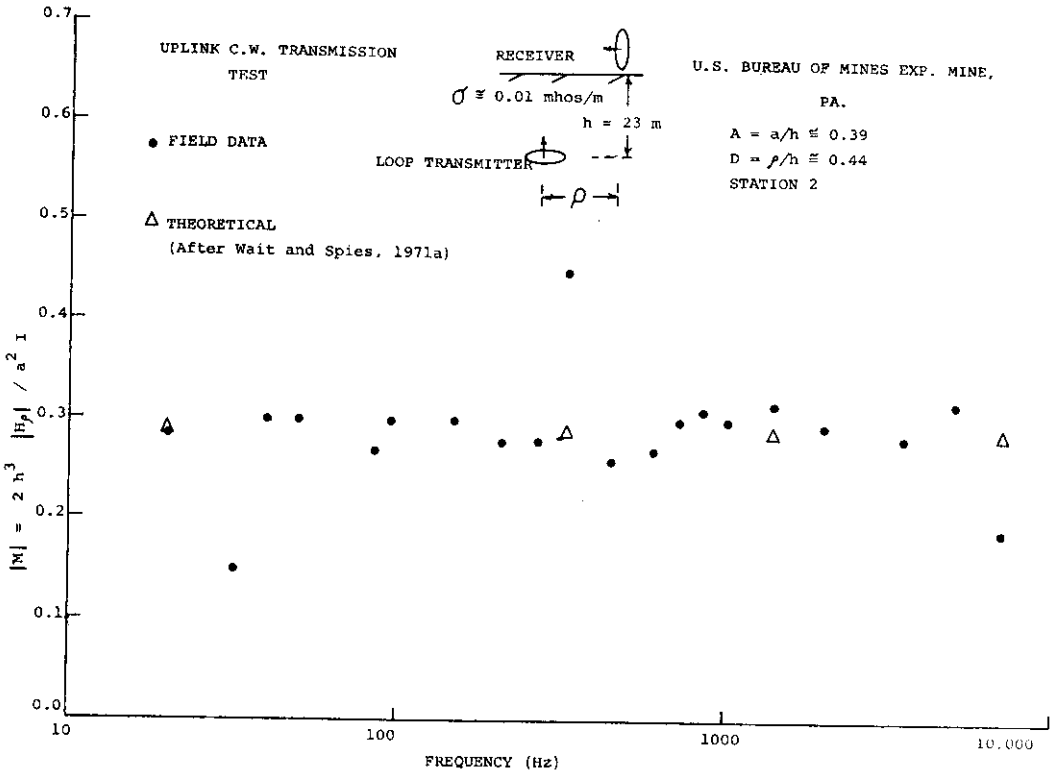
UPLINK C.W. TRANSMISSION TEST
RECEIVER
σ ≅ 0.01 mhos/m
h = 23 m
LOOP TRANSMITTER
ρ
U.S. BUREAU OF MINES EXP. MINE, PA.
A = a/h ≅ 0.39
D = ρ/h ≅ 0.44
STATION 2
FIELD DATA
THEORETICAL
(After Wait and Spies, 1971a)
|M| = 2 h³ |Hρ| / a² I
FREQUENCY (Hz)
0.0
0.1
0.2
0.3
0.4
0.5
0.6
0.7
10
100
1000
10,000

Fig. 68

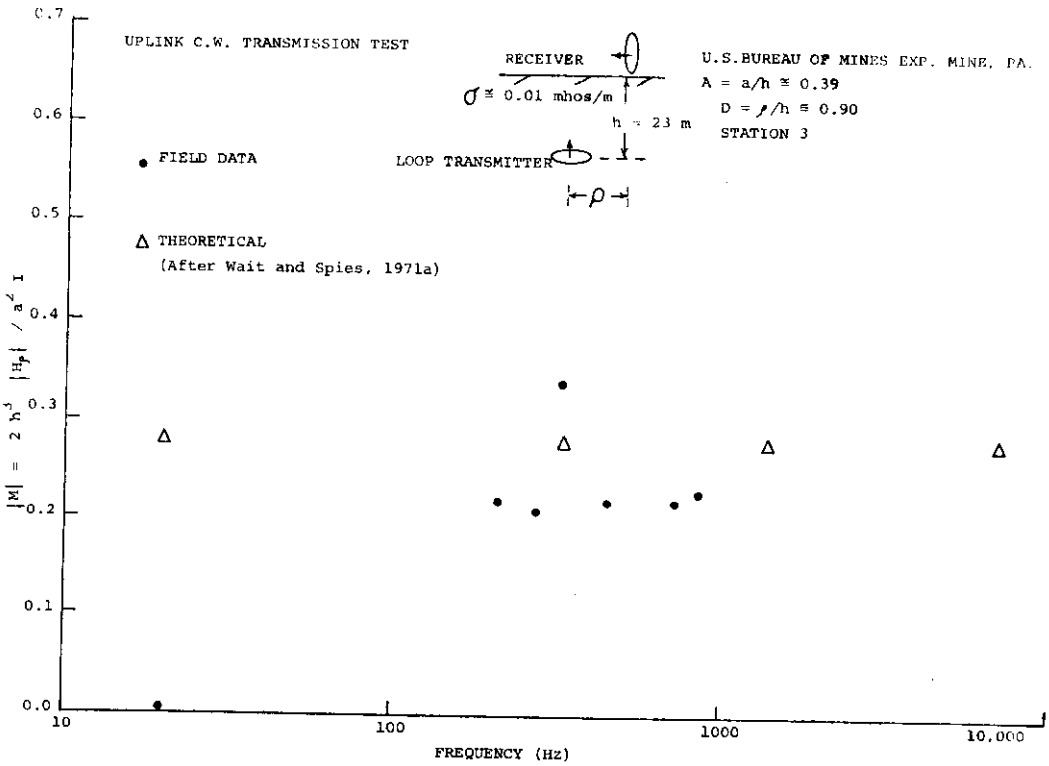
UPLINK C.W. TRANSMISSION TEST
RECEIVER
σ ≅ 0.01 mhos/m
h = 23 m
LOOP TRANSMITTER
ρ
U.S.BUREAU OF MINES EXP. MINE, PA.
A = a/h ≅ 0.39
D = ρ/h ≅ 0.90
STATION 3
FIELD DATA
THEORETICAL
(After Wait and Spies, 1971a)
|M| = 2 h³ |Hρ| / a² I
FREQUENCY (Hz)
0.0
0.1
0.2
0.3
0.4
0.5
0.6
0.7
10
100
1000
10,000

Fig. 69

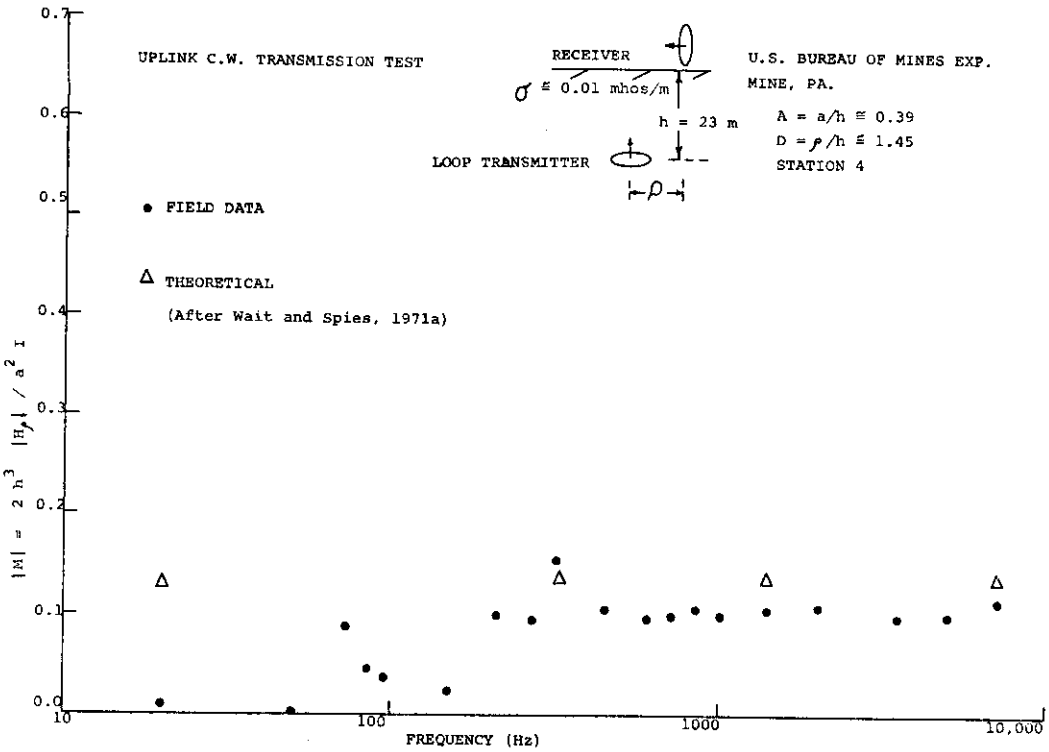
UPLINK C.W. TRANSMISSION TEST
RECEIVER
σ ≅ 0.01 mhos/m
h = 23 m
LOOP TRANSMITTER
ρ
U.S. BUREAU OF MINES EXP. MINE, PA.
A = a/h ≅ 0.39
D = ρ/h ≅ 1.45
STATION 4
FIELD DATA
THEORETICAL
(After Wait and Spies, 1971a)
|M| = 2 h³ |Hρ| / a² I
FREQUENCY (Hz)
0.0
0.1
0.2
0.3
0.4
0.5
0.6
0.7
10
100
1000
10,000

Fig. 70

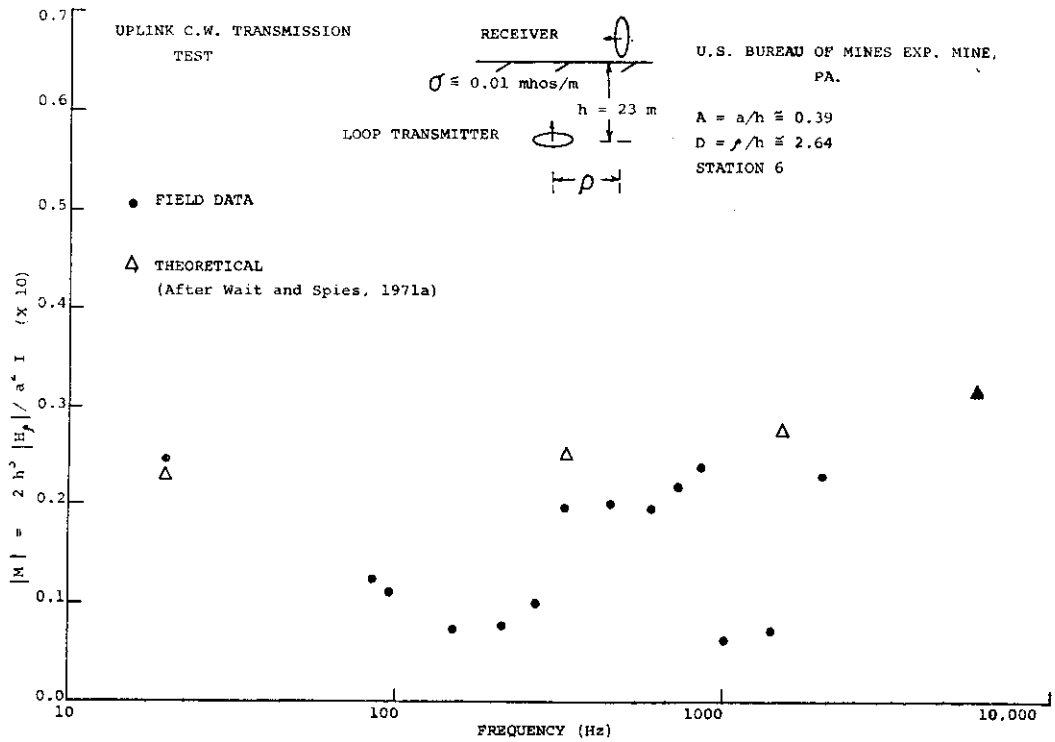
UPLINK C.W. TRANSMISSION TEST
RECEIVER
σ ≅ 0.01 mhos/m
h = 23 m
LOOP TRANSMITTER
ρ
U.S. BUREAU OF MINES EXP. MINE, PA.
A = a/h ≅ 0.39
D = ρ/h ≅ 2.64
STATION 6
FIELD DATA
THEORETICAL
(After Wait and Spies, 1971a)
|M| = 2 h³ |Hρ| / a⁴ I (X 10)
FREQUENCY (Hz)
0.0
0.1
0.2
0.3
0.4
0.5
0.6
0.7
10
100
1000
10,000

Fig. 71

known, the horizontal offset could be determined by the approximate relation $\rho = 0.5$ h. However, if only measurements of the spatial variation of $|M|$ are made, it is firmly recommended that both the null and maximum in $|M|$ be determined either by means of a systematic grid or by rotation of the horizontal-axis induction receiving coil through 360 degrees. In principal, only one profile of $|M|$ would need to be made; whether or not this profile is on a radial through the axis of the transmitting loop could then be determined by analyzing the rate-of-falloff or horizontal gradient of $|M|$ for normalized offset distances greater than $D \simeq 0.5$ and for radials not through the axis of the source loop. However, not always do these gradients coincide with theoretical predictions (gradients presented in Figure 72 for offsets greater than half the source depth of burial are greater than those predicted by theory); therefore discretion would probably dictate the use of a grid.

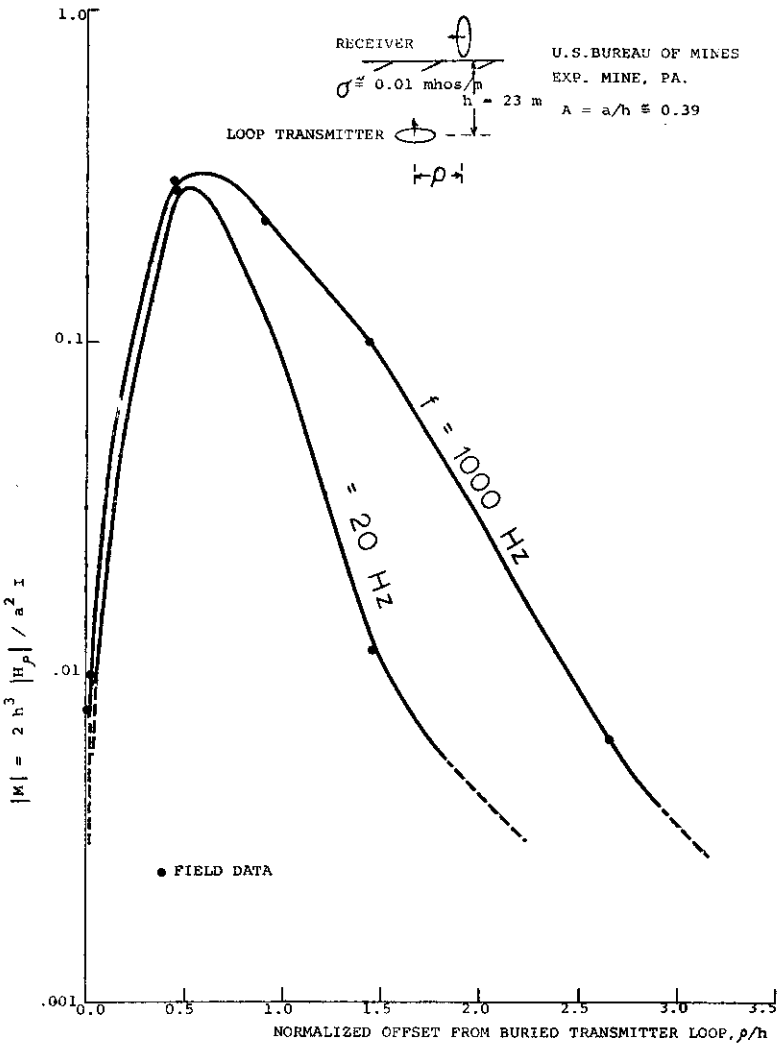
RECEIVER
U.S.BUREAU OF MINES
EXP. MINE, PA.
σ ≅ 0.01 mhos/m
h = 23 m
A = a/h ≅ 0.39
LOOP TRANSMITTER
ρ
f = 1000 Hz
= 20 Hz
FIELD DATA
1.0
0.1
.01
.001
0.0
0.5
1.0
1.5
2.0
2.5
3.0
3.5
|M| = 2 h³ |Hρ| / a² I
NORMALIZED OFFSET FROM BURIED TRANSMITTER LOOP, ρ/h

Fig. 72

SUMMARY

Electrical properties measurements made in several coal mining regions (Gary No. 14 mine, West Virginia; Peabody No. 10 mine, Illinois; Imperial and Eagle mines, Colorado; Montour No. 4 mine, Pennsylvania; U.S. Bureau of Mines Experimental Research Mine, Pennsylvania) enable one to characterize these mining regions by overburden conductivity distributions. Such characterization provides the basis of applicability for various theoretical geoelectric models being examined which predict throuth-the-earth electromagnetic propagation phenomena and also are useful in ensuring the best possible transmitter-receiver coupling for uplink, downlink, or intramine communication. For example, if geoelectric layering is present, the electrical conductivity will be greater parallel to bedding planes (σ_ℓ) than across bedding planes (σ_t). The propagated through-the-earth electromagnetic fields of a loop source antenna depend on the maximum conductivity σ_ℓ; thus, one has maximum coupling through the earth when the axis of the loop transmitting antenna is perpendicular to geoelectric planes of maximum conductivity. In many of the mining regions investigated where electrical layering of the transmission properties was observed, it was such that the planes of maximum conductivity lay in a horizontal plane; in the Gary No. 14 region, however, this layering was tilted.

The electromagnetic fields propagated from a grounded line antenna, on the other hand, depend instead on the geometric average $\sqrt{\sigma_\ell \sigma_t}$ measured along and across the bedding in a laminated sequence of rocks. Thus the fields radiated by a line source antenna will be more sensitive to gross inhomogeneities present in the overburden.

Resistivity measurements in the above coal mining provinces were made both by galvanic and induction techniques; all resistivity values show, in general, for any given region a unimodal character. The spread, however, in the probability density plots of the resistivity values collected in any given area varies. For example, the resistivity probability density plot for the Peabody No. 10 mine appears quite similar to that for the Imperial and Eagle mines. This comparison implies that electromagnetic transmissions through the earth, ambient noise and logistic factors being equal, would be less distorted by the resistivity distribution apparent at the Imperial and Eagle mines or at the Peabody No. 10 mine than by the resistivity distribution apparent at either the Montour No. 4 mine or the Gary No. 14 mine. Consequently, theoretical models of a beacon source antenna immersed in an electrically and magnetically homogeneous halfspace would be applicable in mining provinces which have geoelectric sections similar to those measured at the Imperial and Eagle mines or the Peabody No. 10 mine and should yield insight into the behavior of electromagnetic transmissions. An average resistivity of the overburdens overlying coal mine workings from the data collected and presented here would be about 100 ohm-meters; loss tangents, on the other hand, are generally vanishingly small in the E.L.F. and V.L.F. ranges.

Studies of ambient electromagnetic noise statistics are complimentary to investigations of the overburden electrical transmission properties and are necessary for proper design of any subsurface-surface electromagnetic communications system. Ambient electromagnetic noise levels from 20 Hz to 10 kHz have

been characterized in a number of mining provinces as a function of time of day by amplitude histograms.

In so doing, the signal from either an electric field sensor or magnetic field sensor is first passed through a filter which strongly rejects below some lower frequency limit and above some upper frequency limit. Then, within these frequency bands, the number of times ambient noise events occur which exceed specified levels is determined. The advantage of this approach is that it provides information on the design of a high-sensitivity receiver system not readily available in the more conventional spectral approach. For example, optimum noise rejection could be incorporated into an uplink receiver system by setting thresholds for signal detection just above the median or maximum percent noise levels.

Statistical histogram analyses of ambient background electromagnetic noise data above working faces at the surface show that in most mining provinces the background noise is: (1) independent of time of day while coal mine operations are in progress, and (2) primarily due to artificial, man-made sources as distinct from atmospheric noise in the frequency range 20 Hz - 2 kHz. The magnetic field and electric field noise amplitude density functions presented in this report may be used in conjunction with the measured resistivity data to design and implement a practical operating beacon electromagnetic communications system in which an adequate source strength is determined which will yield a specified signal/noise ratio at the surface. Actual examples of the use of electrical properties data together with electromagnetic surface noise environment data for systems design considerations have been given for a loop-loop source-receiver configuration and a line-line source-receiver configuration. Studies of the ambient electromagnetic noise environment in most coal mine provinces may also be used in analyzing the feasibility of a passive loop detection scheme for location of a subsurface miner. It is deemed that a passive loop detection scheme for location of a subsurface miner would best be employed only as a backup to an active loop detection scheme, because secondary electromagnetic field strengths that are radiated from a buried passive loop excited by an active loop antenna at the surface are too small compared with the ambient noise.

Numerous transmission tests, both uplink and downlink, and both of the C.W. type and pulsed type, were performed with a grounded line transmitter and a vertical-axis loop transmitter and either electric or magnetic field receiving sensors. The feasibility of a pulse electromagnetic communication system is shown both theoretically and by actual field tests for small overburden thicknesses with the qualification that if one wishes to examine the late-time transient coupling response in an operating coal mine environment with transmitter antenna power output levels between 10 and 50 watts, he may have to process (i.e., "stack") the received signals to enhance signal-to-noise ratios.

Several location criteria were also deduced from the uplink C.W. transmission tests. One could, for example, map the surface null along the polar and equatorial axes of a buried line source transmitter when the wavelengths of transmission within the earth are considerably larger than all other distances involved (ELF range).

Another location criterion for positioning a transmitting vertical-axis loop involved the detection of the null in the vertical magnetic field at an offset distance from the buried source of about 1.4 times its depth of burial (low frequency criterion). If only a single profile of surface amplitude measurements were made which was not necessarily along a radial through the axis of the transmitting loop antenna, all that could safely be determined would be a minimum depth of burial of the source antenna in a homogeneous earth. For example, suppose a straight-line profile were made not on a radial from the transmitting loop axis but rather on a radial from a point which was displaced from the antenna axis by a distance equal to the depth of burial of the transmitter. In this perhaps somewhat extreme case, a single profile of amplitude measurements of H_z and detection of a relative null in $|H_z|$ might lead to estimates of the depth of burial of the transmitting antenna which would be as much as 30% too low. This field procedure, which makes use of the behaviorial nature of the amplitude of the surface vertical magnetic field, need not detract from an estimate of the true depth of burial or the true horizontal offset provided one of the following were performed: (1) the maximum in the vertical magnetic field over the transmitting loop were ascertained (as well as the offset null), (2) phase measurements of the vertical magnetic field relative to the horizontal magnetic field were made (as well as amplitude measurements), (3) horizontal gradient measurements of the vertical magnetic field were made (since the horizontal gradient in H_z is dependent on whether or not the measurements are made along a radial through the transmitter axis), or (4) either the depth to the mine working and not necessarily the surface offset distance or perhaps the surface offset distance, but not necessarily the depth to the working where the source antenna is located were known.

Ascertaining the maximum in the vertical magnetic field would involve a systematic grid mapping measurement routine. The second alternative, on the other hand, is particularly attractive since instrumentally it would involve only a highly tuned (perhaps phase-locking) crossed loop ratiometer sensor (commonly used in geophysical mining exploration) and would, with little additional expense, combine information present in both the surface horizontal and vertical magnetic field components from the buried vertical-axis transmitter loop. Gradient field measurements of just $|H_z|$ offer a third alternative and would, in principle, allow the determination of position relative to the axis of the transmitting antenna. However, gradient measurements seem to have an apparent disadvantage in that two measuring coaxial induction coils spaced a finite distance apart (say, in this case a practical distance of one meter) would have to be used and, in a noisy electromagnetic environment, would tend to accentuate noise in the data. On the other hand, the gradient in $|H_z|$could be obtained after measurement and smoothing of $|H_z|$ and compared with graphical nomograms for positioning. Commonly the depth to working levels in mines where men are located during emergency situations is very well known, since there are few multi-level working mines in the United States (Parkinson, 1971). Thus, use of known constraints would yield a large reduction in the scope of the location problem.

Still another criterion for targeting a buried vertical-axis loop beacon is mapping the null conjuctively with the offset maximum in the attenuation function for the horizontal magnetic field, $|M|$. Again the same care would have to be taken in field measurements to ensure a null over the transmitter

were mapped, and the most practical approach seems to lie either in systematically making a series of grid measurements along several profiles at the surface or in rotating the sensor coil 360 degrees horizontally.

It should be noted that the field behavior of a finite loop antenna, as opposed to that of a dipole loop antenna, is useful and necessary in analyzing coupling data from shallow mines. In most coal mines, for instance, the depth of burial of the source loop antenna (for uplink communications) is on the order of 100 meters. A practical buried loop antenna might consist of a single turn of #14 gauge wire wound around a pillar within a coal mine (such as the 10 m by 24 m loop used in uplink transmission in the U.S. Bureau of Mines Experimental Mine) and having an effective circular radius on the order of 8-10 meters. For shallow coal mines (such as the Experimental Research Coal Mine in Bruceton, Pennsylvania) this effective source loop radius is about 1/3 the depth of burial, and finite-size loop behavior should be taken into account. For the same size loop in the visited U.S. Steel Rubina No. 4 Coal Mine in Uniontown, Pennsylvania, however, the above effective source loop radius would only be 1/25th the depth of burial and the limiting case of dipole field behavior would suffice.

As a general rule, it may be said that for the frequency range under consideration, one need only consider dipole field behavior for systems design as long as the separation distances are 10 times larger than the source loop antenna radius. For smaller separations relative to the source loop radius, however, the "size effect" of the transmitting loop can and should be taken into account, for it could affect an accurate location determination scheme, particularly if measurements just of the vertical magnetic field are made. In the analyses given in this report, the size effect of the transmitter loop was shown and taken into consideration for both vertical and horizontal magnetic field measurements. When feasible, it is desirable to make the effective radius of the transmitter loop as large as possible since the source strength of the transmitter is accordingly increased, even if size effects of the transmitter need to be accounted for.

In summary, analysis of the C.W. uplink transmission experiments which made use of a vertical-axis loop transmitter demonstrates close agreement with theoretical considerations. Generally, noise was less of a problem above 1000 Hertz, and attenuation was not as severe as that which would be predicted by plane-wave theory.

It is perhaps appropriate at this point to make some qualified remarks on which source-receiver configuration might be best to use under a given set of circumstances or under a given set of constraints defining the objectives of and limitations on a through-the-earth beacon electromagnetic communications system. For example, is it desired simply to communicate by induction techniques or is the objective to use the source-receiver configuration which in coal mine provinces (based on measured electrical properties of the overburden in coal mine provinces) provides a more useful field for location purposes? In addition, ease and practicality of deployment of the source antenna within a mine must also be considered, particularly in an emergency situation.

Provided the overburden is relatively conductive (less than several hundred ohm-meters) and contact resistance at the current electrodes is no problem, it is often more convenient to directly put current into the ground by a line source. This type of transmitting source, although yielding a very adequate means for communication, is more sensitive to conductivity inhomogeneities (as noted in the field test results above) and for a receiving surface electric-field sensor does not, in our opinion, provide as convenient a means for location as does a loop-loop source-receiver configuration which has been discussed. Thus, received magnetic-field signals in the ELF range are less sensitive in general to secondary scattering sources in the overburden than are electric-field signals.

On the other hand, for general communication purposes, some of the secondary nulls in the produced surface magnetic field from a buried vertical-axis loop antenna may make a horizontal grounded insulated electric-current line a more desirable transmitting source. Of course, the electrical properties of the overburden must always be taken into account, for in the case of a highly resistive overburden (which, although not found usually over coal mines, is frequently found over hard-rock mines), it may not be practically feasible to use an electric line source for communication or location purposes at all, simply because of the difficulty in putting current into the ground. Thus, for the case where a resistive overburden is present, it may necessarily be advantageous to use a loop source antenna.

APPENDICES

AMBIENT SURFACE ELECTROMAGNETIC NOISE MEASUREMENTS

APPENDIX A

Gary No. 14 Coal Mine, W. Virginia

Smoothed Histograms of:

Time Derivative of Vertical Magnetic Field Noise (A-1 - A-8)

NE-SW Horizontal Electric Field Noise (A-9 - A-16)

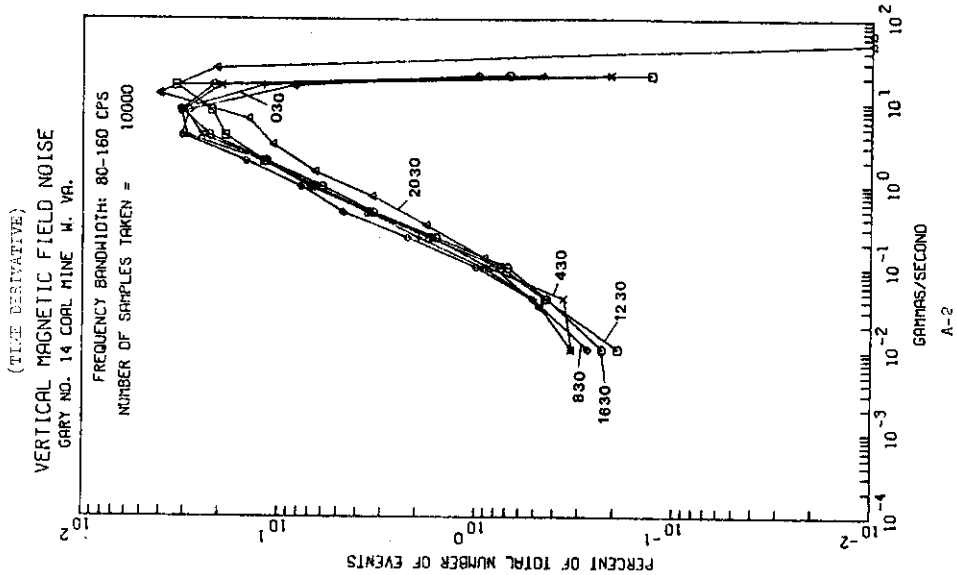
(TIME DERIVATIVE)
VERTICAL MAGNETIC FIELD NOISE
GARY NO. 14 COAL MINE W. VA.
FREQUENCY BANDWIDTH: 80-160 CPS
NUMBER OF SAMPLES TAKEN = 10000
030
2030
430
1230
830
1630
PERCENT OF TOTAL NUMBER OF EVENTS
GAMMAS/SECOND

A-2

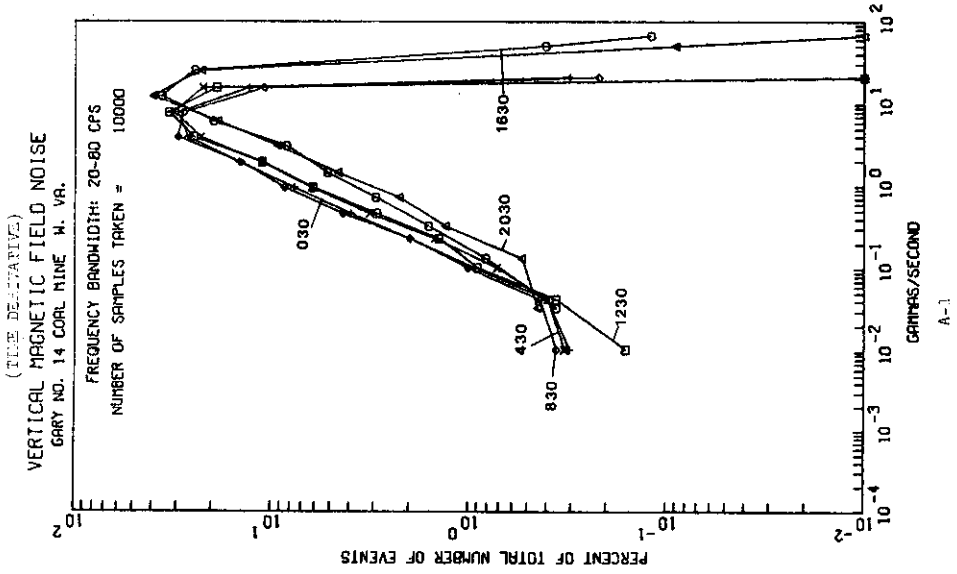
(TIME DERIVATIVE)
VERTICAL MAGNETIC FIELD NOISE
GARY NO. 14 COAL MINE W. VA.
FREQUENCY BANDWIDTH: 20-80 CPS
NUMBER OF SAMPLES TAKEN = 10000
1630
030
2030
1230
430
830
PERCENT OF TOTAL NUMBER OF EVENTS
GAMMAS/SECOND

A-1

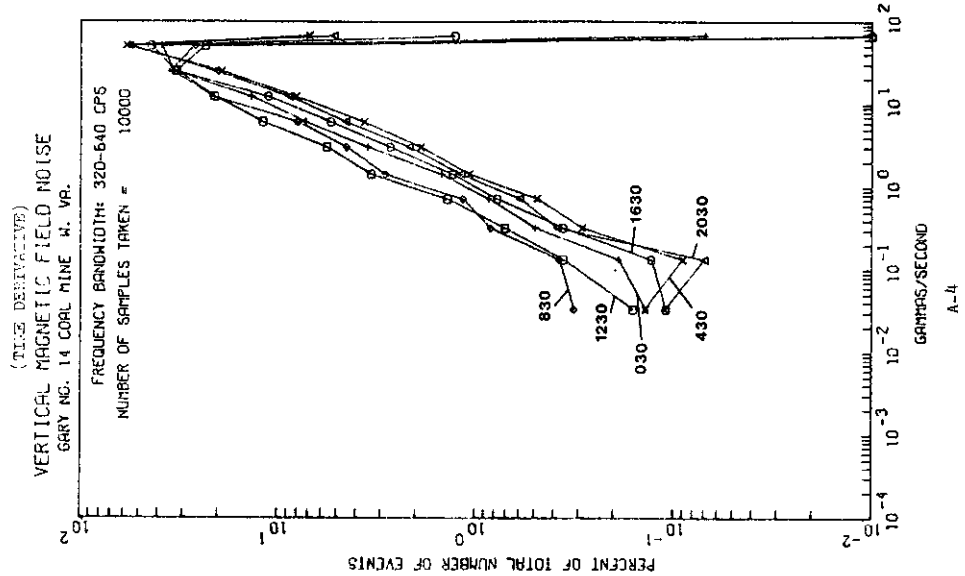
(TIME DERIVATIVE)
VERTICAL MAGNETIC FIELD NOISE
GARY NO. 14 COAL MINE W. VA.
FREQUENCY BANDWIDTH: 320-640 CPS
NUMBER OF SAMPLES TAKEN = 10000
830
1230
030
1630
2030
430
PERCENT OF TOTAL NUMBER OF EVENTS
GAMMAS/SECOND

A-4

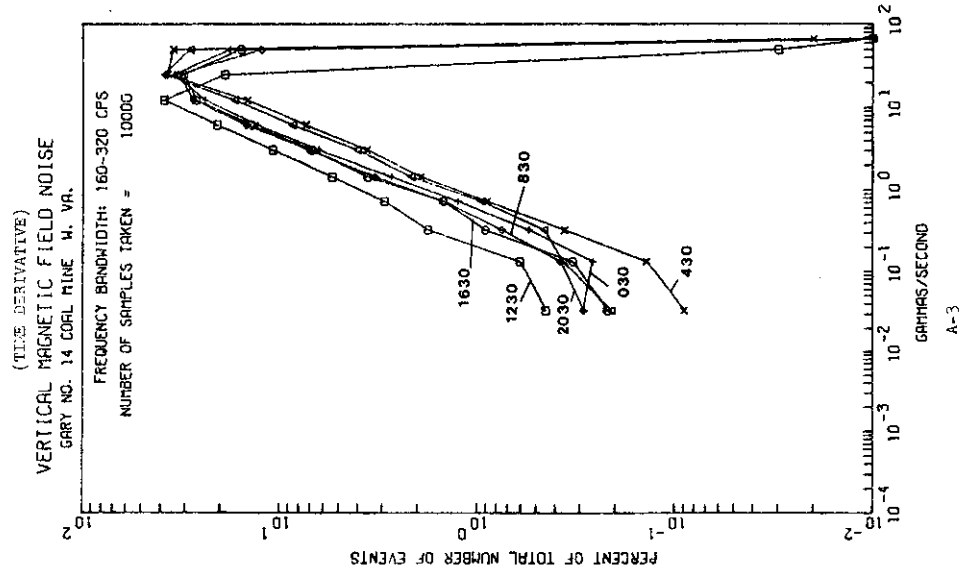
(TIME DERIVATIVE)
VERTICAL MAGNETIC FIELD NOISE
GARY NO. 14 COAL MINE W. VA.
FREQUENCY BANDWIDTH: 160-320 CPS
NUMBER OF SAMPLES TAKEN = 10000
1630
830
1230
2030
030
430
PERCENT OF TOTAL NUMBER OF EVENTS
GAMMAS/SECOND

A-3

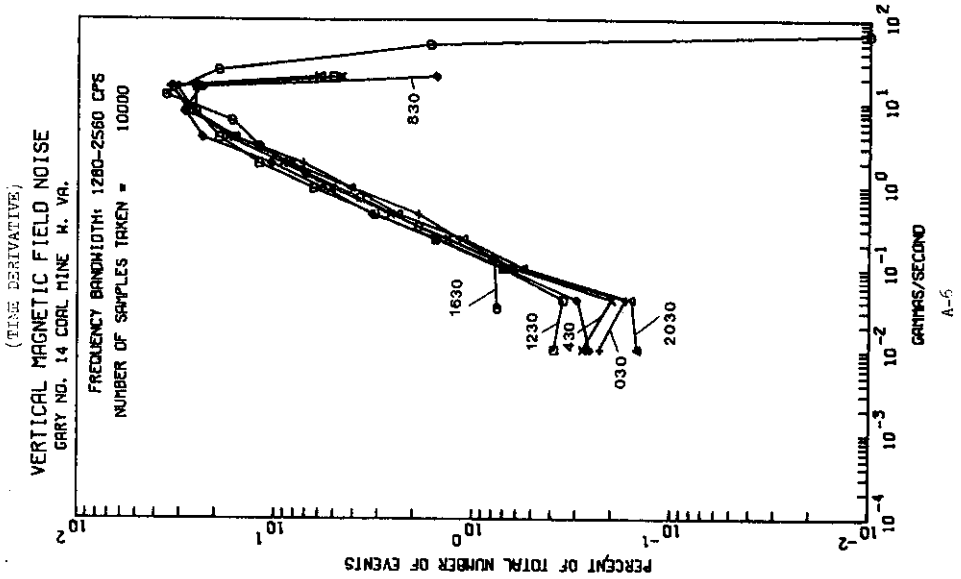
(TIME DERIVATIVE)
VERTICAL MAGNETIC FIELD NOISE
GARY NO. 14 COAL MINE W. VA.
FREQUENCY BANDWIDTH: 1280-2560 CPS
NUMBER OF SAMPLES TAKEN = 10000
830
1630
1230
430
030
2030
PERCENT OF TOTAL NUMBER OF EVENTS
GAMMAS/SECOND

A-6

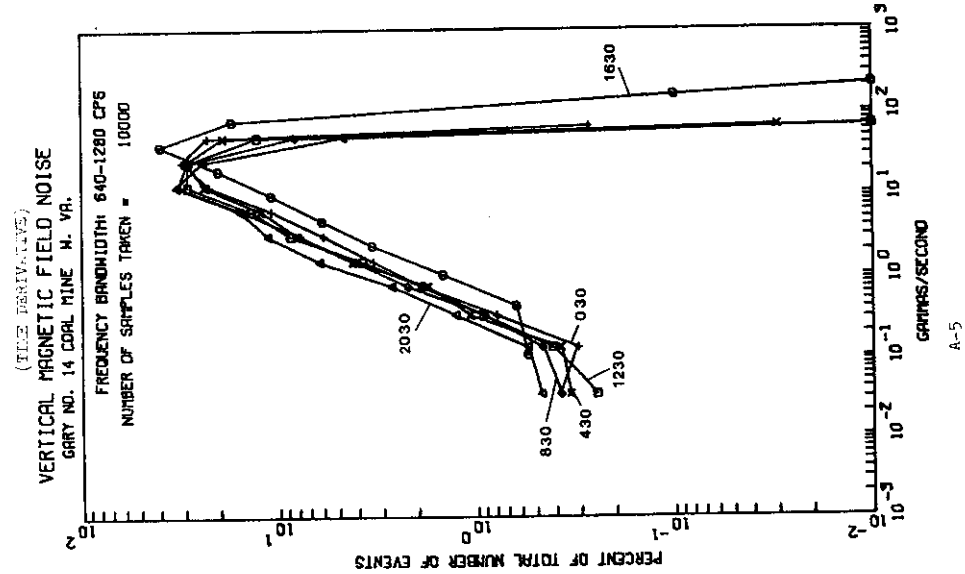
(TIME DERIVATIVE)
VERTICAL MAGNETIC FIELD NOISE
GARY NO. 14 COAL MINE W. VA.
FREQUENCY BANDWIDTH: 640-1280 CPS
NUMBER OF SAMPLES TAKEN = 10000
1630
2030
030
1230
830
430
PERCENT OF TOTAL NUMBER OF EVENTS
GAMMAS/SECOND

A-5

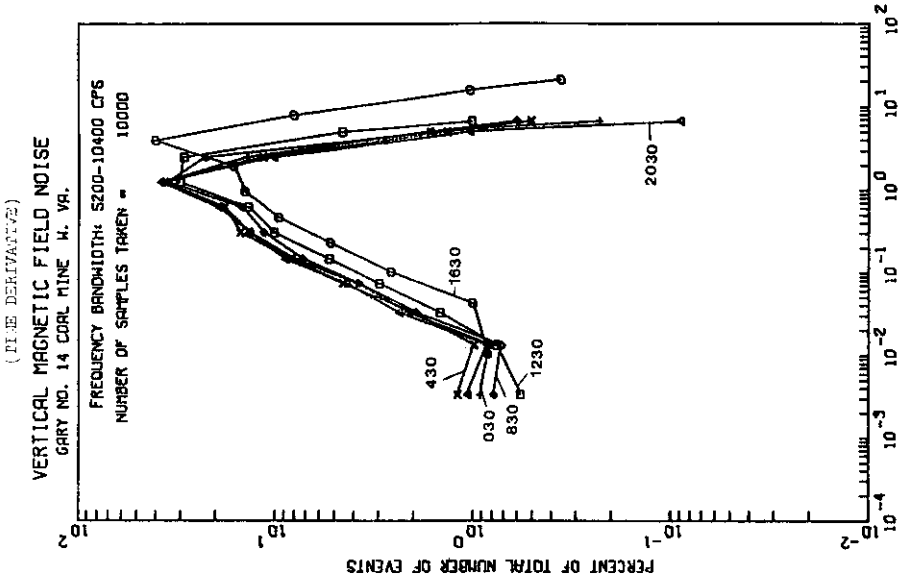
(TIME DERIVATIVE)
VERTICAL MAGNETIC FIELD NOISE
GARY NO. 14 COAL MINE W. VA.
FREQUENCY BANDWIDTH: 5200-10400 CPS
NUMBER OF SAMPLES TAKEN = 10000
2030
1630
430
1230
030
830
PERCENT OF TOTAL NUMBER OF EVENTS
GAMMAS/SECOND

A-6

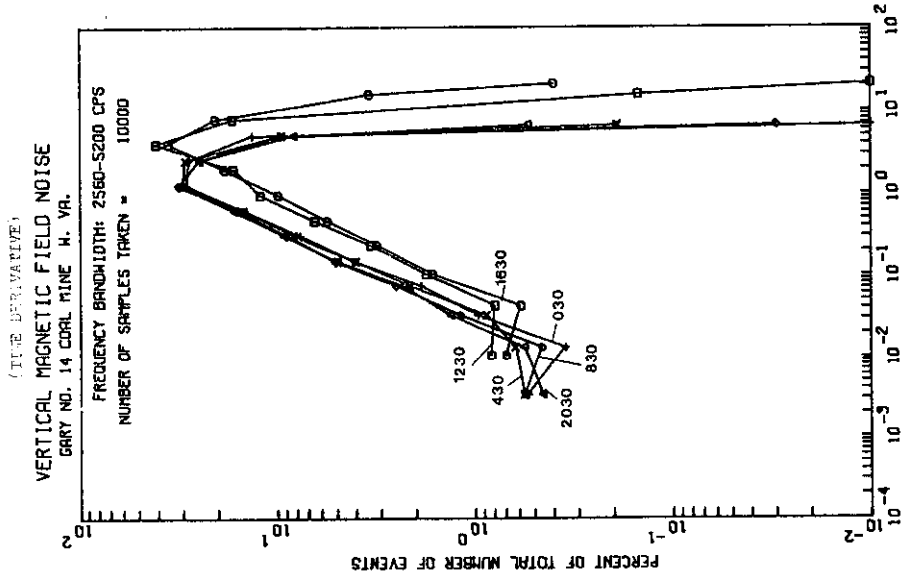
(TIME DERIVATIVE)
VERTICAL MAGNETIC FIELD NOISE
GARY NO. 14 COAL MINE W. VA.
FREQUENCY BANDWIDTH: 2560-5200 CPS
NUMBER OF SAMPLES TAKEN = 10000
1230
1630
030
430
830
2030
PERCENT OF TOTAL NUMBER OF EVENTS
GAMMAS/SECOND

A-7

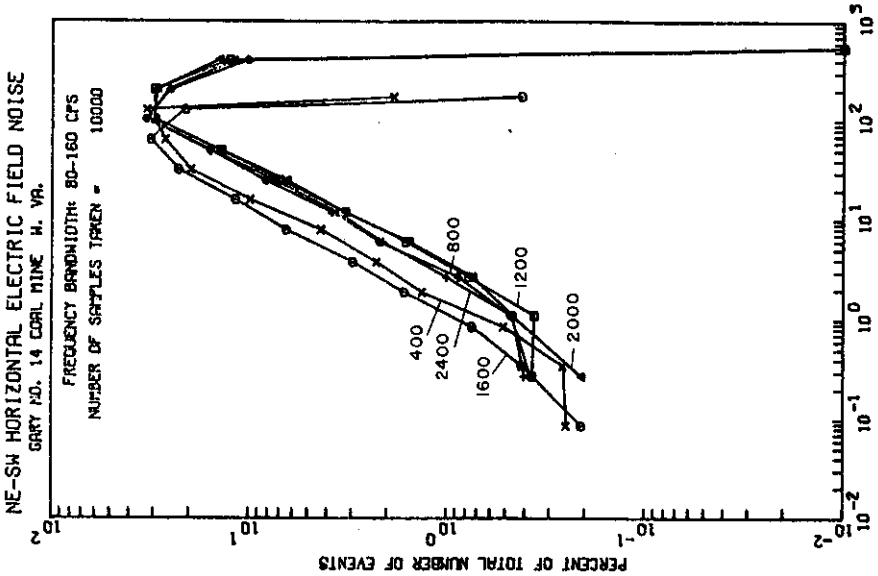
NE-SW HORIZONTAL ELECTRIC FIELD NOISE
GARY NO. 14 COAL MINE W. VA.
FREQUENCY BANDWIDTH: 80-160 CPS
NUMBER OF SAMPLES TAKEN = 10000
400
2400
1600
800
1200
2000
PERCENT OF TOTAL NUMBER OF EVENTS
MILLIVOLTS/KILOMETER

A-10

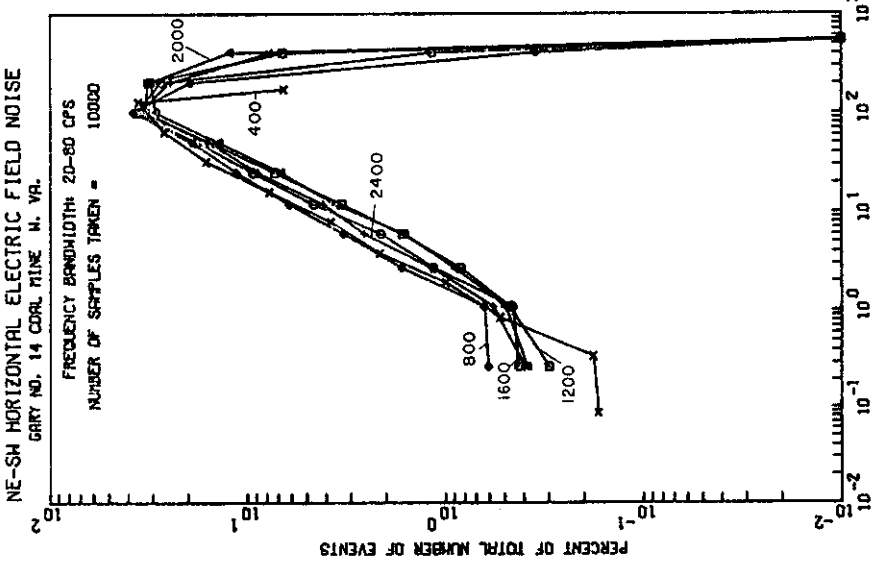
NE-SW HORIZONTAL ELECTRIC FIELD NOISE
GARY NO. 14 COAL MINE W. VA.
FREQUENCY BANDWIDTH: 20-80 CPS
NUMBER OF SAMPLES TAKEN = 10000
2000
400
2400
800
1600
1200
PERCENT OF TOTAL NUMBER OF EVENTS
MILLIVOLTS/KILOMETER

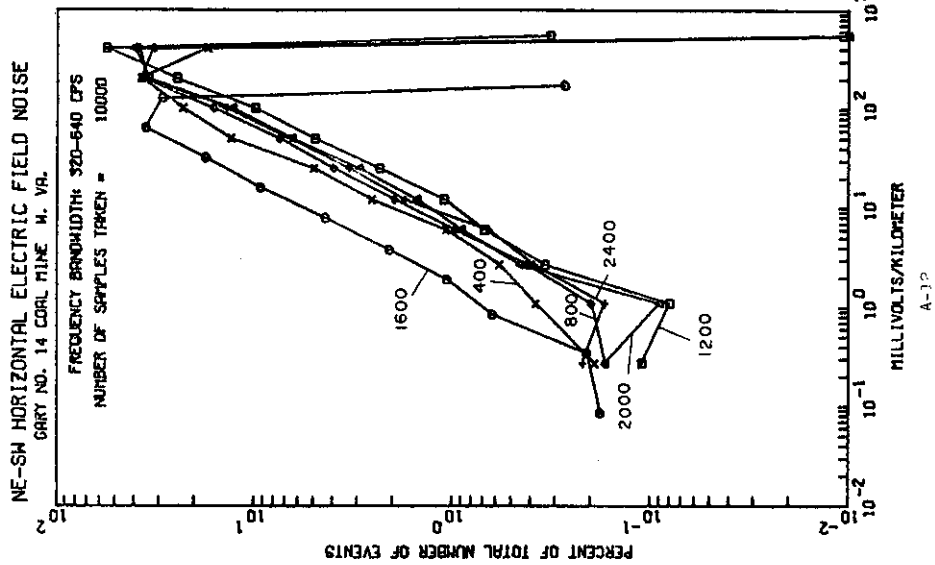
NE-SW HORIZONTAL ELECTRIC FIELD NOISE
GARY NO. 14 COAL MINE W. VA.
FREQUENCY BANDWIDTH: 320-640 CPS
NUMBER OF SAMPLES TAKEN = 10000
1600
400
800
2400
1200
2000
PERCENT OF TOTAL NUMBER OF EVENTS
MILLIVOLTS/KILOMETER

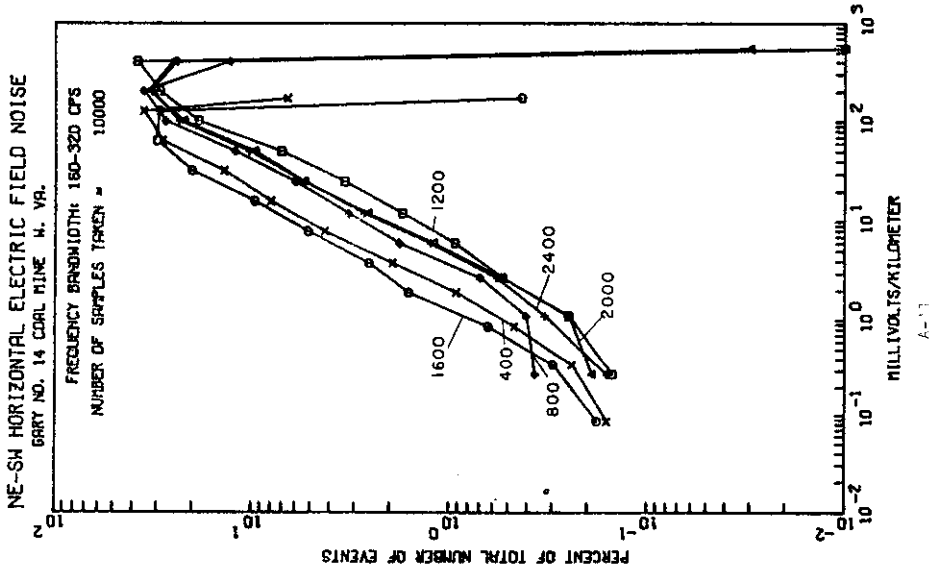
NE-SW HORIZONTAL ELECTRIC FIELD NOISE
GARY NO. 14 COAL MINE W. VA.
FREQUENCY BANDWIDTH: 160-320 CPS
NUMBER OF SAMPLES TAKEN = 10000
1200
2400
2000
1600
400
800
PERCENT OF TOTAL NUMBER OF EVENTS
MILLIVOLTS/KILOMETER

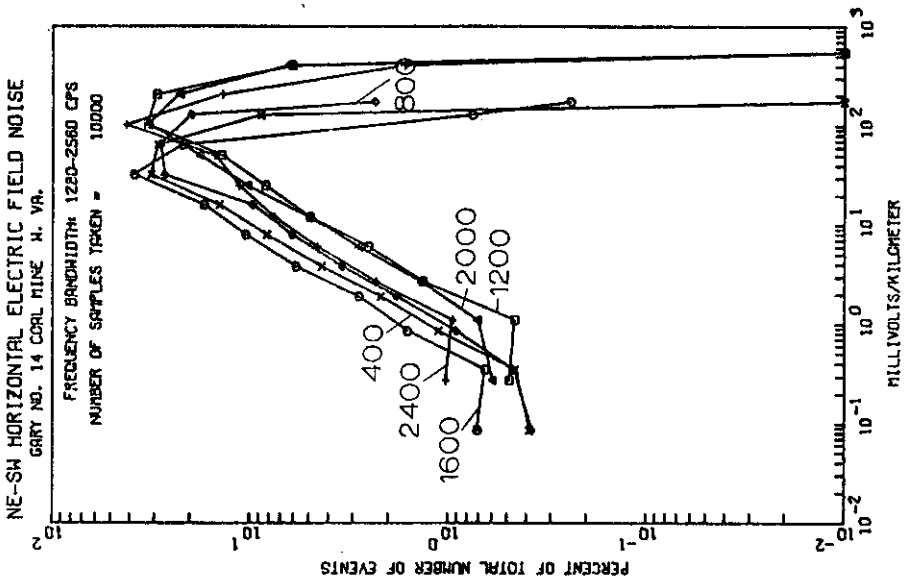
NE-SW HORIZONTAL ELECTRIC FIELD NOISE
GARY NO. 14 COAL MINE W. VA.
FREQUENCY BANDWIDTH: 1280-2560 CPS
NUMBER OF SAMPLES TAKEN = 10000
800
2000
1200
400
2400
1600
PERCENT OF TOTAL NUMBER OF EVENTS
MILLIVOLTS/KILOMETER

A-12

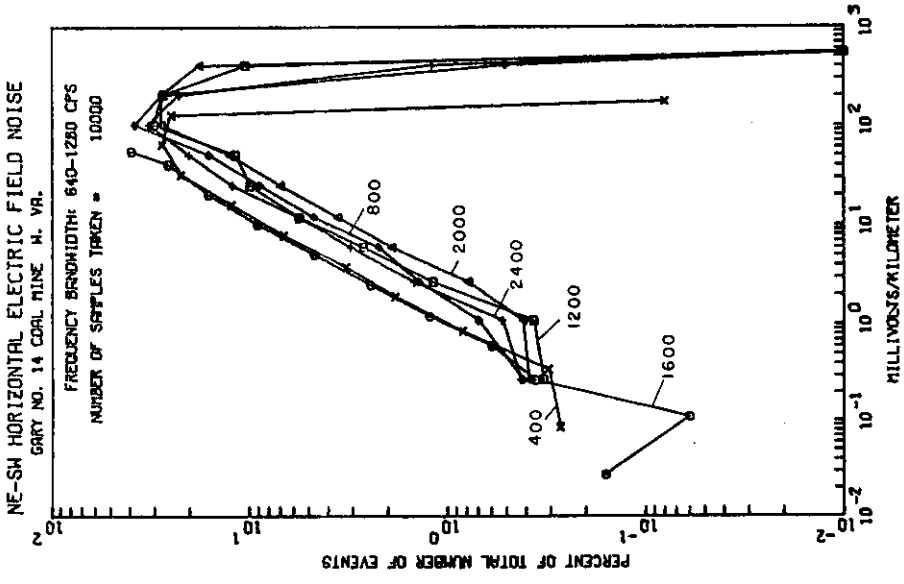
NE-SW HORIZONTAL ELECTRIC FIELD NOISE
GARY NO. 14 COAL MINE W. VA.
FREQUENCY BANDWIDTH: 640-1280 CPS
NUMBER OF SAMPLES TAKEN = 10000
800
2000
2400
1200
1600
400
PERCENT OF TOTAL NUMBER OF EVENTS
MILLIVOLTS/KILOMETER

A-13

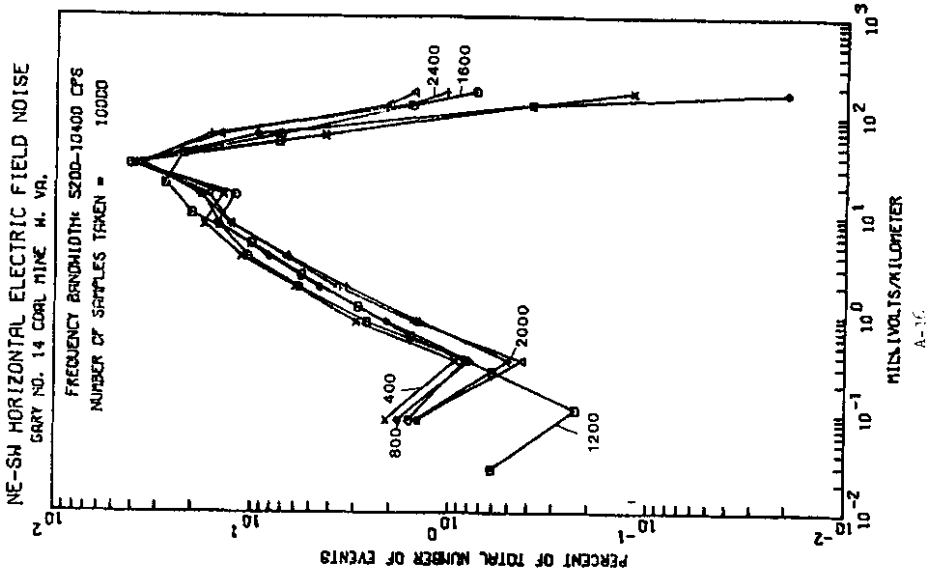
NE-SW HORIZONTAL ELECTRIC FIELD NOISE
GARY NO. 14 COAL MINE W. VA.
FREQUENCY BANDWIDTH= 5200-10400 CPS
NUMBER OF SAMPLES TAKEN = 10000
2400
1600
2000
400
800
1200
PERCENT OF TOTAL NUMBER OF EVENTS
MILLIVOLTS/KILOMETER

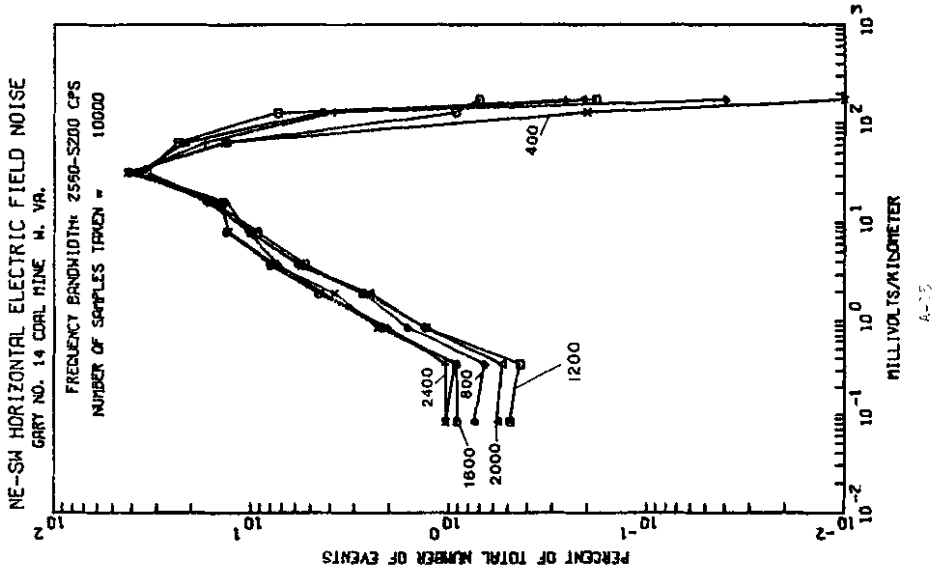
NE-SW HORIZONTAL ELECTRIC FIELD NOISE
GARY NO. 14 COAL MINE W. VA.
FREQUENCY BANDWIDTH= 2560-5200 CPS
NUMBER OF SAMPLES TAKEN = 10000
400
1200
2400
800
1600
2000
PERCENT OF TOTAL NUMBER OF EVENTS
MILLIVOLTS/KILOMETER

APPENDIX B

Peabody No. 10 Coal Mine, Illinois

Smoothed Histograms of:

Time Derivative of Vertical Magnetic Field Noise (B-1 - B-8)

E-W Horizontal Electric Field Noise (B-9 - B-16)

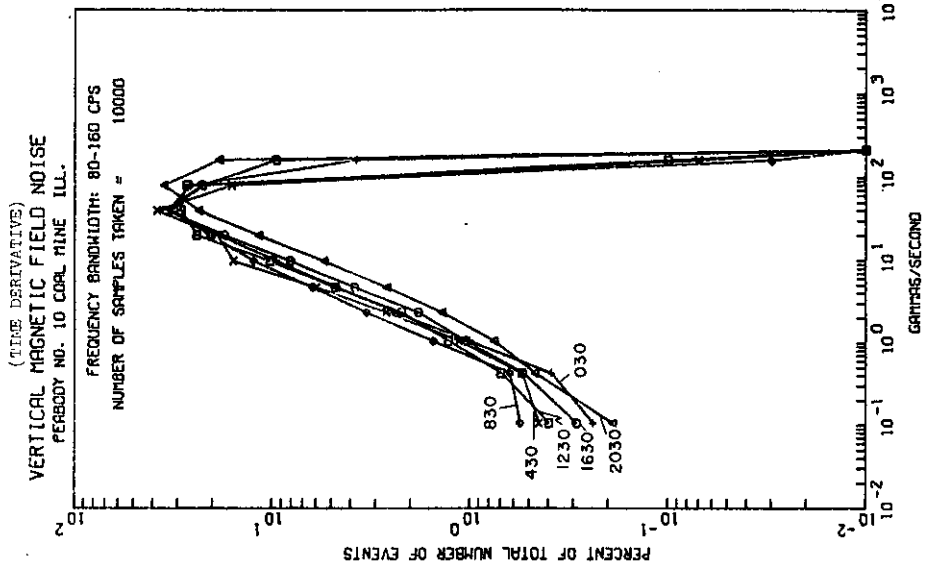
(TIME DERIVATIVES)
VERTICAL MAGNETIC FIELD NOISE
PEABODY NO. 10 COAL MINE ILL.
FREQUENCY BANDWIDTH: 80-160 CPS
NUMBER OF SAMPLES TAKEN = 10000
PERCENT OF TOTAL NUMBER OF EVENTS
GAMMAS/SECOND
830
030
430
1230
1630
20304

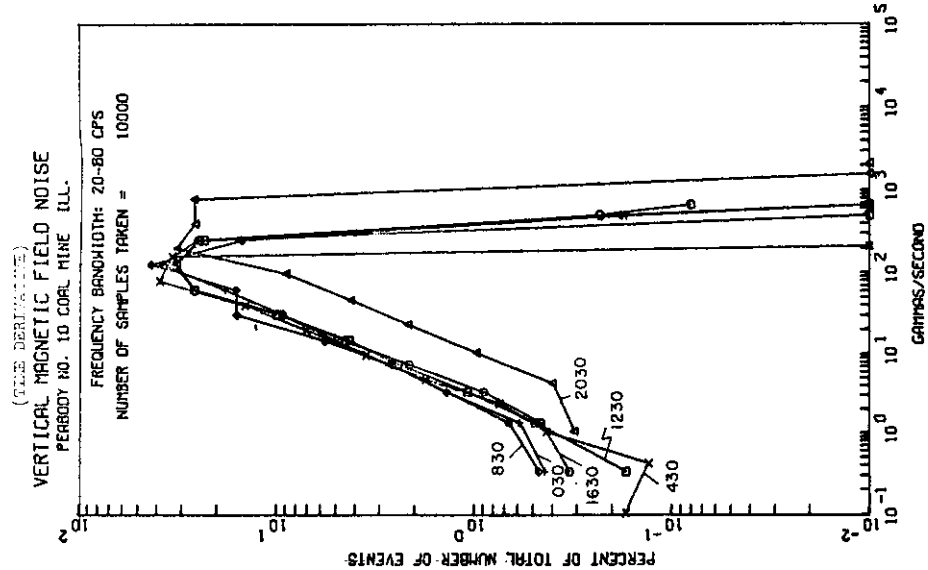
(TIME DERIVATIVES)
VERTICAL MAGNETIC FIELD NOISE
PEABODY NO. 10 COAL MINE ILL.
FREQUENCY BANDWIDTH: 20-80 CPS
NUMBER OF SAMPLES TAKEN = 10000
PERCENT OF TOTAL NUMBER OF EVENTS
GAMMAS/SECOND
830
030
1630
2030
1230
430

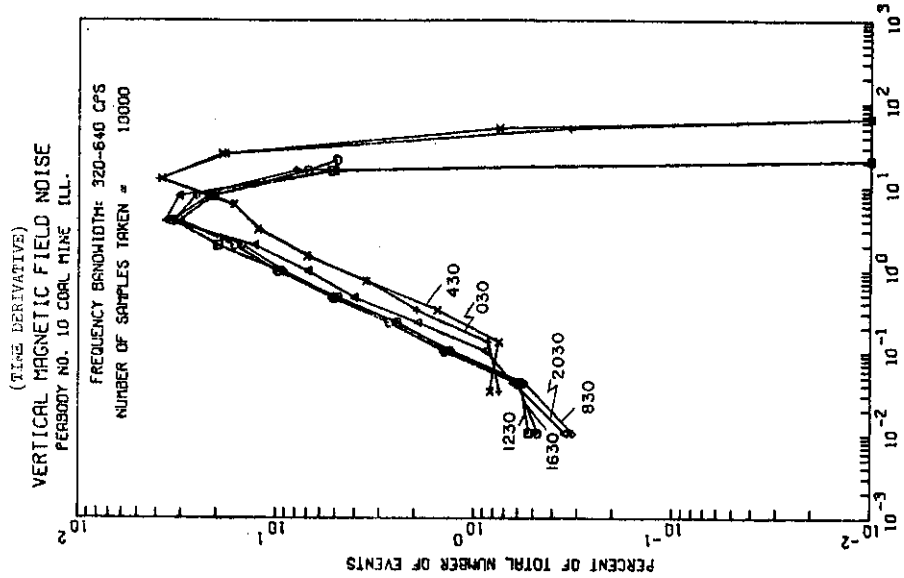
(TIME DERIVATIVE)
VERTICAL MAGNETIC FIELD NOISE
PEABODY NO. 10 COAL MINE ILL.
FREQUENCY BANDWIDTH: 320-640 CPS
NUMBER OF SAMPLES TAKEN = 10000
430
030
2030
830
1230
1630
PERCENT OF TOTAL NUMBER OF EVENTS
GAMMAS/SECOND

B-4

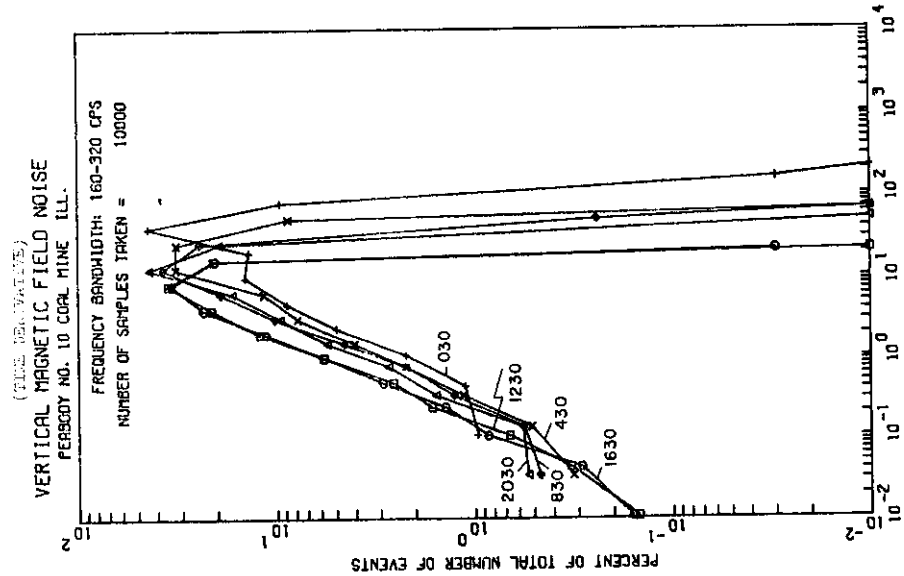
(TIME DERIVATIVE)
VERTICAL MAGNETIC FIELD NOISE
PEABODY NO. 10 COAL MINE ILL.
FREQUENCY BANDWIDTH: 160-320 CPS
NUMBER OF SAMPLES TAKEN = 10000
030
1230
430
1630
2030
830
PERCENT OF TOTAL NUMBER OF EVENTS
GAMMAS/SECOND

B-3

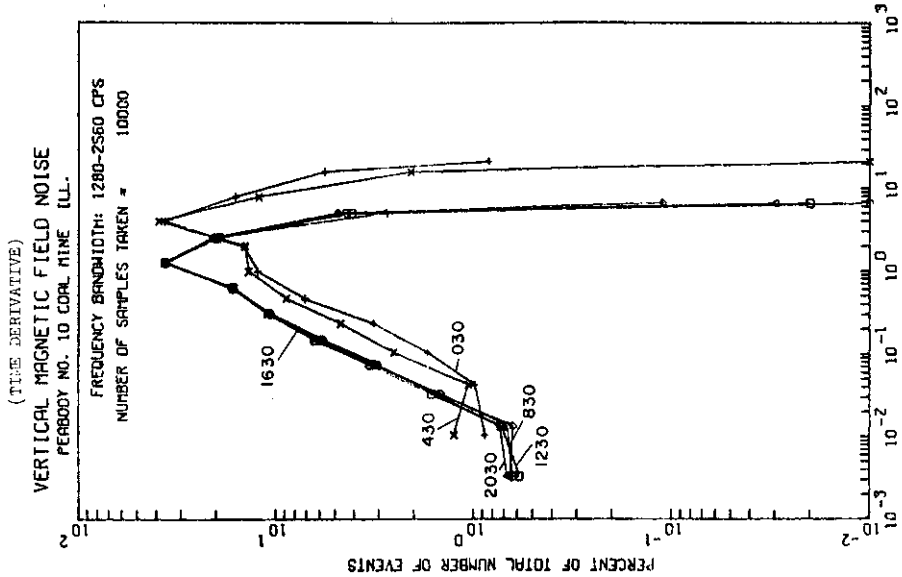
(TIME DERIVATIVE)
VERTICAL MAGNETIC FIELD NOISE
PEABODY NO. 10 COAL MINE ILL.
FREQUENCY BANDWIDTH: 1280-2560 CPS
NUMBER OF SAMPLES TAKEN = 10000
1630
030
430
830
1230
2030
PERCENT OF TOTAL NUMBER OF EVENTS
GAMMAS/SECOND

B-6

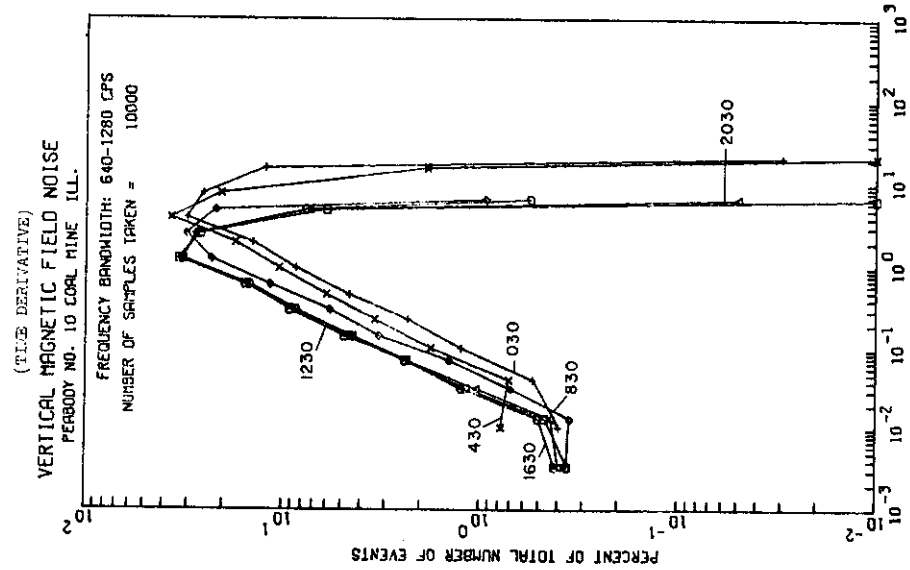
(TIME DERIVATIVE)
VERTICAL MAGNETIC FIELD NOISE
PEABODY NO. 10 COAL MINE ILL.
FREQUENCY BANDWIDTH: 640-1280 CPS
NUMBER OF SAMPLES TAKEN = 10000
2030
1230
030
830
430
1630
PERCENT OF TOTAL NUMBER OF EVENTS
GAMMAS/SECOND

B-5

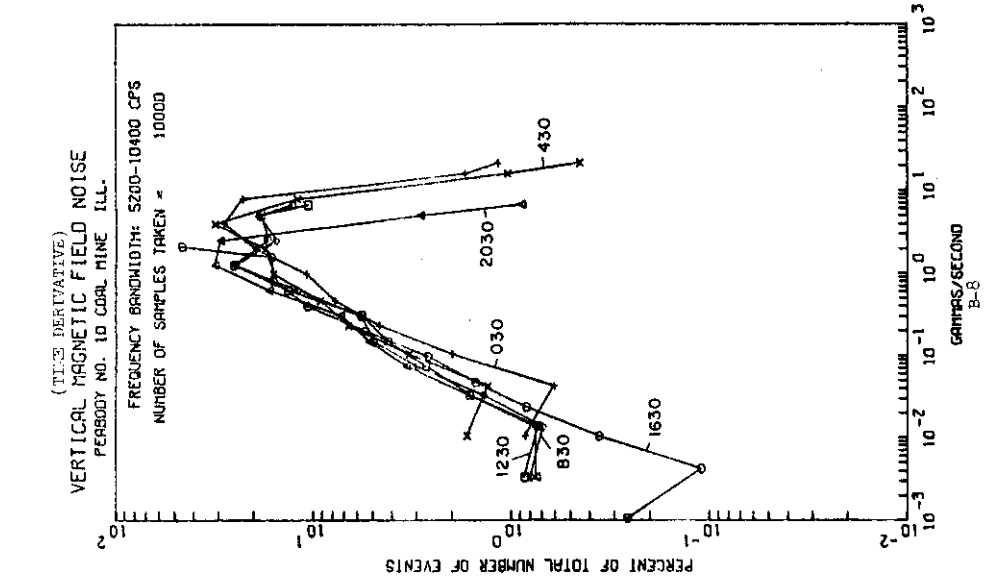
(TIME DERIVATIVE)
VERTICAL MAGNETIC FIELD NOISE
PEABODY NO. 10 COAL MINE ILL.
FREQUENCY BANDWIDTH: 5200-10400 CPS
NUMBER OF SAMPLES TAKEN = 10000
430
2030
030
1630
1230
830
PERCENT OF TOTAL NUMBER OF EVENTS
GAMMAS/SECOND
B-8

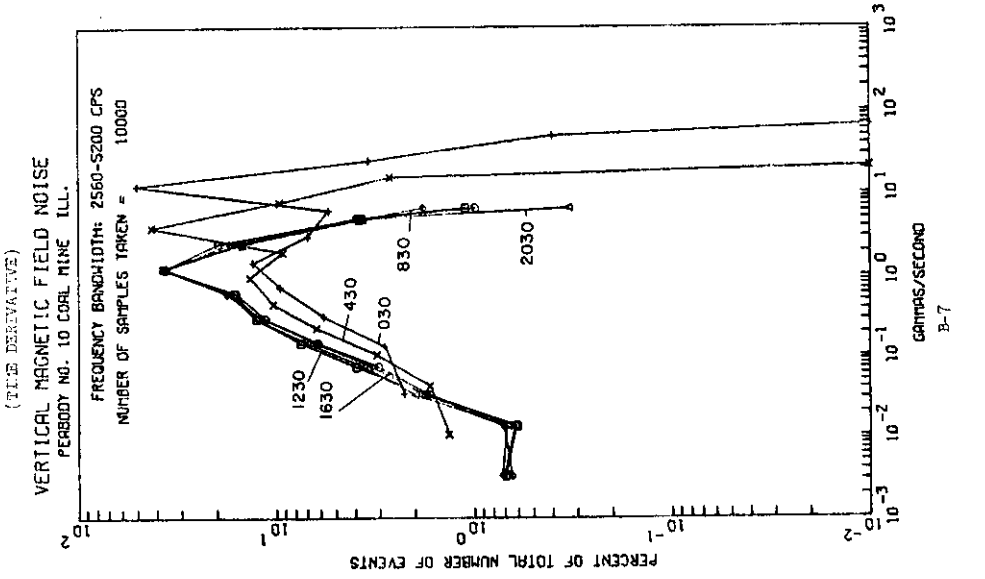
(TIME DERIVATIVE)
VERTICAL MAGNETIC FIELD NOISE
PEABODY NO. 10 COAL MINE ILL.
FREQUENCY BANDWIDTH: 2560-5200 CPS
NUMBER OF SAMPLES TAKEN = 10000
830
2030
430
030
1230
1630
PERCENT OF TOTAL NUMBER OF EVENTS
GAMMAS/SECOND
B-7

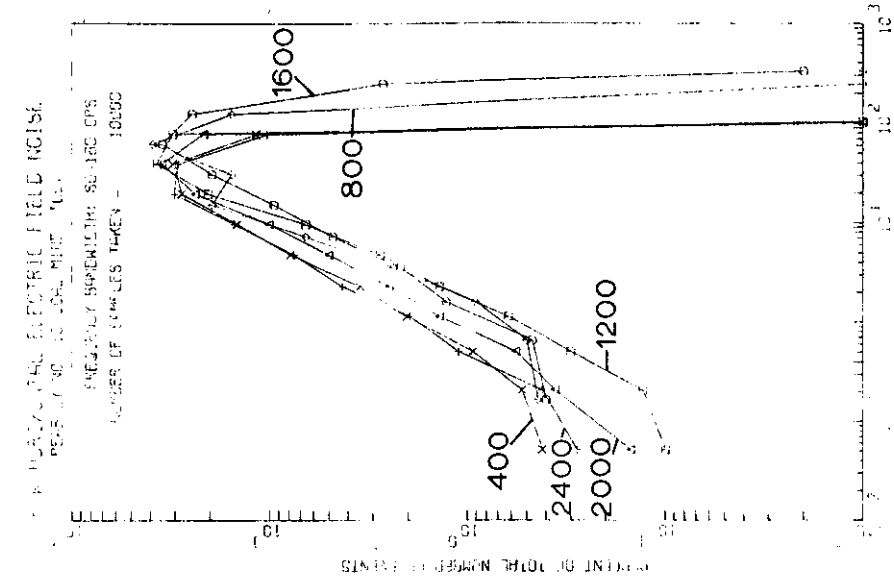
1600
800
1200
400
2400
2000

B-10

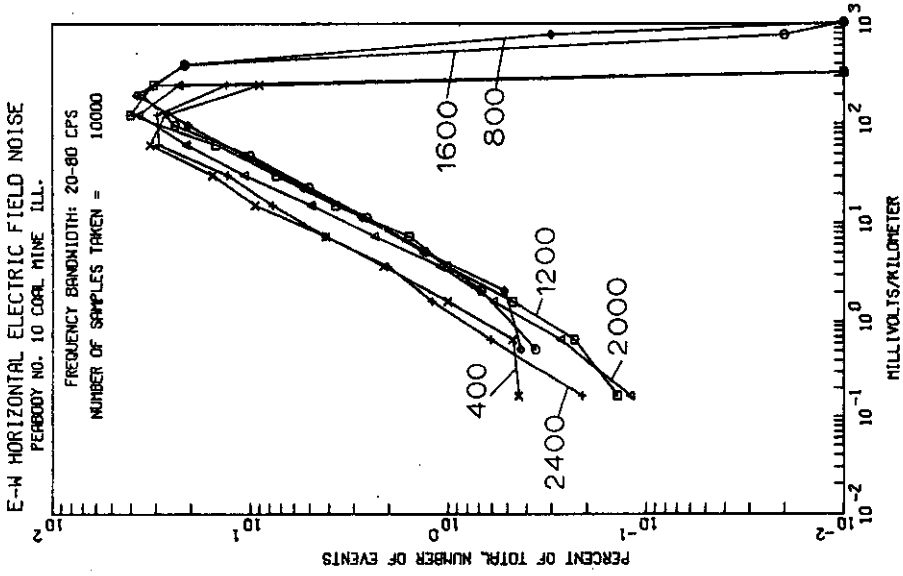
E-W HORIZONTAL ELECTRIC FIELD NOISE
PEABODY NO. 10 COAL MINE ILL.
FREQUENCY BANDWIDTH: 20-60 CPS
NUMBER OF SAMPLES TAKEN = 10000
1600
800
1200
2000
400
2400
PERCENT OF TOTAL NUMBER OF EVENTS
MILLIVOLTS/KILOMETER

B-9

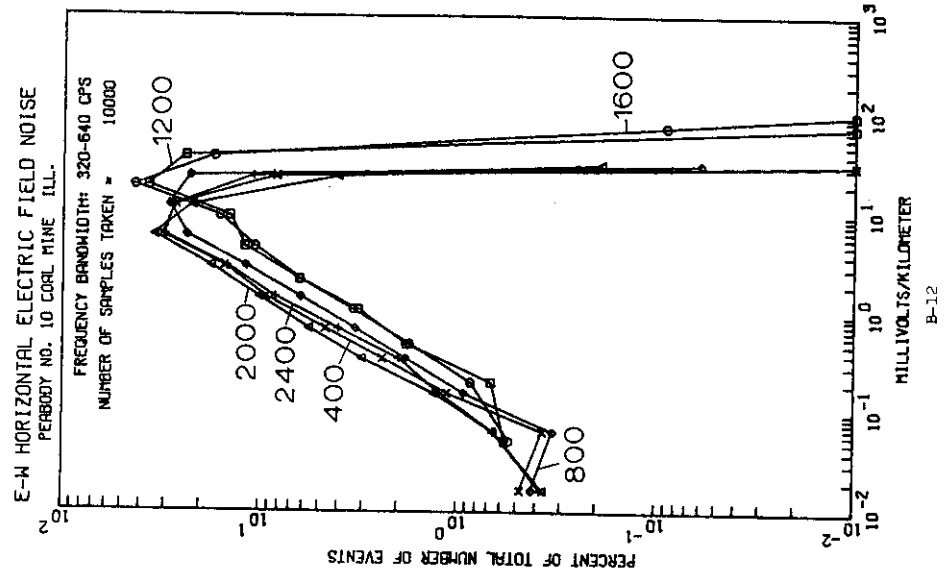
E-W HORIZONTAL ELECTRIC FIELD NOISE
PEABODY NO. 10 COAL MINE ILL.
FREQUENCY BANDWIDTH: 320-640 CPS
NUMBER OF SAMPLES TAKEN = 10000
1200
1600
2000
2400
400
800
PERCENT OF TOTAL NUMBER OF EVENTS
MILLIVOLTS/KILOMETER

B-12

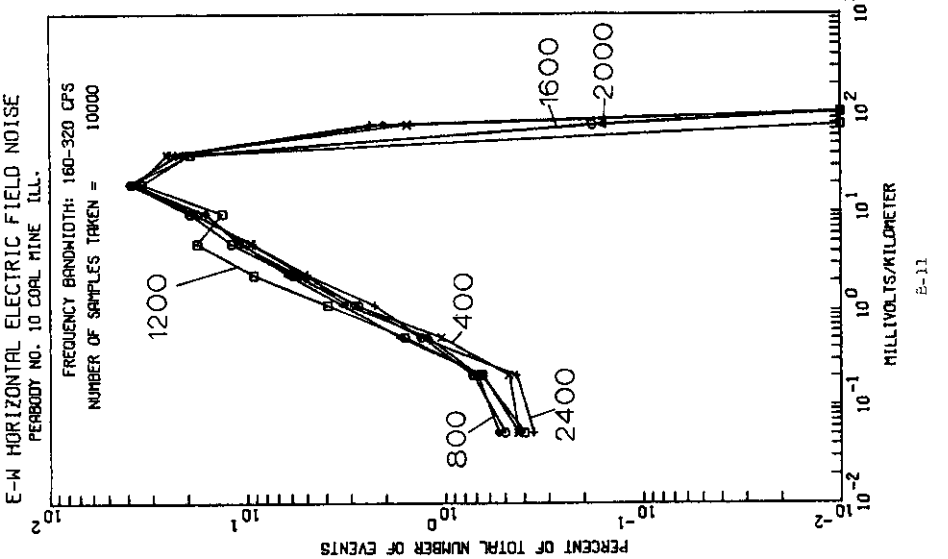
E-W HORIZONTAL ELECTRIC FIELD NOISE
PEABODY NO. 10 COAL MINE ILL.
FREQUENCY BANDWIDTH: 160-320 CPS
NUMBER OF SAMPLES TAKEN = 10000
1200
1600
2000
400
800
2400
PERCENT OF TOTAL NUMBER OF EVENTS
MILLIVOLTS/KILOMETER

B-11

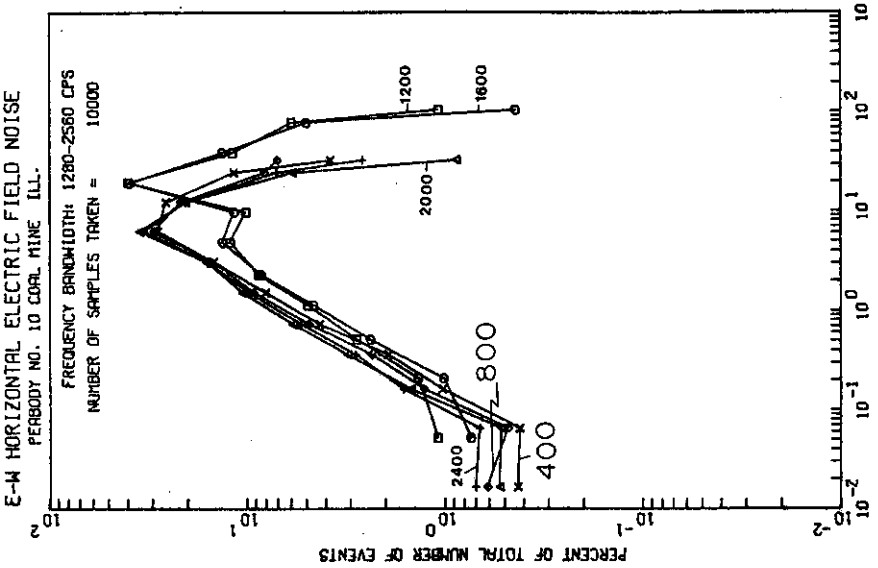
E-W HORIZONTAL ELECTRIC FIELD NOISE
PEABODY NO. 10 COAL MINE ILL.
FREQUENCY BANDWIDTH: 1280-2560 CPS
NUMBER OF SAMPLES TAKEN = 10000
1200
1600
2000
800
2400
400
PERCENT OF TOTAL NUMBER OF EVENTS
MILLIVOLTS/KILOMETER

B-14

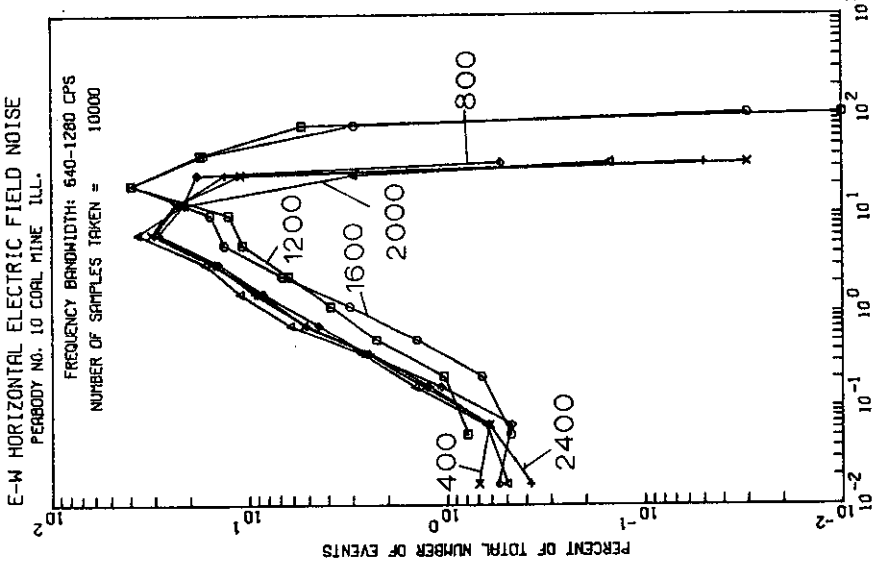
E-W HORIZONTAL ELECTRIC FIELD NOISE
PEABODY NO. 10 COAL MINE ILL.
FREQUENCY BANDWIDTH: 640-1280 CPS
NUMBER OF SAMPLES TAKEN = 10000
800
1200
1600
2000
400
2400
PERCENT OF TOTAL NUMBER OF EVENTS
MILLIVOLTS/KILOMETER

B-13

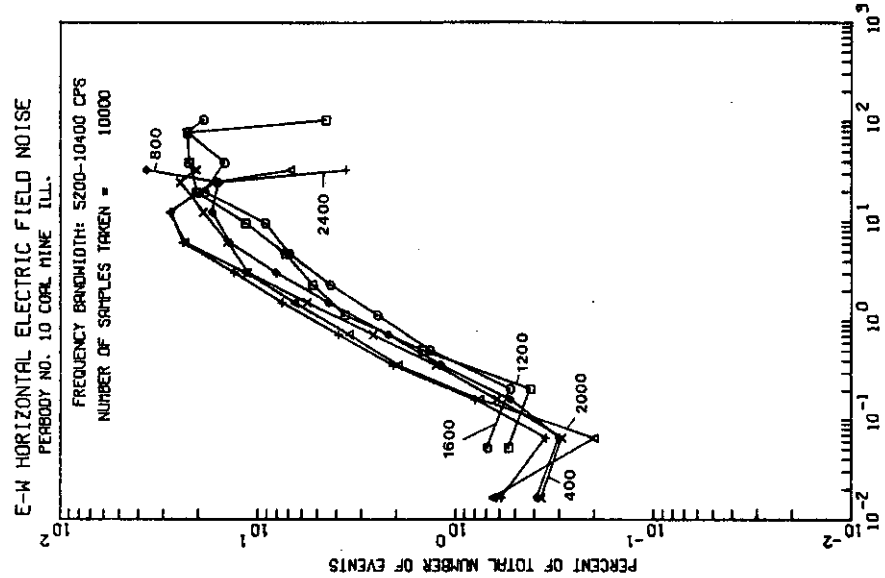
E-W HORIZONTAL ELECTRIC FIELD NOISE
PEABODY NO. 10 COAL MINE ILL.
FREQUENCY BANDWIDTH: 5200-10400 CPS
NUMBER OF SAMPLES TAKEN = 10000
800
2400
1200
1600
2000
400
PERCENT OF TOTAL NUMBER OF EVENTS
MILLIVOLTS/KILOMETER

B-16

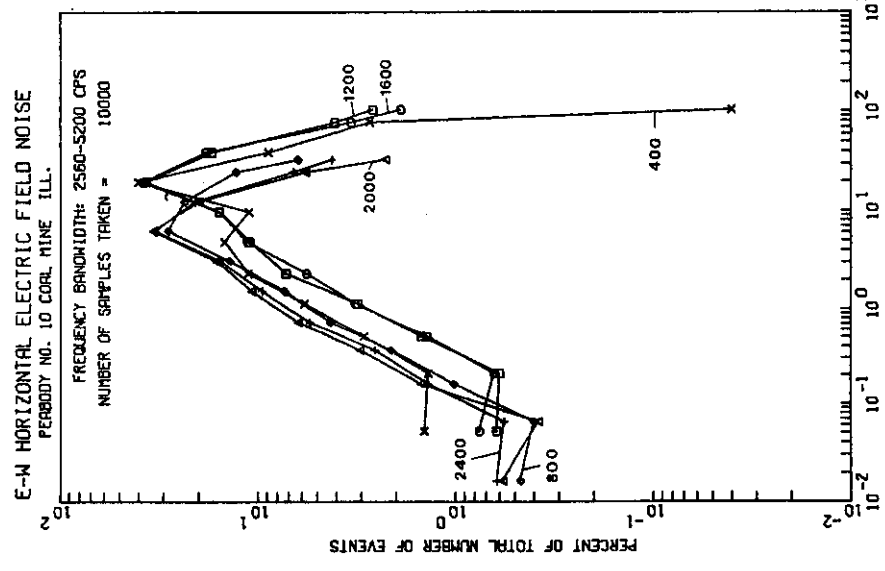
E-W HORIZONTAL ELECTRIC FIELD NOISE
PEABODY NO. 10 COAL MINE ILL.
FREQUENCY BANDWIDTH: 2560-5200 CPS
NUMBER OF SAMPLES TAKEN = 10000
1200
1600
2000
400
2400
800
PERCENT OF TOTAL NUMBER OF EVENTS
MILLIVOLTS/KILOMETER

B-15

APPENDIX C

Eagle Coal Mine, Colorado

Smoothed Histograms of:

Time Derivative of Vertical Magnetic Field Noise (C-1 - C-8)

N-S Horizontal Electric Field Noise (C-9 - C16)

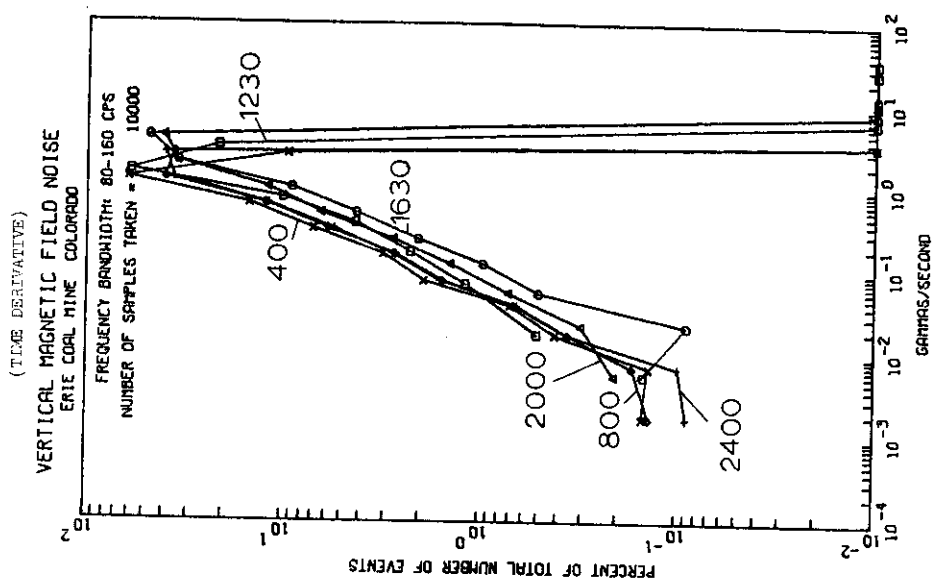
(TIME DERIVATIVE)
VERTICAL MAGNETIC FIELD NOISE
ERIE COAL MINE COLORADO
FREQUENCY BANDWIDTH: 80-160 CPS
NUMBER OF SAMPLES TAKEN = 10000
1230
1630
400
2000
800
2400
PERCENT OF TOTAL NUMBER OF EVENTS
GAMMAS/SECOND
C-2

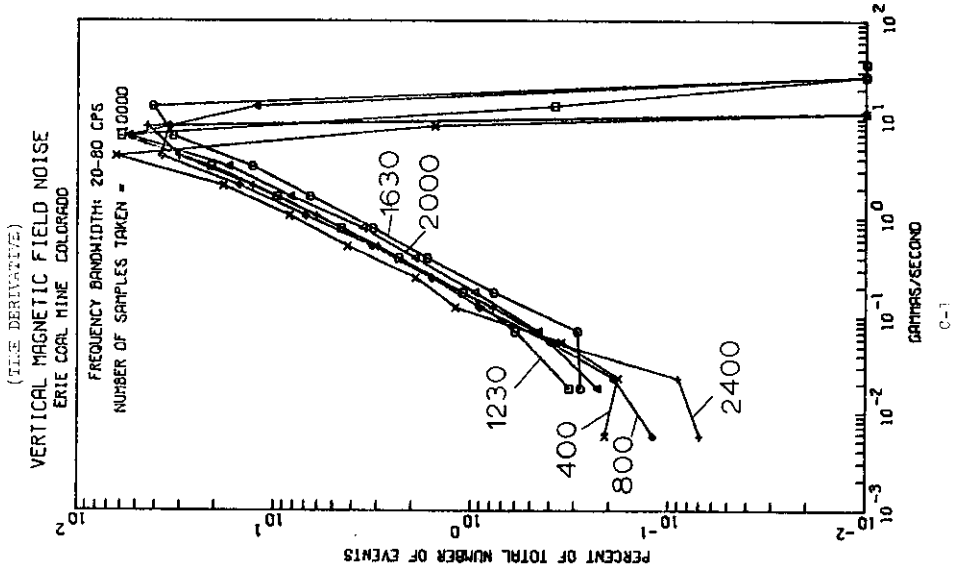
(TIME DERIVATIVE)
VERTICAL MAGNETIC FIELD NOISE
ERIE COAL MINE COLORADO
FREQUENCY BANDWIDTH: 20-80 CPS
NUMBER OF SAMPLES TAKEN = 10000
1630
2000
1230
2400
400
800
PERCENT OF TOTAL NUMBER OF EVENTS
GAMMAS/SECOND
C-1

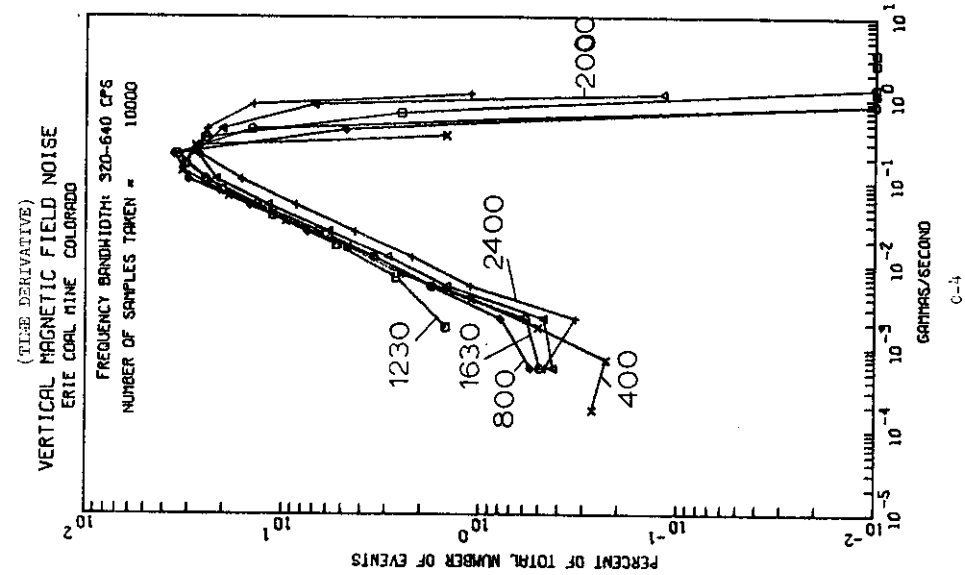
(TIME DERIVATIVE)
VERTICAL MAGNETIC FIELD NOISE
ERIE COAL MINE COLORADO
FREQUENCY BANDWIDTH: 320-640 CPS
NUMBER OF SAMPLES TAKEN = 10000
2000
2400
1230
1630
800
400
PERCENT OF TOTAL NUMBER OF EVENTS
GAMMAS/SECOND

C-4

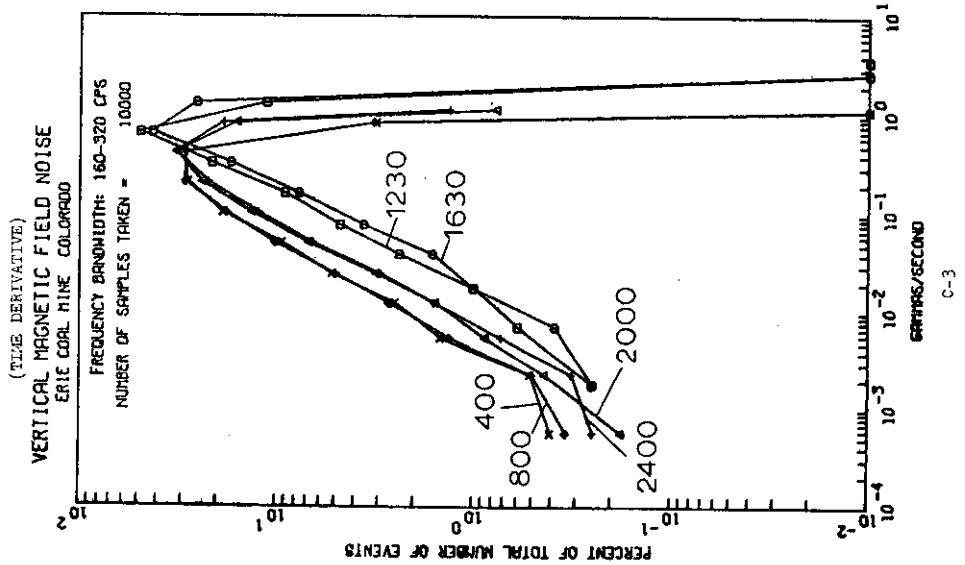
(TIME DERIVATIVE)
VERTICAL MAGNETIC FIELD NOISE
ERIE COAL MINE COLORADO
FREQUENCY BANDWIDTH: 160-320 CPS
NUMBER OF SAMPLES TAKEN = 10000
1230
1630
2000
400
800
2400
PERCENT OF TOTAL NUMBER OF EVENTS
GAMMAS/SECOND

C-3

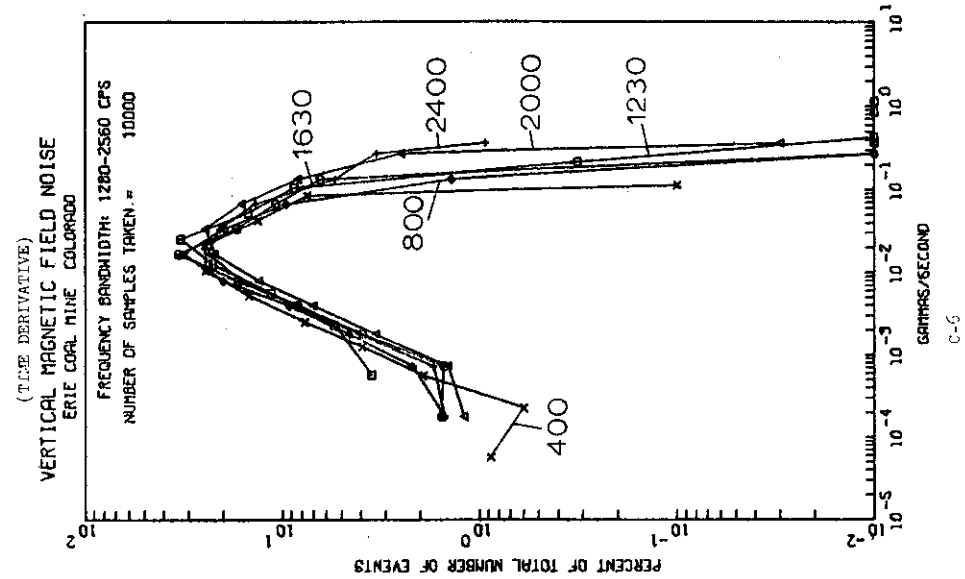
(TIME DERIVATIVE)
VERTICAL MAGNETIC FIELD NOISE
ERIE COAL MINE COLORADO
FREQUENCY BANDWIDTH: 1280-2560 CPS
NUMBER OF SAMPLES TAKEN = 10000
1630
2400
2000
1230
800
400
PERCENT OF TOTAL NUMBER OF EVENTS
GAMMAS/SECOND
C-5

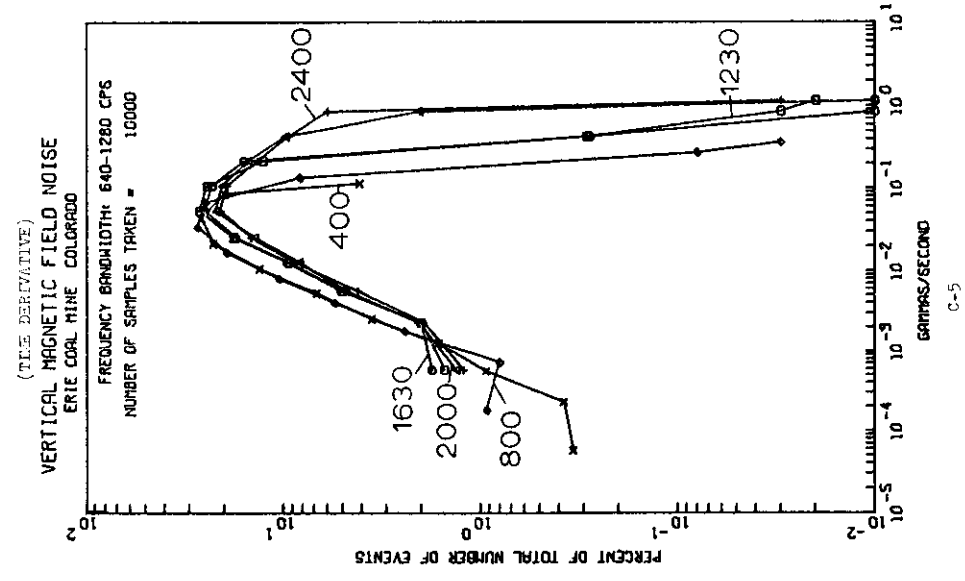
(TIME DERIVATIVE)
VERTICAL MAGNETIC FIELD NOISE
ERIE COAL MINE COLORADO
FREQUENCY BANDWIDTH: 640-1280 CPS
NUMBER OF SAMPLES TAKEN = 10000
2400
1230
400
1630
2000
800
PERCENT OF TOTAL NUMBER OF EVENTS
GAMMAS/SECOND
C-5

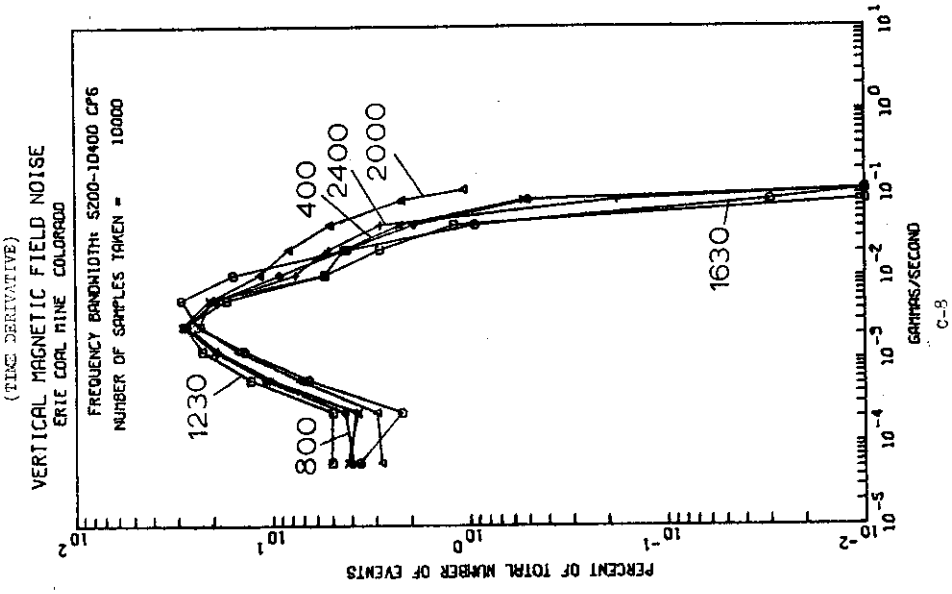
(TIME DERIVATIVE)
VERTICAL MAGNETIC FIELD NOISE
ERIE COAL MINE COLORADO
FREQUENCY BANDWIDTH: 5200-10400 CPS
NUMBER OF SAMPLES TAKEN = 10000
400
2400
2000
1630
1230
800
PERCENT OF TOTAL NUMBER OF EVENTS
GAMMAS/SECOND
C-8

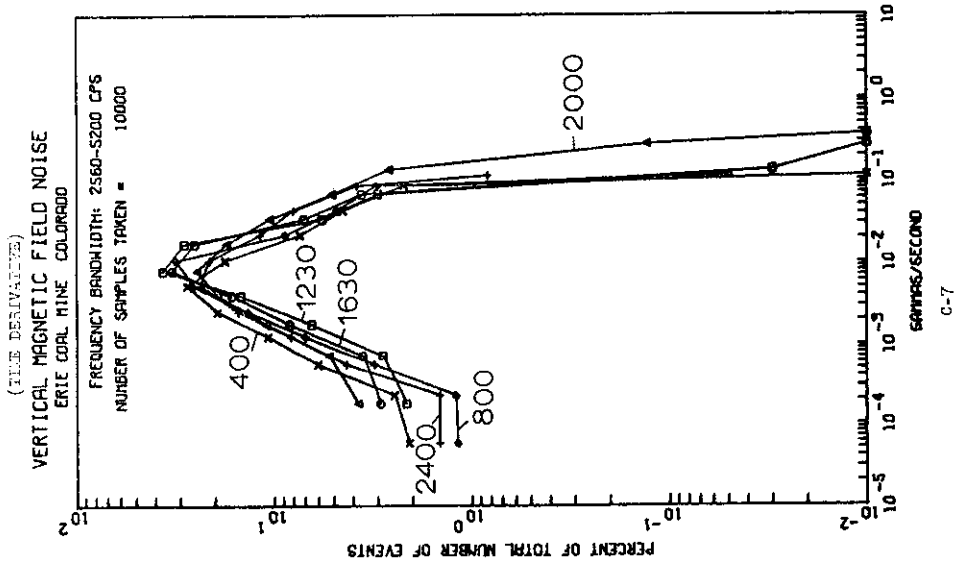
(TIME DERIVATIVE)
VERTICAL MAGNETIC FIELD NOISE
ERIE COAL MINE COLORADO
FREQUENCY BANDWIDTH: 2560-5200 CPS
NUMBER OF SAMPLES TAKEN = 10000
2000
1230
1630
400
800
2400
PERCENT OF TOTAL NUMBER OF EVENTS
GAMMAS/SECOND
C-7

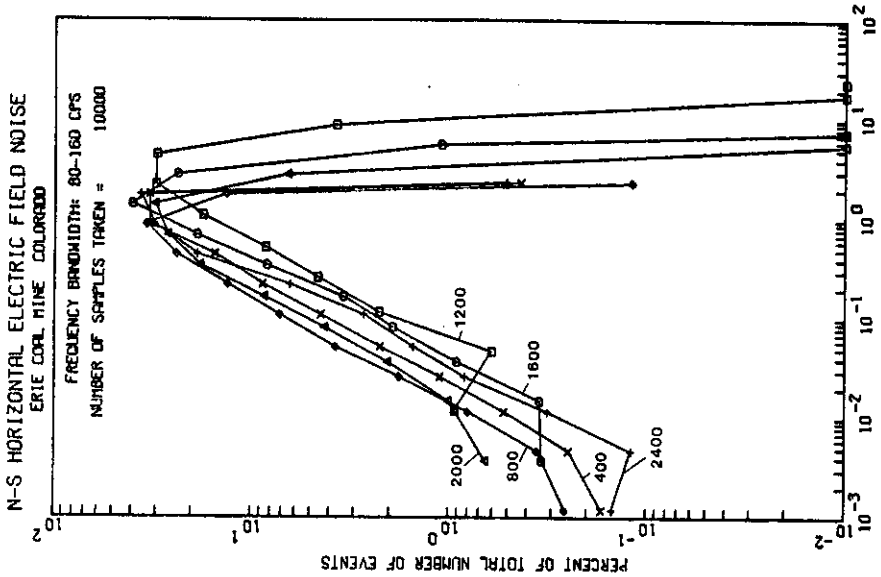
N-S HORIZONTAL ELECTRIC FIELD NOISE
ERIE COAL MINE COLORADO
FREQUENCY BANDWIDTH: 80-160 CPS
NUMBER OF SAMPLES TAKEN = 10000
2000
1200
1600
800
400
2400
PERCENT OF TOTAL NUMBER OF EVENTS
MILLIVOLTS/KILOMETER
C-10

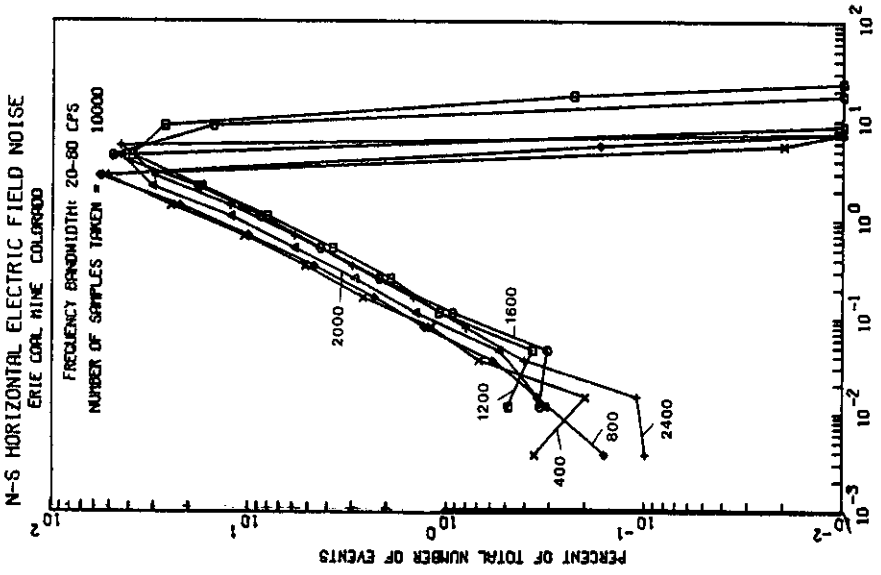
N-S HORIZONTAL ELECTRIC FIELD NOISE
ERIE COAL MINE COLORADO
FREQUENCY BANDWIDTH: 20-80 CPS
NUMBER OF SAMPLES TAKEN = 10000
2000
1600
1200
800
400
2400
PERCENT OF TOTAL NUMBER OF EVENTS
MILLIVOLTS/KILOMETER
C-9

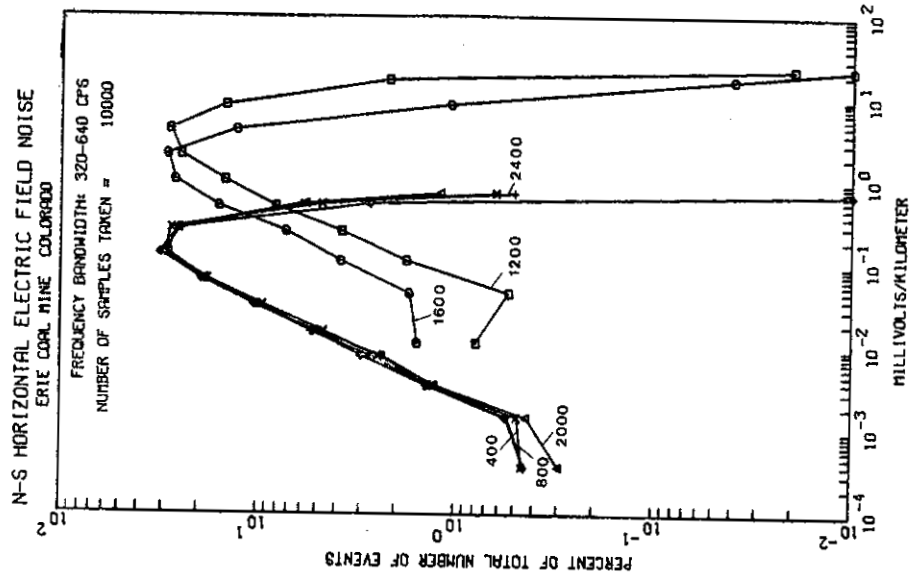
N-S HORIZONTAL ELECTRIC FIELD NOISE
ERIE COAL MINE COLORADO
FREQUENCY BANDWIDTH: 320-640 CPS
NUMBER OF SAMPLES TAKEN = 10000
400
800
1600
2000
1200
2400
PERCENT OF TOTAL NUMBER OF EVENTS
MILLIVOLTS/KILOMETER

C-11

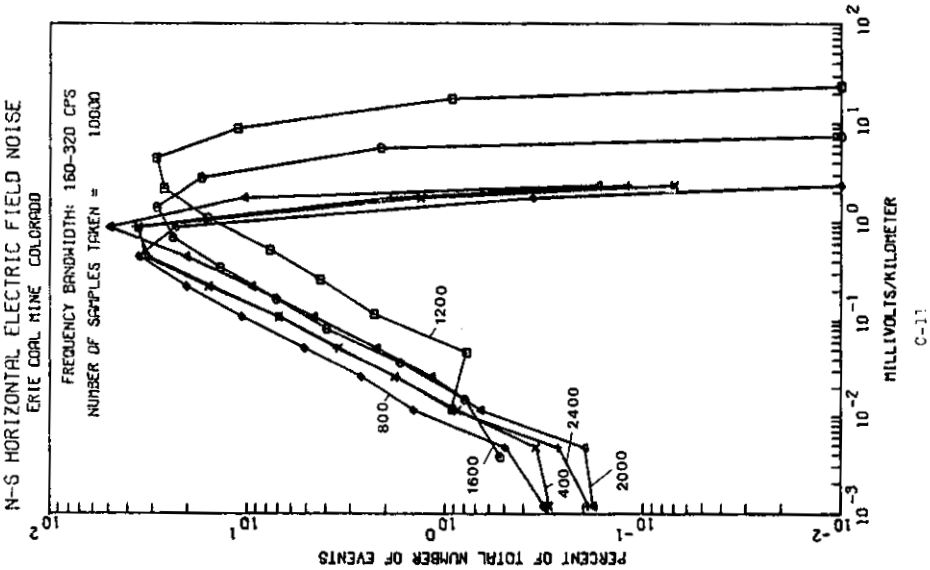
N-S HORIZONTAL ELECTRIC FIELD NOISE
ERIE COAL MINE COLORADO
FREQUENCY BANDWIDTH: 160-320 CPS
NUMBER OF SAMPLES TAKEN = 10000
1200
800
2400
1600
400
2000
PERCENT OF TOTAL NUMBER OF EVENTS
MILLIVOLTS/KILOMETER

C-11

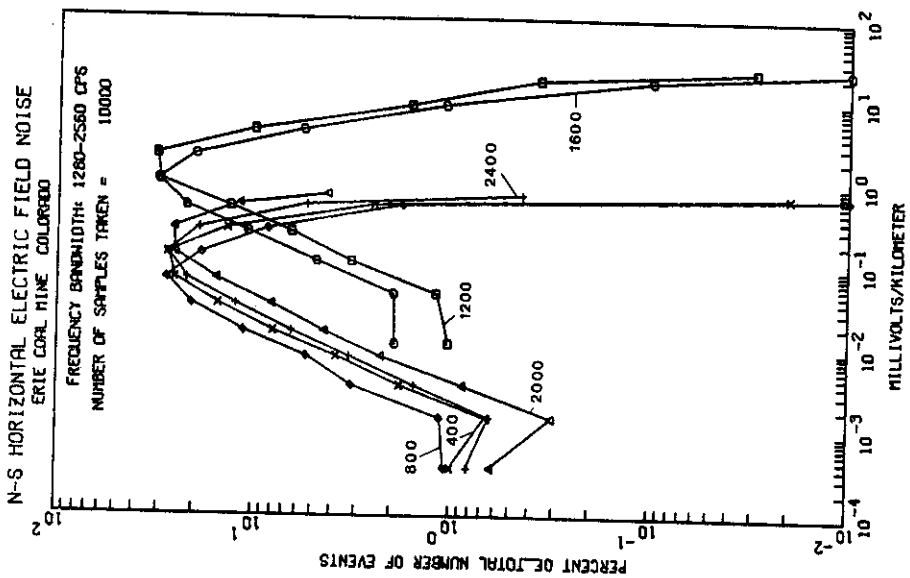
N-S HORIZONTAL ELECTRIC FIELD NOISE
ERIE COAL MINE COLORADO
FREQUENCY BANDWIDTH= 1280-2560 CPS
NUMBER OF SAMPLES TAKEN = 10000
1600
2400
1200
2000
800
400
PERCENT OF TOTAL NUMBER OF EVENTS
MILLIVOLTS/KILOMETER

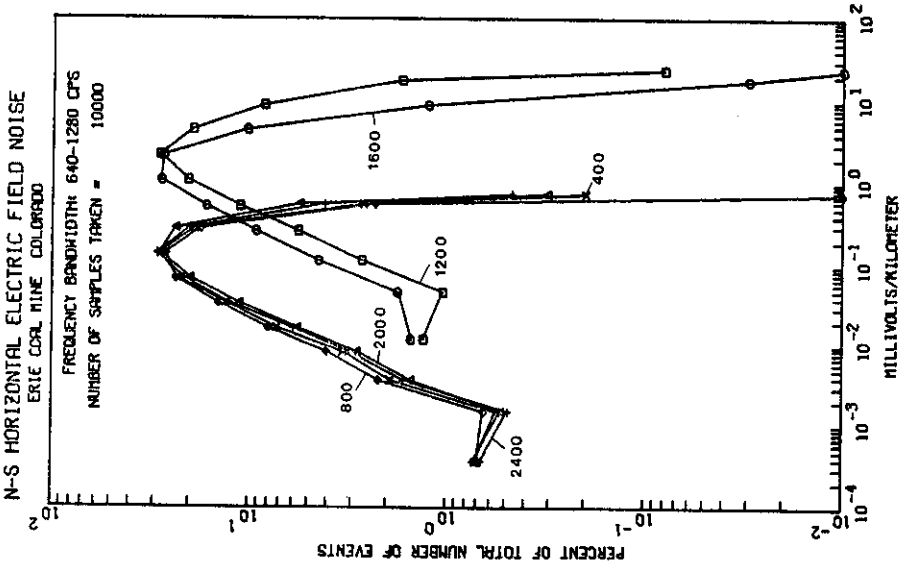
N-S HORIZONTAL ELECTRIC FIELD NOISE
ERIE COAL MINE COLORADO
FREQUENCY BANDWIDTH= 640-1280 CPS
NUMBER OF SAMPLES TAKEN = 10000
1600
400
1200
2000
800
2400
PERCENT OF TOTAL NUMBER OF EVENTS
MILLIVOLTS/KILOMETER

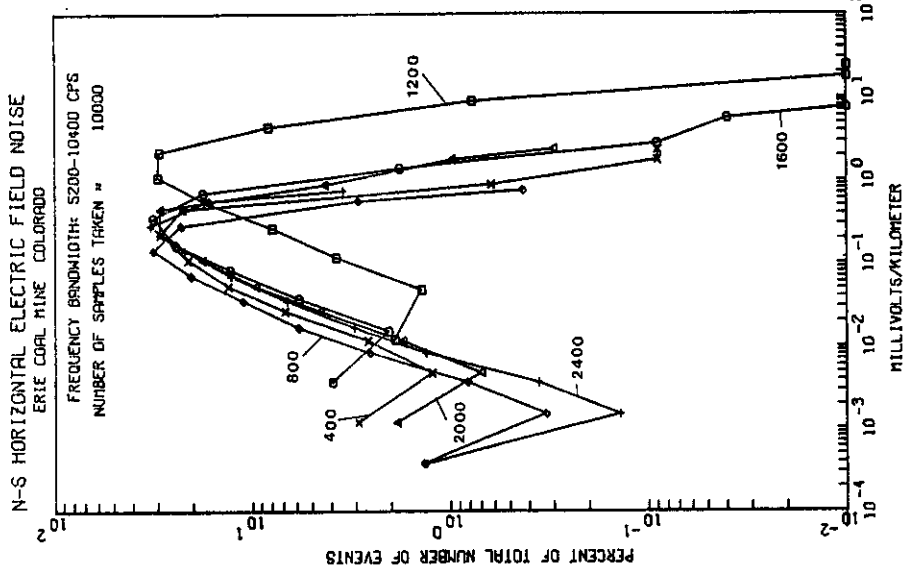
N-S HORIZONTAL ELECTRIC FIELD NOISE
ERIE COAL MINE COLORADO
FREQUENCY BANDWIDTH: 5200-10400 CPS
NUMBER OF SAMPLES TAKEN = 10000
1200
1600
800
400
2400
2000
PERCENT OF TOTAL NUMBER OF EVENTS
MILLIVOLTS/KILOMETER

C-16

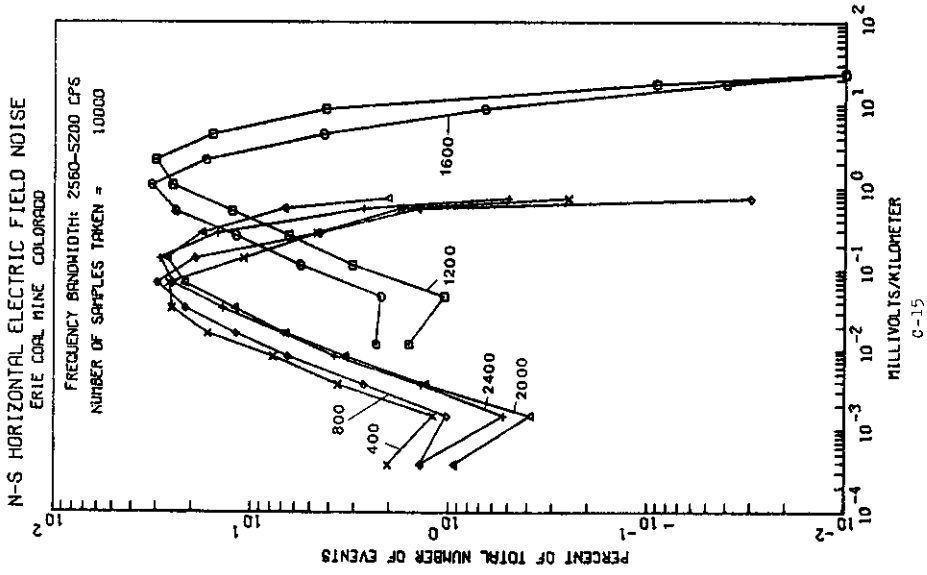
N-S HORIZONTAL ELECTRIC FIELD NOISE
ERIE COAL MINE COLORADO
FREQUENCY BANDWIDTH: 2560-5200 CPS
NUMBER OF SAMPLES TAKEN = 10000
1600
1200
2400
2000
800
400
PERCENT OF TOTAL NUMBER OF EVENTS
MILLIVOLTS/KILOMETER

C-15

REFERENCES

Baker, A. F., Brady, G. A., and Eckerd, J. W., 1966, A method for determining the electrical resistivity of solid anthracite specimens: U.S. Bureau of Mines Report of Investigations 6788.

Bannister, P. R., 1966, The quasi-static fields of dipole antennas - Part I: USL Report No. 701, 34 p.

Banõs, A., Jr., 1966, Dipole radiation in the presence of a conducting half-space: Pergamon Press, New York, 245 p.

Clark, S. P., Jr. (Editor), 1966, Handbook of physical constants: Geol. Soc. Am. Memoir 97.

Frischknecht, F. C., 1967, Fields about an oscillating dipole: Quart. Colo. Sch. Mines, v. 62, n. 1, 326 p.

Geyer, R. G., and Keller, G. V., 1971a, Research related to the development of emergency mine communication systems: Quart. Tech. Rpt. prepared for the U.S. Bureau of Mines for the period July 1, 1971 to September 30, 1971, 42 p.

_____ 1971b, Research on the transmission of acoustic and electromagnetic signals between mine workings and the surface: Quart. Tech. Rpt. to U.S. Bureau of Mines for the period Oct. 1, 1971 to Dec. 30, 1971, 106 p.

Geyer, R. G., 1972a, Evaluation of an impulsively driven line current source at the surface for downlink communications to mine workings: Quart. Tech. Rpt. to U.S. Bureau of Mines for the period Jan. 1, 1972 to March 30, 1972, 51 p.

Geyer, R. G., and Keller, G. V., 1972b, Uplink field transmission tests using a vertical-axis loop source: Quart. Tech. Rpt. to U.S. Bureau of Mines for the period Oct. 1, 1972 to Dec. 31, 1972, 52 p.

Hill, D. A., 1973a, Electromagnetic surface fields of an inclined buried cable of finite length: Preliminary Rpt. to U.S. Bureau of Mines, April 16, 1973, 22 p.

Hill, D. A., and Wait, J. R., 1973b, Electromagnetic response of a conducting cylinder of finite length for various source types: Preliminary Rpt. to U.S. Bureau of Mines (August 1, 1973), 32 p.

_____ 1973c, Perturbation of magnetic dipole fields by a perfectly conducting prolate spheroid: Preliminary Rpt. to U.S. Bureau of Mines (August 22, 1973), 10 p.

Howard, A. Q., Jr., 1972, The electromagnetic fields of a subterranean cylindrical inhomogeneity excited by a line source: Geophysics, v. 37, n. 6, p. 975-984.

Kirby, R. S., Harman, J. G., Capps, F. M., and Jones, D. N., 1954, Effective radio ground conductivity measurements in the United States: Nat. Bur. Stan. Circ. 546, U.S.G.P.O., Washington, D.C.

Krasnovskii, F. Z., 1969, The electrical conductivities of coals and their relations with the mechanical properties: Soviet Mining Science 1969, no. 5, p. 570-572.

Madden, T. R., and Cantwell, T., 1967, Induced polarization, a review, in Mining Geophysics, v. II, Soc. Expl. Geophys., Tulsa.

Parkhomenko, E. I., 1967, Electrical properties of rocks: Plenum Press, New York, p. 314.

Parkinson, H. E., 1971, Private communication.

Parkinson, H. E., Powell, J., and Wait, J. R., 1972, Private communication.

Sinha, A. K., and Bhattacharya, P. K., 1966, Vertical magnetic dipole buried inside a homogeneous earth: Radio Science, v. 1, n. 3, p. 379-395.

Tonkonogov, M. P., and Veksler, V. A., 1971, Electrical properties of Karaganda coal: Soviet Mining Science, v. 7, no. 6, p. 640-645.

Vanian, L. L., 1965, Electromagnetic depth soundings (translated): Consultants Bureau, New York, 312 p.

Wait, J. R., and Campbell, L. L., 1953, The fields of an oscillating magnetic dipole immersed in a semi-infinite conducting medium: Jour. Geophys. Res., v. 58, n. 2, p. 167-178.

Wait, J. R., 1955, Mutual coupling of loops over a homogeneous ground: Geophysics, v. 20, n. 3, p. 630-637.

_____ 1962, Electromagnetic waves in stratified media: New York, Pergamon Press, 608 p.

_____ 1969, Electromagnetic fields of sources in lossy media in Antenna Theory, Part II (ed. by Collin and Zucker): McGraw-Hill, New York, p. 438-513.

_____ 1970, Criteria for locating an oscillating magnetic dipole buried in the earth: Informal Rpt. to U.S. Bureau of Mines (Dec. 28, 1970, 11 p.

Wait, J. R., and Spies, K. P., 1971a, Subsurface electromagnetic fields of a circular loop of current located above ground: Informal Rpt. to U.S. Bureau of Mines (Nov. 15, 1971), 16 p.

Wait, J. R., 1971b, Influence of earth curvature on the subsurface electromagnetic fields of a line source: Electronics Letters, v. 7, n. 23.

Wait, J. R., 1971c, Electromagnetic fields of a small loop buried in a stratified earth: IEEE Trans. Antennas and Propagation, v. AP-19, n. 5, p. 717-718.

_____ 1971d, Criteria for locating an oscillating magnetic dipole buried in the earth: Proc. IEEE, p. 1033-1035.

_____ 1971e, Subsurface electromagnetic fields of a line source on a conducting half-space: Radio Science, v. 6, n. 8, 9, p. 781-786.

_____ 1971f, The effect of a buried conductor on the subsurface fields of line source excitation (Private communication).

Wait, J. R., and Hill, D. A., 1972a, Electromagnetic surface fields produced by a pulse-excited loop buried in the earth: Preliminary Rept. to U.S. Bureau of Mines (June 15, 1972), 14 p.

_____ 1973a, Excitation of a homogeneous conductive cylinder of finite length by a prescribed axial current distribution: Preliminary Rpt. to U.S. Bureau of Mines (July 10, 1973), 27 p.